PETROLEUM SOURCE ROCK ANALYSIS OF THE JURASSIC SARGELU

FORMATION, NORTHERN IRAQ

by

Rzger Abdula

A thesis submitted to the Faculty and the Board of Trustees of the Colorado School of Mines in partial fulfillment of the requirements for the degree of Master of Science (Geology).

Golden, Colorado

Date 6/29/10

Signed: _____

Rzger Abdula

Signed: _____

Dr. Stephen A. Sonnenberg

Thesis Advisor

Golden, Colorado

Date 6/29/10

Signed: _____

Dr. John D. Humphrey

Department Head

Geology and Geological Engineering

ii

ABSTRACT

The Sargelu Formation is one of the major petroleum source rocks in Iraq and the Middle East. In an effort to build on the previous work and add new interpretations, this study focuses on four outcrops, cuttings from four wells in various localities and crude oil samples from eight wells in three oil fields in northern Iraq (Kirkuk, Taq Taq, and Tawke oil fields).

The Late Toarcian–Late Bathonian Sargelu Formation has rather uniform lithology with variable thickness throughout northern Iraq. The thickness progressively decreases from about 485 m west of the Tigris River in the Mosul area toward north where it is 20-30 m thick and northeastern Iraq where it is 49 m thick.

The pyrolysis analysis for the studied samples shows that the total organic carbon of the Sargelu Formation decreases toward the north and northeastern parts of Iraq. The mean of TOC wt. percent is 11.1 in northwestern part in Tawke-15 and it is only 0.5 wt. percent in eastern part in Hanjeera locality. The organic material is characterized by type II and III kerogens. The thermal maturity increases to the east of the studied area. The organic matter is within the dry gas zone in the eastern part of the study area and is mature and immature in both the western and northwestern parts of the study area.

Various diagrams and relationships between bulk properties and biomarkers help recognize different oil families in the eight oil wells in northern Iraq. Four main oil families are recognized: (1) the Upper Jurassic Taq Taq; (2) the Lower Jurassic Tawke; (3) the Upper Jurassic Kirkuk; and (4) the Tertiary Kirkuk. The geochemical parameters suggest carbonate source deposited in reducing environments for the oils.

The biomarker parameters show no evidence of molecular contribution from the Sargelu Formation to the oils in Taq Taq, but Tawke and Kirkuk oils show a molecular contribution from the Sargelu Formation.

TABLE OF CONTENTS

LIST OF FIGURES

LIST OF TABLES

LIST OF PLATES

LIST OF ABBREVIATIONS

Aj-8　　　　　Ajil-8

°API　　　　　degrees API gravity (American Petroleum Institute)

bbls　　　　　barrels

C, H, N, O, S　carbon, hydrogen, nitrogen, oxygen, and sulfur

cf.　　　　　　Latin word confer, meaning "compare"

cm　　　　　　centimeter

comm.　　　　communication

Corg.　　　　　organic carbon

CPI　　　　　carbon preference index

CV　　　　　canonical variable

D　　　　　　degrees

Eh　　　　　redox potential—a measure of the oxidizing or reducing intensity of the environment

GC　　　　　gas chromatography

GC-MS　　　gas chromatography-mass spectrometry

GP　　　　　genetic potential

HC　　　　　hydrocarbon

H/C　　　　　hydrogen to carbon ratio

HI　　　　　hydrogen index

H-1　　　　　Hawler-1

IIS　　　　　type 2 sulfur rich

K-109   Kirkuk-109

K-156   Kirkuk-156

K-247   Kirkuk-247

K-331   Kirkuk-331

L.   lower

M   minutes

M.   middle

Ma 10^6 years ago

MK-2   Makhul-2

O/C   oxygen to carbon ratio

OI   oxygen index

PCI   pyrolyzable carbon index

pers.   personal

pH   the negative logarithm of the hydrogen ion concentration: a measure of the
            acidity or alkalinity of a solution (acids, less than 7; bases, more than 7)

PI   production index

ppm   parts per million

ppt   parts per thousand

Pr/Ph   pristane to phytane ratio

QC-1   Qara Chugh-1

QC-2   Qara Chugh-2

Qu-2   Guwear-2

Ro   reflectance in oil immersion

S   seconds

S/C	sulfur to oxygen ratio
SEM	scanning electron microscope
S_1	the total free hydrocarbons
S_2	amount of hydrocarbon obtained by heating during pyrolysis (kerogen breakdown)
S_3	the amount of carbon dioxide (CO_2) released through heating organic matter
TA-3	Tawke-3
TA-4	Tawke-4
TA-15	Tawke-15
TT-1	Taq Taq-1
TT-6	Taq Taq-6
TT-7	Taq Taq-7
TT-8	Taq Taq-8
TT-9	Taq Taq-9
TOC	total organic carbon
T_{max}	highest temperature for generating a maximum amount of hydrocarbon during pyrolysis
U.	upper
V	vanadium
W-3	well number 3
W-19	well number 19
W-120	well number 120
W-421	well number 421
Zb-4	Zubair-4

$\delta^{13}C_{\text{aro.}}$ aromatic carbon 13 isotope

$\delta^{13}C_{\text{sat.}}$ saturate carbon 13 isotope

ACKNOWLEDGEMENTS

CHAPTER 1

INTRODUCTION

Northern Iraq lies within the northern part of the Zagros Folded Belt and is estimated to contain about 45 billion barrels (bbls) of Iraq's 115 billion barrels of oil reserves, making Iraq the sixth largest oil reserve in the world (Al-Zubaidi and Al-Zebari, 1998; Jassim and Al-Gailani; 2006; Hill and Shane, 2009).

The Middle Jurassic contains very significant source rocks over all southern, northeastern, and northern Iraq owing to the high total organic carbon (TOC) content of the Sargelu and Naokelekan formations that were deposited throughout the Jurassic basin that exists in these areas (Jassim and Al-Gailani, 2006). Only a few published studies exist on the stratigraphy and sedimentology of these source rocks so other information including TOC content, thermal maturation, and burial history are required for understanding the existence of other hydrocarbon resources (Pitman et al., 2003).

1.1   Objectives and Purpose

Relatively little work has been published on the correlation between the hydrocarbon types and the source rocks in Iraq (oil-source rock correlations). This study has several exploration objectives. The main objective is to determine the possible genetic relationships between crude oil samples from wells in the giant Kirkuk, Taq Taq, and Tawke oil fields and outcrop and subsurface samples of the Jurassic Sargelu Formation source rock. The outcrop and subsurface locations include: Sargelu village, Hanjeera village, Barsarin village, Gara Mountain, Tawke village, Banenan village, Guwear city, and Qara Chugh Mountain (Fig. 1.1). Source rock characterization of the Jurassic Sargelu was performed to determine if it is indeed the source for these large fields. The stratigraphy, paleogeography and sedimentology are important for the

proposed work. The study will include data on thermal maturity, TOC and Rock-Eval pyrolysis of kerogen in the Sargelu Formation to determine the source rock capability and kerogen type.

Other objectives include:

(1) define the lower and upper boundaries of the Sargelu Formation and determine the thickness of the Sargelu Formation for each location;

(2) correlate the lithofacies within the Sargelu Formation; and

(3) predict hydrocarbon migration pathways from the source units to the reservoirs in field.
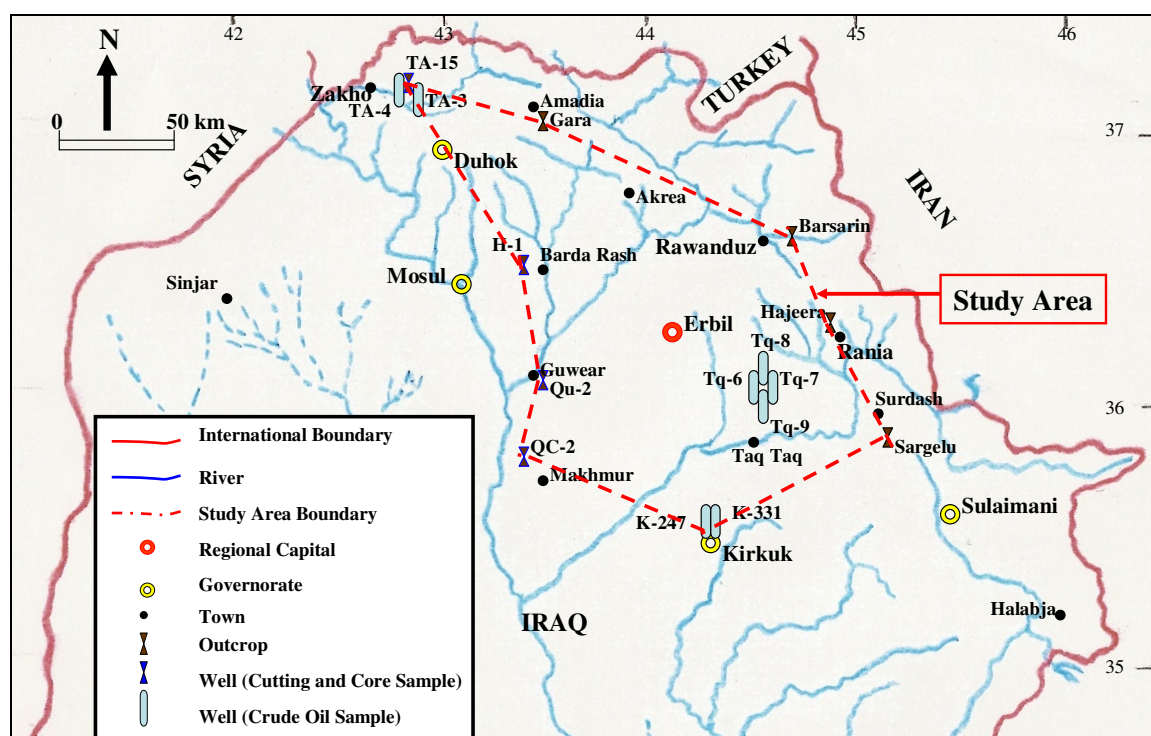
Figure 1.1: Map of northern Iraq showing the study area.

1.2   Study Area

This study focuses on the northern part of Iraq (Fig. 1.1) and includes four surface outcrops, four subsurface stratigraphic sections of the Sargelu Formation, and crude oil samples in eight wells from three fields (Table 1.1). All the outcrop sections and wells

are located in the High Folded and Foothill zones of the mountain front (Fig. 1.2).

The outcrops locations are:

(1) Sargelu village near Surdash town;

(2) Hanjeera village two km north west of Rania town;

(3) Barsarin village near Rawanduz in Balak valley; and

(4) Gara Mountain in Gali-Zewki south of Amadia.

The subsurface well sections are in:

(1) Tawke village east of Zakho town;

(2) Banenan village south of Barda Rash town;

(3) Guwear town near Great Zab River south east of the Erbil; and

(4) Qara Chugh northwest of Makhmur town.

The crude oil samples are from:

(1) Kirkuk Oil Field wells K-247 and K-331 in Kirkuk governorate, 250 km north of the capital, Baghdad. The Kirkuk region lies among the Pir Magrun (Gudrun) Mountains to the northeast, the Zab River and the Tigris River to the west, the Hamrin Mountains to the south, and the Sirwan (Diyala) River to the southeast;

(2) Tawke Oil Field wells TA-3 and TA-4 east of Zakho (TA-3 is located thirteen km east of TA-4); and

(3) Taq Taq Oil Field wells TT-6, TT-7, TT-8, and TT-9 located near Shiwashok village 60 km north of the Kirkuk Oil Field (TT-7 is located on south east plunge, TT-6 is located on north west plunge while TT-9 is located on north east limb and TT-8 is located on south west limb).

1.3   Methods

The data base for the study consists of both surface outcrop and subsurface well, cuttings sample, and fluid data. Field work on Sargelu outcrops was performed during the summer of 2009. A preliminary assessment of the stratigraphy was made by observing and describing outcrops in different parts of the area. The geometry of the sedimentary rock units and general relationships in each sequence were described. The selected

Table 1.1: Location names, tectonic zones, longitude/latitude, and number of samples that were collected from each locality for geochemical analysis.

Serial Number	Location	Tectonic Zones	Longitude			Latitude			Number of Samples
			D	M	S	D	M	S	
1	Qara Chugh-2	Foothill	43	34	39	35	46	35	5
2	Guwear-2	Foothill	43	29	44	36	2	52	8
3	Hawler-1	Foothill	43	35	2	36	30	7	5
4	Tawke-15	High Folded	42	46	47	37	7	55	6
5	Sargelu	High Folded	45	9	25	35	52	44	12
6	Barsarin	High Folded	44	39	18	36	37	13	7
7	Hanjeera	High Folded	44	51	52	36	17	8	5
8	Gara	High Folded	43	25	30	37	00	28	2
	Rock Samples					Subtotal			50
9	Taq Taq-6	Foothill	44	31	32	36	4	44	1
10	Taq Taq-7	Foothill	44	33	36	36	0	37	1
11	Taq Taq-8	Foothill	44	32	30	36	3	38	1
12	Taq Taq-9	Foothill	44	32	30	36	2	42	1
13	Kikuk-247	Foothill	44	24	36	35	28	12	1
14	Kirkuk-331	Foothill	44	27	29	35	28	12	1
15	Tawke-3	High Folded	42	47	49	37	7	60	1
16	Tawke-4	High Folded	42	45	48	37	8	3	1
	Crude Oil Samples					Subtotal			8
						Total			58
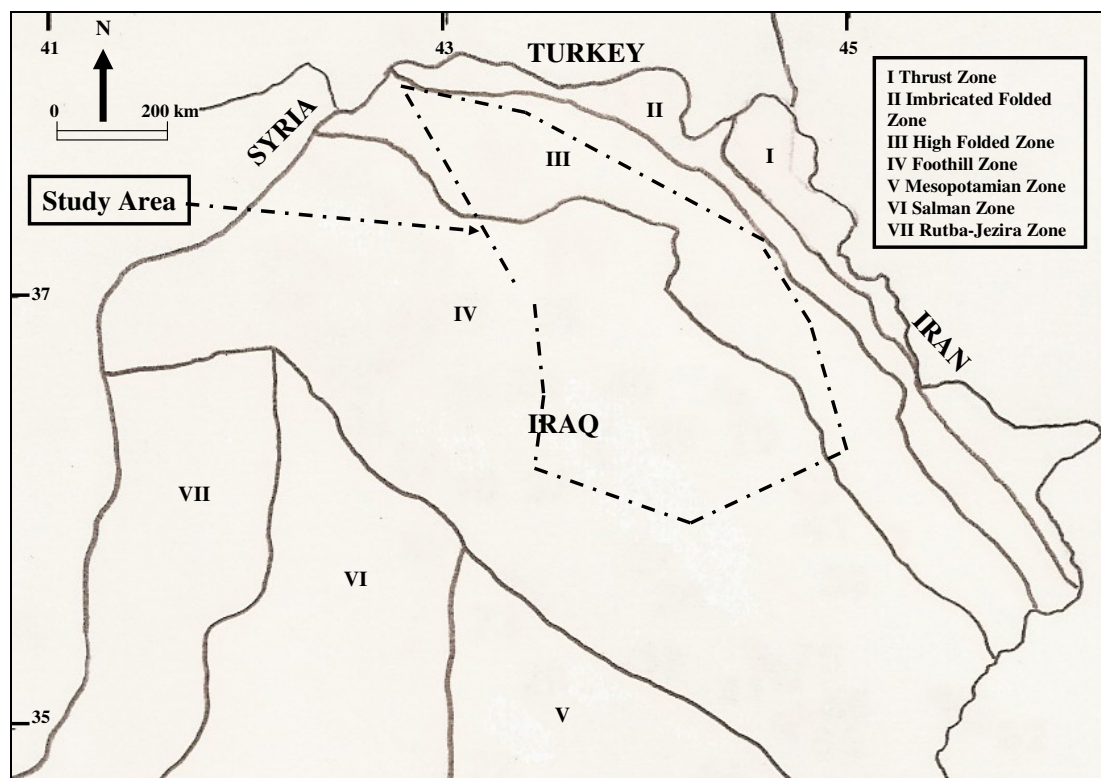
Figure 1.2: Tectonic zones of northern Iraq (redrawn after Buday, 1980; Ameen, 1992; Numan, 2000; Jassim and Buday, 2006a; Rasoul Sorkhabi, 2008).

outcrop sections have excellent sequences that reflect the main components of the depositional system.

The outcrop sections were measured from the base to the top of the Sargelu outcrops using a Jacob's staff and Brunton compass. The thickness, mineral composition, grain size, color, and sedimentary structures were recorded. Mineral composition was determined by hand specimen descriptions, petrographic thin sections, and scanning electron microscope (SEM).

The metric scale was used to measure sections. The true thickness was calculated for each outcrop separately. The thicknesses for some sections are approximate because of the steepness (inaccessibility) of the cliffs. The map scale for the measured sections is 1 cm equals 2 m while the horizontal scale for the measured correlation panel is 1 cm equals 3 km. Topographic maps were used to locate the outcrops, and photomosaic maps were taken to illustrate facies changes both vertically in each of the outcrops and laterally across the various outcrops.

Cutting samples were also collected from a number of wells. These cuttings were stored at the North Petroleum Company Office in Kirkuk and at the Geological Survey Office in Duhok. Because of Kurdistan Regional Government restrictions, seismic lines are restricted and not available for this study.

Crude oil samples were also collected in the summer of 2009 from eight wells in the Kirkuk, Taq Taq, and Tawke oil fields for organic geochemical analyses. Representative samples of source rocks were also collected at the outcrops in Sargelu village, Hanjeera village, Barsarin village, Gara Mountain, and in the wells in Banenan, Guwear, Qara Chugh, and Tawke.

Samples were submitted to GeoMark Research, Ltd. in Houston, Texas for organic geochemical analysis. The geochemical analyses included: (1) Rock Eval pyrolysis to identify the type and maturity of organic matter and to detect petroleum potential; (2) soxhlet extraction to remove the bitumen and to determine the major hydrocarbon fractions (saturates, aromatics, resins, asphaltenes) in which the elemental carbon, hydrogen, oxygen, nitrogen, and sulfur (C, H, O, N, S) composition was determined; (3) liquid chromatographic separation of crude oil to identify compound classes; (4) gas chromatography-mass spectrometry (GC-MS) to analyze biomarkers in petroleum; (5) trace metals; and (6) American Petroleum Institute (API) gravity.

To interpret these data, I used the guidelines presented in a class taken at Colorado School of Mines, Organic Geochemistry of Fossil Fuels and Ore Deposits (Curtis and Lillis, 2008, pers. comm.).

These combined source rock and oil data were used to:

(1) determine the amount of generated oil from the source rock;

(2) make source rock-oil ties; and

(3) establish reasonable migration paths.

1.4 Geologic Setting

The stratigraphy of Iraq is influenced by the structural position of the country within the Middle East area and the structure within the country itself (Al-Juboury, 2009)

1.4.1. Tectonic Evolution of the Area

The Arabian Plate was a part of Gondwana during much of the Paleozoic and Mesozoic eras. Late Precambrian suturing brought together a number of basic and dense volcanic and plutonic terranes to make the Arabian Plate (Haq and Al-Qahtani, 2005). Throughout Late Ordovician times, a glacial event occurred and affected the western part of the Arabian Plate. At that time, the Arabian Plate occupied a high southern latitudinal position. In the Early Silurian Period, the sea level rose due to deglaciation (Haq and Al-Qahtani, 2005).

The first main tectonic event that broadly affected the Arabian Plate was the Hercynian Orogeny (Haq and Al-Qahtani, 2005; Konyuhov and Maleki, 2006). The term Hercynian, or Variscan (Variscan is a term that refers to the European part of the Hercynian orogen), is generally used for Late Devonian to Permian diastrophic movements in Europe and North America (Wilson et al., 2004; Haq and Al-Qahtani, 2005). The Arabian Plate was extensively uplifted in the Carboniferous time by the Hercynian orogeny that caused a break and erosion of most Paleozoic sequences in the area (Ahlbrandt, 2000; Konyuhov and Maleki, 2006). In the Zagros Foothills, Devonian and Carboniferous rocks are completely missing due to the erosion related to this unconformity (Konyuhov and Maleki, 2006).

In the Early Permian Period, the Neo-Tethys Ocean began to open (Muttoni et al., 2009) (Fig. 1.3). In the Late Permian Period, the Arabian-Gondwana/Iranian-Laurasia supercontinent was fragmented due to crustal extension and rifted along the Zagros line to form the Neo-Tethys Sea by the Early Triassic time (Beydoun, 1991). In pre-Late Triassic time, the area was fairly stable. The facies of the Upper Triassic strata are noticeably different from older beds due to expansion of the Tethys Seaway as a result of movement of blocks in Turkey and northern and eastern Iraq and Iran (Sharief, 1981).

The opening of the Neo-Tethys took place in two stages. The first began when the Iranian Plate, or microplate, moved away from Arabian Plate toward the Eurasian Plate during the Permian and Triassic periods. The next stage occurred as the Neo-Tethys reached its maximum width of 4000 km during the Late Triassic to Middle Jurassic periods (Sadooni and Alsharhan, 2004) (Fig. 1.4).
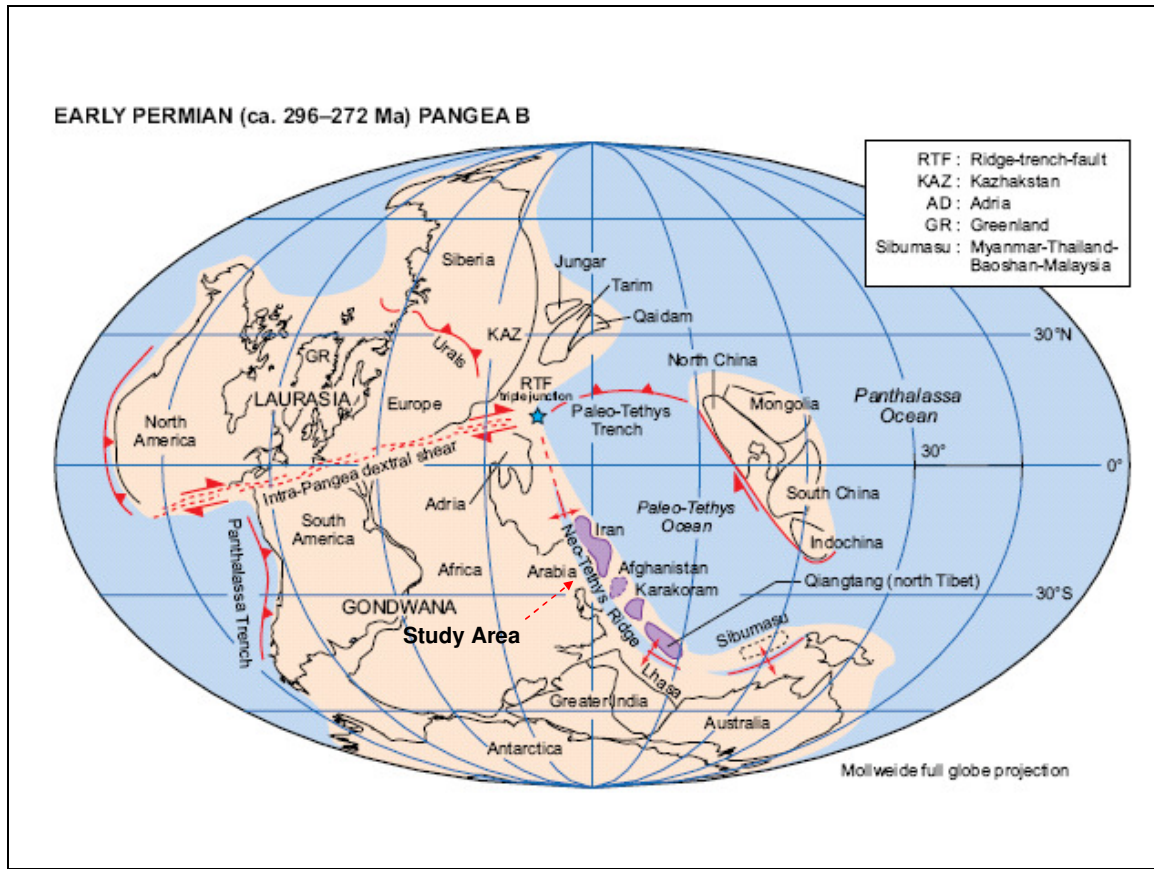
Figure 1.3: Opening of the Neo-Tethys Ocean during the Permian Period (Muttoni et al., 2009).

The Neo-Tethys started to close during the Cretaceous Period, creating a belt of junction from Turkey to Oman. This belt, Taurus-Zagros, was affected by low-relief folding and shear effects which extended to the rest of the platform area from Syria to Egypt (May, 1991). Accordingly, a foredeep next to the Tethys edge formed, following an ophiolite-radiolarite nappe emplacement from the north (Murris, 1980).

The collision of the continental segments of the Eurasian margin with the continental Arabian Plate created the Zagros Mountain as a result of subduction of the oceanic Arabian Plate crust under the Eurasian Plate (Beydoun et al., 1992). This continent-to-continent collision started during the late Eocene time and the junction continues at present (Beydoun et al., 1992).
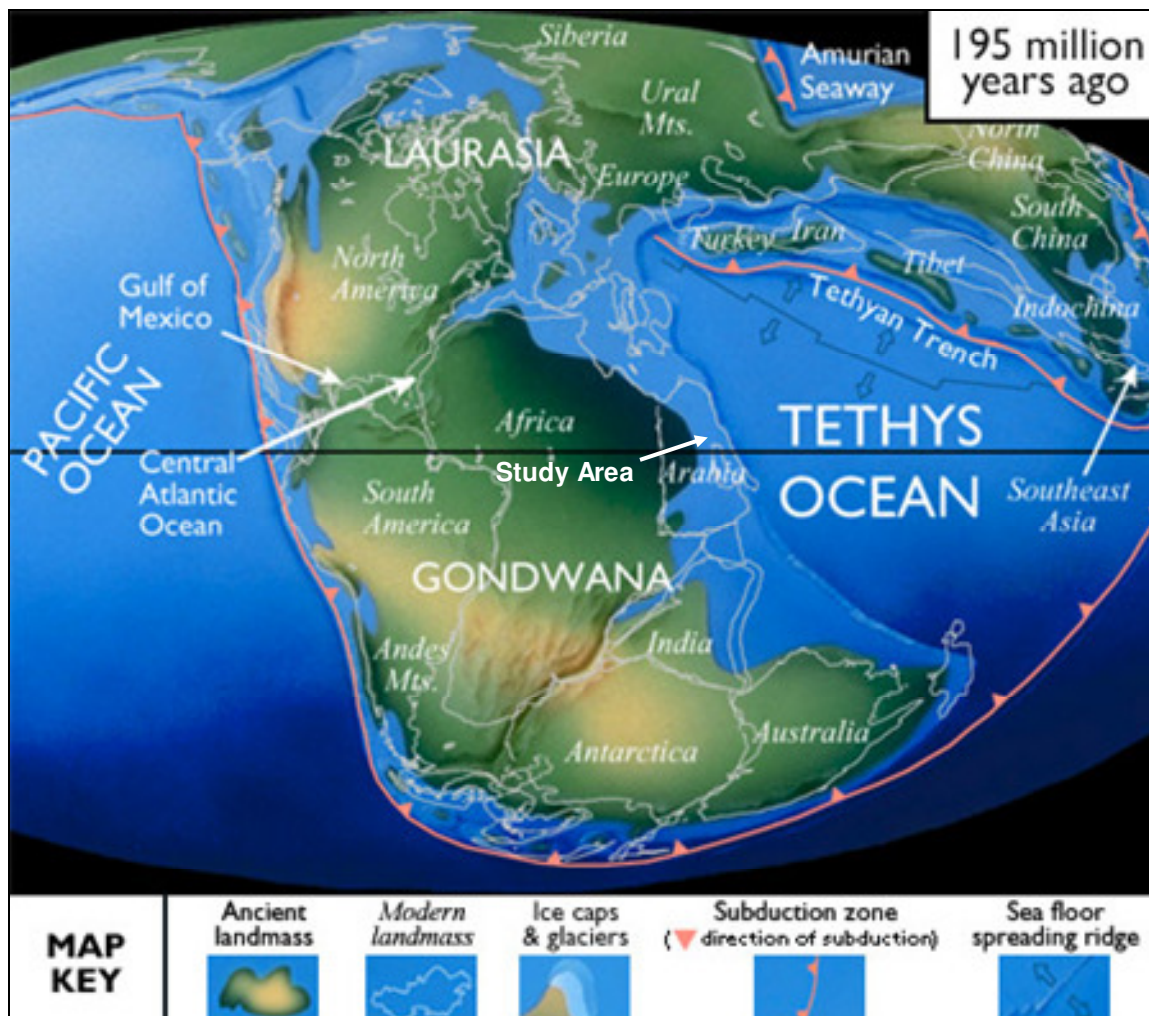
Figure 1.4: Paleo-plate reconstruction map of the Early Jurassic Period showing the well developed Tethys Seaway (Scotese Paleomap Project, Accessed January 19, 2010).

1.4.2   Structural Setting of the Area

The northern and northeastern parts of Iraq are a part of an Alpine mountain belt (Fig. 1.2). This belt has a northwest-southeast trend in northeastern Iraq and east-west direction in northern Iraq (Ameen, 1992) (Fig. 1.5, Plate Ia, and Plate Ib).

Two main zones can be recognized within the Taurus—Zagros belt: (1) the thrust zone; and (2) the folded zone (Fig. 1.2). The thrust zone is located next to the border between Iraq and Iran in the northeast and outside the border between Iraq and Turkey in
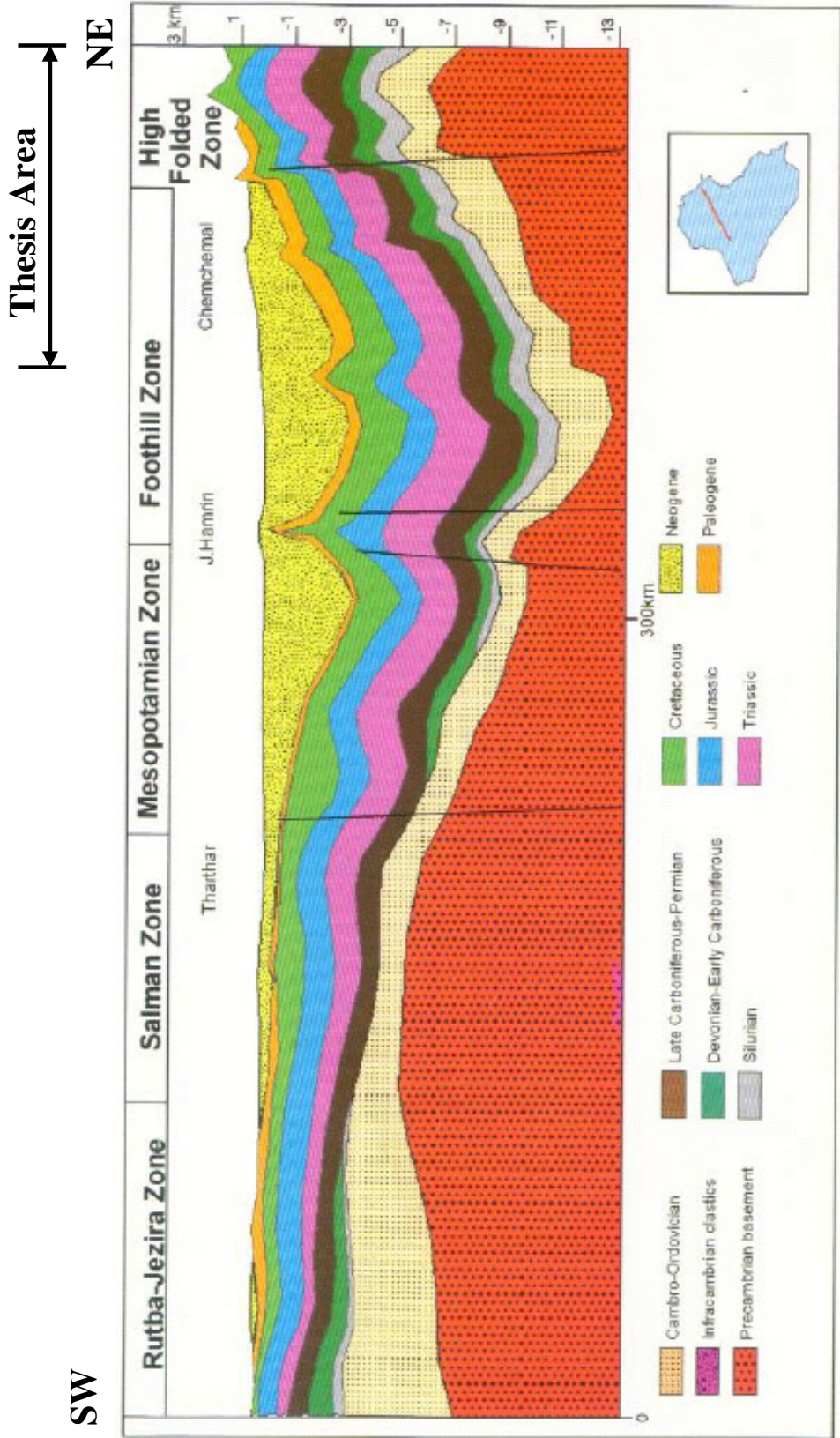
Figure 1.5: Cross section through central Iraq (NE-SW) passing through different tectonic zones showing the deepest basement in Iraq in the Foothill Zone (Jassim and Buday, 2006a).

the north (Buday, 1980; Ameen, 1992; Jassim and Buday, 2006a). According to Ameen (1992), the latter can be subdivided into two parts based on the intensity of folding. These are the imbricated (crushed) folds zone, which is extremely deformed and the simply folded zone which occurs as a less distorted smaller fold zone. The simple folded zone includes two additional subzones: the high folded (mountainous) zone, which consists of asymmetric anticlines and associated narrow synclines; and the foothills zone, which appears as comparatively small anticlines (Buday, 1980; Ameen, 1992; Jassim and Buday, 2006a).

The basement rocks in northern Iraq are broken into several blocks (Ameen, 1992) (Fig. 1.6). The Kirkuk and northern Mosul blocks are the main ones. The tectonic stability of the area stems from the activity of these fragmented pieces (Ameen, 1992).
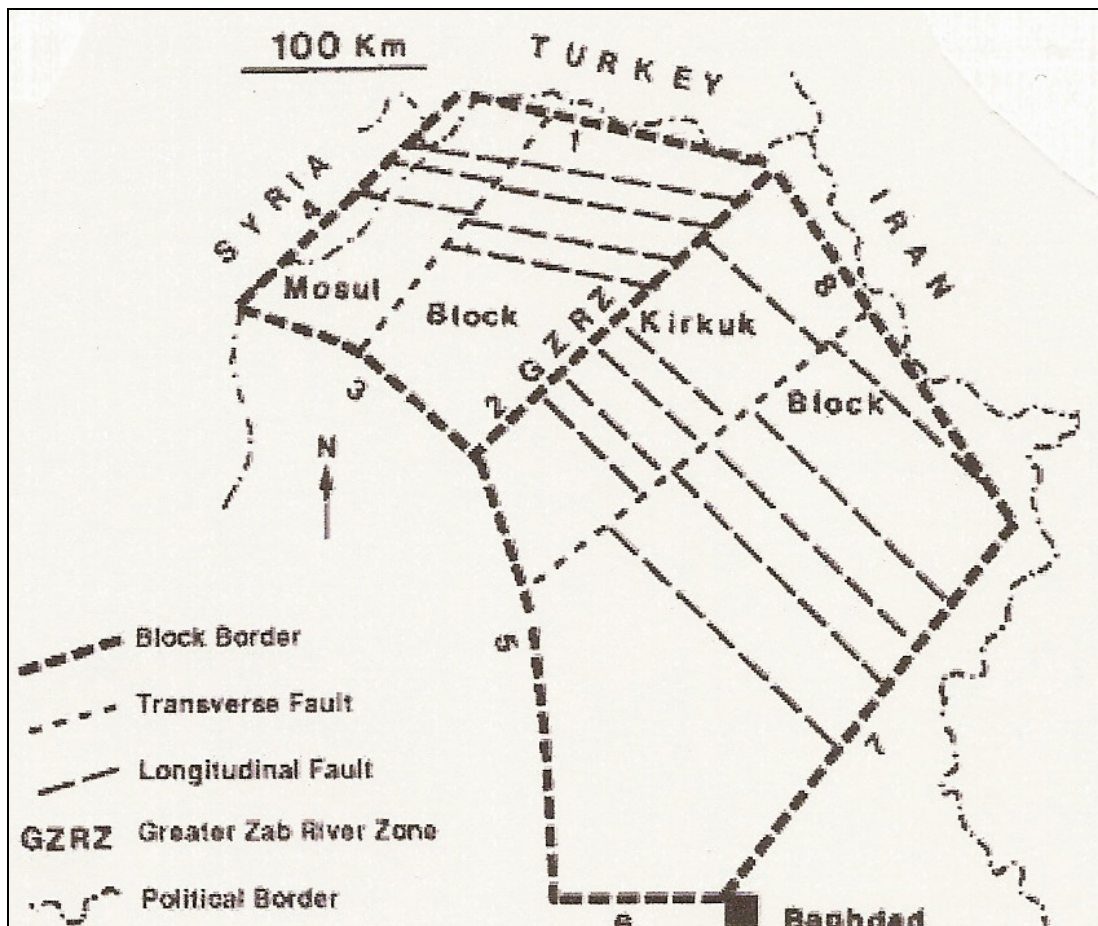
Figure 1.6: The regional basement tectonic pattern of northern Iraq showing the borders (lines 1-8) of the Mosul and Kirkuk blocks and the longitudinal and transverse faults which break the blocks into smaller subblocks (Ameen, 1992).

1.5   Previous Work

The reader is referred to the column in Figure 1.7 for the following remarks.

Period	Epoch	Age	Units		
			Foothill Zone		High Folded Zone
Jurassic	Late (Malm)	Tithonian	Gotnia		Barsarin
		Kimmeridgian	Najmah		Naokelekan
		Oxfordian			
	Middle (Dogger)	Callovian	Sargelu		
		Bathonian			
		Bajocian			
		Aalenian			
	Early (Liassic)	Toarcian	Alan		Sehkaniyan
		Pliensbachian	Mus		
		Sienmurian	Adaiyah		
		Hittangian	Butmah		Sarki

Figure 1.7: Geologic column of Jurassic succession in northern Iraq—not to scale (modified from Al-Omary and Sadiq, 1977; Al-Sayyab et al., 1982; Sadooni, 1997).

The Sargelu Formation on the Surdash anticline, Sulaimani district of the High Folded Zone in northeastern Iraq, was first recognized and described by Wetzel (1948). The sequence at Emam Hasan and at Masjed-e Suleyman in Iran was correlated by James and Wynd (1965) with the Adaiyah, Mus, Sargelu, Najmah, and Gotnia formations of Iraq, which were described and defined in the Lexique Stratigraphique International for Iraq by Bellen et al. (1959). Altinli (1966) and Dubertret (1966) compared the Sargelu Formation to the Cudi group of southern Turkey and to the black shale of the uppermost part of the Dolaa Group in Syria, respectively. Qaddouri (1972) studied the Sargelu Formation in the Benavi area in northern Iraq. Al-Omari and Sadiq (1977), in a general geological overview of northern Iraq, included the Sargelu Formation within the Middle

Jurassic.

Murris (1980), in his classic stratigraphic evolution and oil habitat study of the Middle East, identified various parts of the petroleum system in the Middle East including the Middle Jurassic. In a general review of the formation, Buday (1980) agreed with the original description given by Wetzel (1948) and interpreted the depositional environment as an euxinic marine environment. This interpretation was also accepted by Al-Sayyab et al. (1982). Ibrahim (1984) used local geothermal gradients in southern Iraq to calculate the time-temperature indices of Cretaceous, Jurassic, Triassic and Paleozoic source rock maturation. Al-Mashhadani (1986) discussed regional paleogeography of sedimentary basins during the Mesozoic and Cenozoic eras and the relationship with the geological system of Arabia. Another investigation of biostratigraphy and lithostratigraphy of Upper Triassic-Jurassic formations in Iraq was presented by Qaddouri (1986). Beydoun (1986) studied the oil migration and accumulation in conventional traps in general within the Middle East region. Moshrif (1987) investigated the sedimentary history and paleogeography of Lower and Middle Jurassic rocks in central Saudi Arabia; he stated that during the expansion of the Tethys Sea in Bajocian-Bathonian time, the Dhruma Formation (equivalent in age to the Sargelu Formation) was deposited. Al-Barzanji (1989) studied the Muhaiwir Formation in the Iraqi Western Desert, pointing out that this formation was deposited within the same sedimentary cycle in which the Sargelu Formation belongs. The more detailed study regarding the age and depositional environment of the Muhaiwir Formation was performed by Al-Hadithi (1989), who focused on the ostracods to estimate the age.

Bordenave and Burwood (1990) studied source rock distribution and maturation in the Zagros Orogenic Belt, a provenance of the Asmari and Bangestan Reservoir oil accumulations. They pointed out that the Sargelu Formation can be considered to be a good but not effective source rock due to isolation of its organically rich layers from good reservoirs by thick evaporitic layers. Outhman (1990) studied the generation, migration, and maturation of the Upper Jurassic-Lower Cretaceous hydrocarbons in northern Iraq, and identified the types of kerogen which are II and III that occurs in the Sargelu Formation. Beydoun et al. (1993) stated that the Sargelu Formation is a source rock that entered the oil generation phase at the end of Eocene. Al-Dujaily (1994) studied

the Middle-Upper Jurassic stratigraphic section in northern Iraq, and determined the age of the Sargelu Formation to be Aalenian-Bajocian. Ahmed (1997) described the sedimentary facies and depositional environments of Jurassic rocks in northwestern Iraq. The lower contact of the Sargelu Formation with Early Jurassic formations was described by Surdashy (1999) in his sequence stratigraphic analysis of the Early-Jurassic formations in central and northern Iraq.

Salae (2001), in a stratigraphic and sedimentologic study of the Upper Jurassic succession in northern Iraq, described the upper contact of the Sargelu Formation with the Naokelekan Formation. Al-Ahmed (2001) used palynofacies to indicate depositional environment and source potential for hydrocarbon of the Sargelu Formation in northern Iraq. Al-Kubaisy (2001) analyzed the depositional basin and evaluated petroleum of Middle-Upper Jurassic succession in northern Iraq. Abdullah (2001), in his preliminary evaluation of Jurassic source rock potential in Kuwait, indicated that most of the Jurassic succession is mature.

Fox and Ahlbrandt (2002) studied the petroleum geology and total petroleum systems of the Widyan Basin and interior platform of Saudi Arabia and Iraq. In the study, they stated that most of the petroleum is sourced from cyclically bedded Jurassic shales and carbonates. Pitman et al. (2003) investigated the generation and migration of petroleum in Iraq and stated that Jurassic marine shales and carbonates are the major sources of hydrocarbons produced in the Zagros Basin and Fold Belt. Alsharhan and Nairn (2003) studied sedimentary basins and petroleum geology of the Middle East, and included the Sargelu Formation within the Middle Jurassic. Balaky (2004) studied the stratigraphy and sedimentology of the Sargelu Formation in three localities in Iraqi Kurdistan. He divided the Sargelu Formation into four main lithofacies and investigated a variety of diagenetic processes.

Erik et al. (2005) studied the Cudi Group in the eastern part of southeast Turkey. The Sargelu Formation is equivalent to the upper part of this group. The oils in six oilfields in the Persian Gulf were studied by Rabbani and Kamali (2005). The oil in these oilfields was found to come from Mesozoic and Tertiary source rocks. Abboud et al. (2005) geochemically correlated oils and source rocks from central and northeastern Syria. They found two oil families which were generated by different source rock types

of different ages. Alsharhan and Habib (2005) studied organic matter and maturation of the Sargelu Formation in southern Iraq. Al-Ameri et al., (2006) classified oils in the northern and central part of Iraq into two subfamilies. In the same way, Al-Ahmed (2006) recognized two types of facies in source rock samples and two subfamilies of carbonate Jurassic oils in the middle and northern part of Iraq. Jassim and Buday (2006b) stated that the age equivalent of the Sargelu Formation is the lower part of the Surmeh Formation of southwestern Iran and the Dhruma Formation of Saudi Arabia. Jassim and Al-Gailani (2006) studied hydrocarbons of all geological times including petroleum from the Jurassic Period.

Al-Ameri et al. (2008) studied the stratigraphic section between the Alan Anhydrite and Lower Fars formations in northeastern Iraq. The study showed that the Sargelu Formation has no molecular contribution to the oil found in the Jeribe Formation. Al-Ameri et al. (2009) studied the hydrocarbon potential of the Middle Jurassic Sargelu Formation in the Zagros Fold Belt from exploratory wells and outcrops in northern Iraq. They found that the Middle Jurassic Sargelu Formation contains abundant oil-prone organic matter. They also concluded that generation and expulsion of oil from the Sargelu began and ended in the late Miocene time.

CHAPTER 2

STRATIGRAPHY

2.1   Stratigraphy

        The Sargelu Formation is underlaid by either the Sehkaniyan or Alan formations

and is overlaid by the Najmah or Naokelakan formations (Fig. 1.7 and Plate IVb).

2.1.1   Formations Underlying Sargelu

        The Sehkaniyan Formation at its type locality is comprised from the base to the

top of:

(1) dark dolomites and dolomitic limestones with some solution breccias;

(2) fossiliferous limestones, repeatedly dolomitized with some chert bands that become

more common near the top; and

(3) dolomitic limestones and dark, fetid, saccharoidal dolomites, locally with chert

interbeds (Wetzel and Morton, 1950b; Al-Omari and Sadik, 1977; Buday, 1980; Al-

Sayyab et al., 1982; Alsharhan and Nairn, 2003; Jassim et al., 2006).

        In the Rania area, the formation is composed only of dark dolomites (Buday,

1980; Jassim et al., 2006). The formation shows both lagoonal evaporitic and euxinic

conditions in the lower part and in the middle and upper parts, respectively (Buday,

1980). The formation is comparable to the Alan-Mus-Adaiyah formations of the Foothill

Zone (Surdashy, 1999; Alsharhan and Nairn, 2003).

        The Alan Formation at its type section comprises bedded anhydrites with

secondary pseudo-oolitic limestones. The thickness of the formation varies significantly

laterally (Dunnington, 1953a; Buday, 1980; Jassim et al., 2006). In some localities, the

presence of halite is observed (Alsharhan and Nairn, 2003). The Alan Formation is

superlatively developed in the Foothill Zone in the southern and western part of Iraq. The formation was deposited in a sabkha environment (Buday, 1980; Jassim et al., 2006).

2.1.2 Formations Overlying Sargelu

The Najmah Formation at its type locality is comprised from the base to the top of:

(1) fine-grade, dense, recrystallized limestone;

(2) oolitic and pseudo-oolitic limestones with macrofossil fragments;

(3) coarse grainy dolomite with bulky crystals of dolomite; and

(4) feathery textured limestone and thin anhydrite.

In some localities, a thin division of limestone and black shale is found in the lower part (Dunnington, 1953c; Al-Omari and Sadik, 1977; Buday, 1980; Al-Sayyab et al., 1982; Jassim and Buday, 2006b). The formation was deposited under neritic conditions for the most part and restricted lagoonal influences appear on other parts (Buday, 1980).

The Gotnia Formation is comprised of anhydrite; brown calcareous shales; black bituminous shales; and recrystallized limestones at its type section (Dunnington, 1953b; Al-Omari and Sadik, 1977; Buday, 1980; Al-Sayyab et al., 1982; Jassim and Buday, 2006b). The formation was deposited in a hypersaline lagoonal environment (Alsharhan and Nairn, 2003).

The Najmah Formation intertongues laterally with the Gotnia Formation. The interfingering appears to be in the Kirkuk division (Buday, 1980; Alsharhan and Nairn, 2003; Jassim and Buday, 2006b). Presently, the location of the boundary of the Najmah Formation is inadequately determined but may overlap with the Duhok-Chemchemal Paleo-uplift (Ditmar et al., 1971). This, on the other hand, conflicts with the existence of the assumed Naokelekan and Barsarin formations in K-109 Well. A 307 meter thick unit in well K-109 was assigned to the Barsarin Formation with a thickness of 283 m and Naokelekan Formation with a thickness of 24 m (North Oil Company, 1953; Al-Habba and Abdullah, 1989; Petroleum Geological Analysis, 2000; Lewan and Ruble, 2002;

Ahmed, 2007; Mohyaldin and Al-Beyati, 2007; Mohyaldin, 2008). Consequently, the interfingering between Najmah and Gotnia formations is more plausible than between the Naokelekan and Barsarin formations in the Kirkuk division (Buday, 1980; Jassim and Buday, 2006b). A few unexpected meters of shaly beds may belong to other (for example Najmah or Sargelu) formations (Buday, 1980). The age equivalent units to Najmah and Gotnia formations, in the High Folded and northern Thrust zones, are the Barsarin and Naokelekan formations (Alsharhan and Nairn, 2003). The Najmah Formation is transitional to the north with the argillaceous and condensed basinal Naokelekan Formation (Buday, 1980).

The Naokelekan Formation at Naokelekan village (type locality) is comprised of three units from the base to the top of:

(1) a thin-bedded, extremely bituminous dolomite and limestone with intercalated black shale;

(2) a thin-bedded, bluish, hard, fossiliferous dolomitic limestone; and

(3) a laminated argillaceous bituminous limestone alternating with shaly limestone (Wetzel and Morton, 1950a).

The formation was deposited in brackish lagoon and shallow open marine environments (Salae, 2001). Al-Sayyab et al. (1982) and Jassim and Buday (2006b) also described the type section but they have reversed the sequence.

2.2   Sargelu Formation

The stratigraphic studies of the Sargelu Formation can be summarized in the following sections.

2.2.1   Areal Distribution

The Sargelu Formation is characterized by broad geographic distribution in Iraq and surrounding countries. In Iraq, this formation occurs on the surface in several

localities including: (1) Northern Thrust Zone; (2) High Folded, Balambo—Tanjero tectonic zones; and (3) within the Qulqula—Khwakurk tectonic zones. It exists all over Iraq with the exception of the Rutba Subzone, in western Iraq south of the Euphrates River, where it is transitional into the Muhaiwir Formation (Buday, 1980; Jassim and Buday, 2006b). The formation outcrops at many localities other than the measured sections of this study, including Sirwan, Sehkaniyan, Qal'Gah, Naokelekan, Kurrek, Rawanduz, Ru Kuchuk, Isumaran, Ser Amadia, Ora, Chalki, Shiranish, Banik and also occurs in many subsurface wells (Wetzel, 1948).

The Sargelu Formation is comparable in age to some stratigraphic units in surrounding countries. These units are: the Dhruma Formation of Saudi Arabia; the uppermost part of the Dolaa Group in northeastern and in central Syria; the upper parts of the Cudi Group of southeastern Turkey; and the lower part of the Surmeh Formation of southwestern Iran (James and Wynd, 1965; Altinli, 1966; Dubertret, 1966; Buday, 1980; Jassim and Buday, 2006b) (Figs. 2.1 and 2.2).

2.2.2   Formation Contacts

Eight localities were chosen for the present study, including four outcrops (Sargelu village, Hanjeera village, Barsarin village, and Gara Mountain) and four subsurface wells (TA-15 in Tawke area, H-1 in Banenan village, Qu-2 in Guwear town, and QC-2 in Qara Chugh Mountain northwest of Makhmur).

In all outcrop sites and the TA-15 Well, the Sargelu Formation is underlain by the Sehkaniyan Formation. Because of partial dolomitization, the position of the lower boundary is doubtful at the type locality (Buday, 1980), but Sehkaniyan's dark brownish color in outcrop exposures is an important feature for recognizing the Shehkaniyan Formation in the field (Al-Omary and Sadik, 1977; Balaky, 2004). Regularly, the lower contact is gradational and conformable in northern and northeastern Iraq (Buday, 1980; Jassim and Buday, 2006b). This contact occurs below massive to bedded, blue on weathering, cherty, brittle, laminated limestones that belong to the Sargelu Formation and above the massive, dark brown on weathering, dolomitic limestone of the Shehkaniyan

Formation (Balaky, 2004). A petrographic study shows no detectable changes between these two units (Shehkaniyan and Sargelu formations) due to increased dolomitization affecting them both (Salae, 2001; Balaky, 2004). In the Gara locality, minor variations are observed in the absence of a massive interval of dolomitic limestone near the base of the Sargelu Formation and in the presence of some bitumen pockets (Balaky, 2004).

The lower contact of all subsurface sections is rather clear cut and is defined by the last occurrence of anhydrite at the top of the Alan Formation. It is conformable and
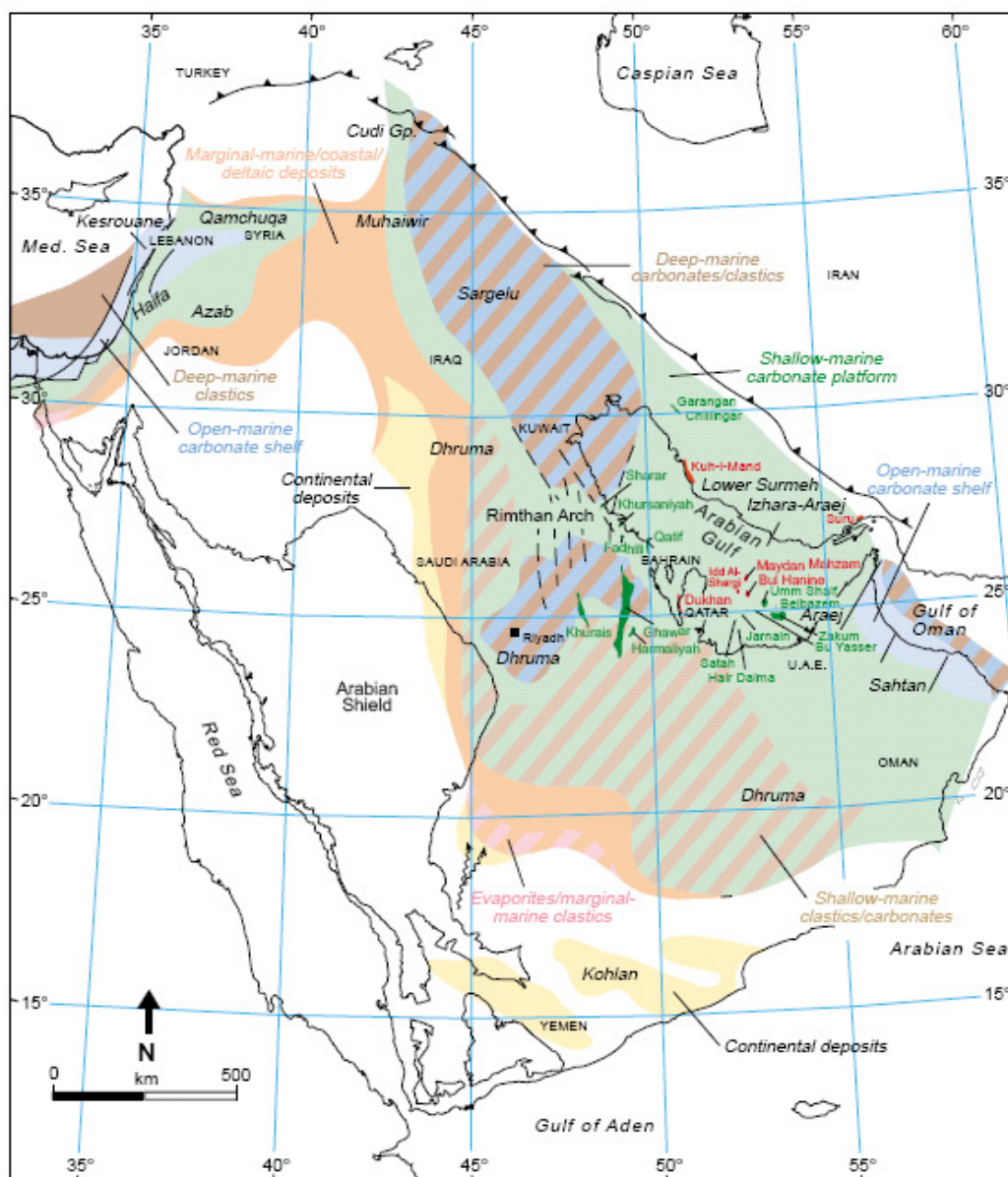
Figure 2.1: Paleofacies of the Middle Jurassic Sargelu Formation (Ziegler, 2001).
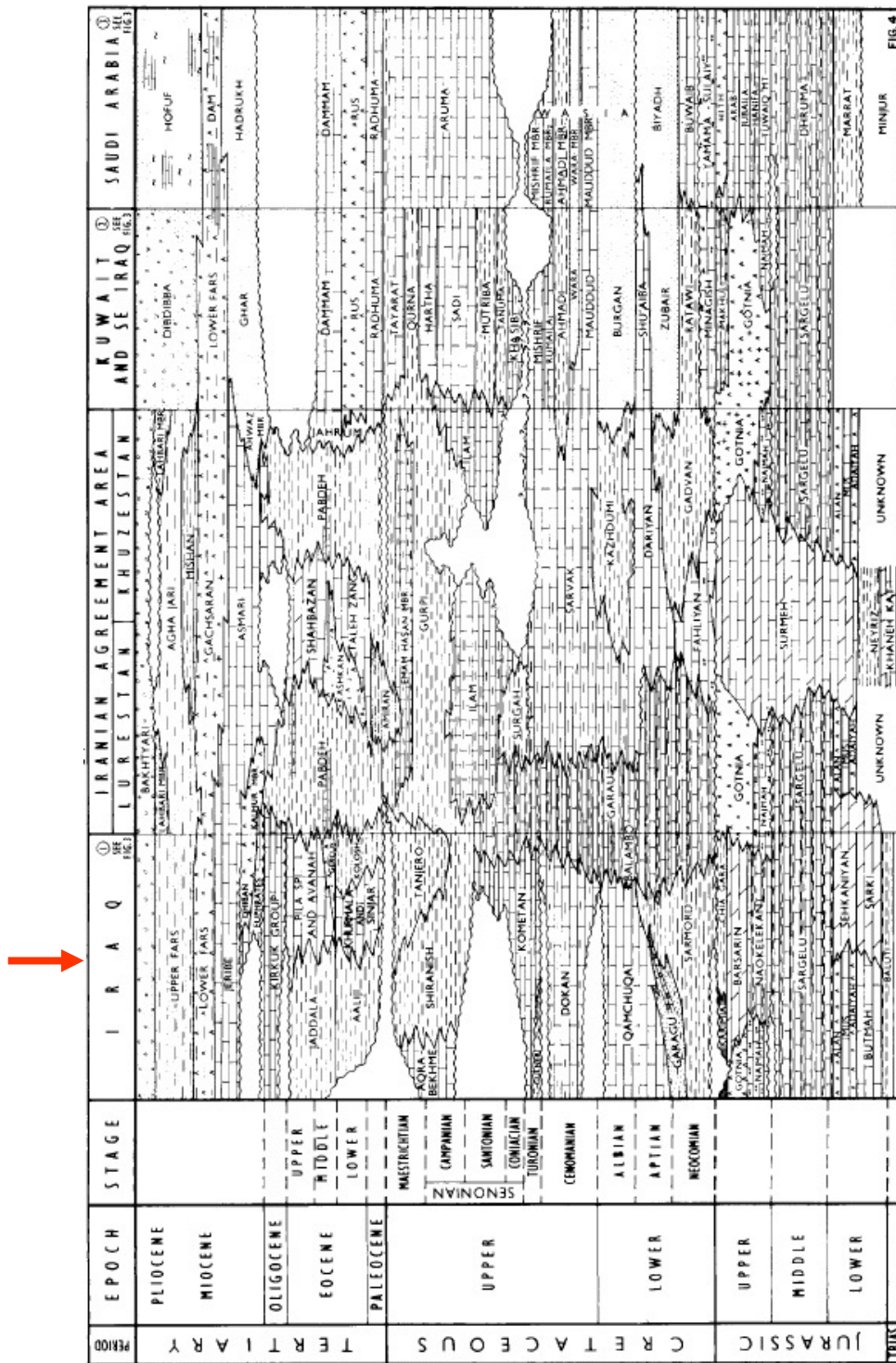
Figure 2.2: Mesozoic stratigraphy in Iraq (arrow) in relation to other Middle East countries (James and Wynd, 1965).

gradational.

In all the outcrop sites and the TA-15 Well, the Sargelu Formation is overlain by the Naokelekan Formation. In the Northern Thrust, Imbricated, and High Folded zones, the recognition of the upper contact of the formation is more difficult. This is due to vagueness between the shale of the Sargelu Formation and lower units of the overlying Naokelekan; thus, the change is assumed to be gradational (Buday, 1980). The upper boundary of the Sargelu can be found within a basically analogous thin-bedded limestone sequence. The lack of chert and abundant *Posidonia* and ammonites distinguishes the Sargelu Formation from the overlying Naokelekan Formation (Wetzel, 1948; Salae, 2001; Balaky, 2004). Moreover, the exceedingly bituminous and typically distorted nature of the bed is identifiable from the Sargelu Formation (Wetzel, 1948). At the Gara section, a similarity is observed between limestones from the upper part of the Sargelu and lower part of the Naokelekan formations (Balaky, 2004). The upper Sargelu Formation, at the Hanjeera village locality, is analogous to that of the Barsarin village locality and is characterized by the abundance of solution collapse breccia (Salae, 2001).

The upper boundary of the Sargelu with the Najmah Formation in the examined subsurface sections is unconformable. This contact occurs at the top of dark grey, dolomitized, calcareous shales which contain *Posidonia* that belong to the Sargelu Formation and at the base of light grey limestones with pseudo-ooliths that are moderately hard and belong to the Najmah Formation (Wetzel, 1948).

The Callovian break is a well-known break at the upper boundary of the formation all over western and southwestern Iraq where sufficient uplift occurred (Buday, 1980; Marouf, 1999; Balaky, 2004). In subsurface sections, north and west of Mosul, considerable amounts of the Middle Jurassic succession, including the Sargelu Formation and the entire sequence of the Upper Jurassic and Berriasian rock succession, are absent (Wetzel, 1948; Ameen, 1992). In this area, the Sargelu Formation is overlain by Aptian (or Albian?) Sarmord Formation and appears to be eroded. The total number of eroded beds is different throughout the area (Wetzel, 1948). The Callovian break is reported at western Khuzestan and Lurestan in Iran (Setudehnia, 1978). Similarly, this disconformity was confirmed at Emam Hasan and at Masjed-e Suleyman in Iran (James and Wynd, 1965).

2.2.3   Age

The ages of the underlying Upper Sehkaniyan and Alan formations are not determined on faunal evidence. Age is determined based on the stratigraphic position and relationship to other (Mus and Middle Sehkaniyan) formations. Determination of the Toarcian age for the upper part of the Sehkaniyan and Alan formations is based on their position between the Pliensbachian Mus and Middle Sehkaniyan formations and the Sargelu Formation (Surdashy, 1999).

The ages of the overlying Najmah and Naokelekan formations have been determined based on their fossil content which has been found to be Middle Callovian-Kimmeridgian and Early Callovian-Kimmeridgian (Buday, 1980; Jassim and Buday, 2006b, respectively).

The lower boundary is gradational, conformable, and unidentifiable, which is represented by gradual facies that change from brownish dolomitic limestone to bluish dolomitic limestone. The upper part of the Sargelu Formation represents shallow facies. There is no evidence for nonconformity at the lower and upper boundaries. The marine transgression led to a facies change at the beginning of Late Toarcian megasequence, thus, the Late Toarcian-Late Bathonian age for the Sargelu Formation was determined by Wetzel (1948), Al-Omari and Sadiq (1977), Buday (1980), Al-Sayyab et al. (1982), Qaddouri (1986), Alsharhan and Nairn (2003), and Jassim and Buday(2006b). This age, avoids all other assumptions, such as those offered by Qaddouri (1972), Al-Dujaily (1994), Surdashy (1999), Al-Ahmed (2001), Balaky (2004), Peters et al. (2005b), and Zumberge (2010, pers. comm.) including Bajocian, Aalenian-Bajocian, Aalenian-Bathonian, Aalenian-Bathonian, Late Bathonian-Early Callovian, Bajocian-Callovian, Bajocian-Bathonian, respectively.

The age-equivalent formation for the upper Sargelu Formation in Iraq is the Muhaiwir Formation, which Wetzel (1951) dated as Bathonian, as did Al-Sayyab et al. (1982), Alsharhan and Nairn (2003), and Jassim and Buday (2006b). Al-Hadithi (1989) dated it as Bathonian-Callovian.

2.2.4   Thickness

The thickness of the Sargelu Formation is variable (Fig. 2.3). The thickness of the formation in the Northern Thrust, Imbricated, and Simply Folded zones has a range from 20 m in northwestern Iraq (Ora and the Chalki region) to 125 m in northeastern Iraq in the Sirwan valley near Halabja. It is 115 m thick at the type locality (Wetzel, 1948; Buday, 1980; Balaky, 2004; Jassim and Buday, 2006b). In the Foothill Zone, the thickness is significantly high and has a range between 250–500 m (Ditmar et al., 1971; Buday, 1980; Jassim and Buday, 2006b). The thickness of the Sargelu Formation in the Iran (Lurestan, Khuzestan) area is 152–213 m, and in Kuwait has a range between 75–83 m, in Burgan and Umm Gudair, respectively (James and Wynd, 1965; Jassim and Buday, 2006b).

The thickness of the Sargelu Formation of 110 m and 148 m at type locality that Al-Sayyab et al. (1982) and Al-Ahmed (2006) reported, respectively, was not confirmed during my field investigation. This discrepancy could result from (1) not determining the boundaries properly or (2) counting the folded part in the lower part of the formation without taking repetition into consideration.

The thickness of the Sargelu Formation from Dunnington' (1955) Middle Jurasic-facies map was not confirmed by my field observations in Barsarin, Gara, and Hanjeera. Similarly, the newly drilled wells in northern Iraq, such as in the Zakho and Hawler areas where Jurassic formations were penetrated, are shown to have different thicknesses than those offered in the mentioned isopach map. In the same way, the thickness of the Sargelu Formation in Tawke, Guwear, Qara Chugh, Hawler, Gara, Barsarin, Hanjeera from the isopach contours map drawn by Pitman et al. (2004) was not confirmed by the data I obtained from the field nor by those from newly drilled wells. In the same way, the thickness of the formation in the Late Toarcian–Early Tithonian Megasequence map performed by Jassim and Buday (2006b) was not confirmed by the thickness of the formation in Hawler and Tawke which was obtained from the newly drilled wells.
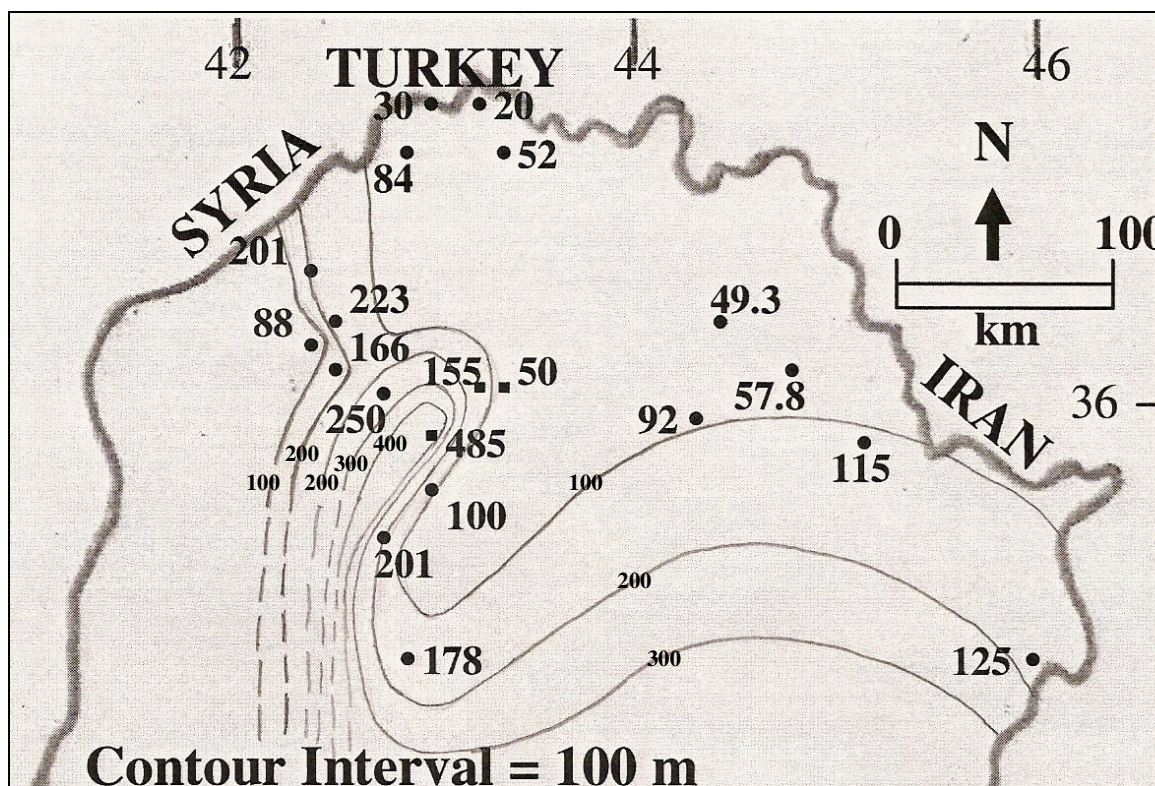
Figure 2.3: Isopach map for the Sargelu Formation. The data from Wetzel (1948); Jassim and Buday (2006b), Duhok Geological Survey (2009, pers. Comm.), North Oil company (2009, pers. Comm.), and measured outcrops within this Study.

2.2.5   Lithology

The lithological composition of the Sargelu Formation is very consistent and can be correlated over a distance of more than 350 km (Buday, 1980). The correlation of lithofacies among the studied sections of the Sargelu Formation in northern Iraq is shown in Plate VII. The facies is uniform throughout, inspite of the thickness changes. It is comprised of thin-bedded, black, bituminous limestones, dolomitic limestone, and black papery shales with streaks of thin black chert in the upper parts. The Sargelu Formation also includes the succession of thin-bedded, calcareous-argillaceous sediments (Wetzel, 1948; Buday, 1980; Balaky, 2004; Jassim and Buday, 2006b).

In most outcrops, a comparable lithology is expected. Subsurface sections contain a higher proportion of shale, and a sandy admixture has occasionally been found towards

the west (Buday, 1980; Jassim and Buday, 2006b). The formation is rich in fossils in both surface and subsurface sections.

Generally, the depositional environment was anoxic; however, some layers show either shallowing or a higher degree of oxygenation. The shallower environment occurred mainly to the western part of Iraq (Buday, 1980; Alsharhan and Nairn, 2003). In the Hanjeera section, the upper part noticeably contains detrital limestone. According to Wetzel (1948), at Ru Kuchuk in northeast Barzan town, the lower part is obviously silty and contains plant impressions. The detailed lithological composition of the Sargelu Formation in different localities is shown in Plates II, III, IVa, V, and VI.

2.2.6   Depositional System and Depositional Environment

The Sargelu facies consist of argillaceous-lime mudstone/wackestone/packstone, including a diverse open marine biota. Read (1985) describes the following as a characteristic facies of the deeper depositional system "Deeper ramp argillaceous lime packstone/mudstone, containing open marine, diverse biota, whole fossils, nodular bedding, upward-fining storm sequences, and burrows." A sandy admixture towards the west indicates that the ramp was proximal to land that emerged west of Iraq (Buday, 1980; Alsharhan and Nairn, 2003; Jassim and Buday, 2006b). Towards the northeast, the silty admixture was also observed at Ru Kuchuk northeast of Barzan town near the Great Zab River. At Ru Kuchuk, the *Posidonia-* and chert-bearing unit from the lower part of the Sargelu is noticeably silty, and plant impressions of the *Bradyphyllum-Pagiophyllum* group, cf. *Pagiophyllum expansum* (Feistmantel) has been observed (Wetzel, 1948). At the same time, the Sargelu Formation in the Sabriyah Structure in Kuwait is comprised of packstone facies deposited in the middle ramp (Khan et al., 2009).

Deposition during the Middle Jurassic Period continued throughout the same basin that was present during the Early Jurassic time. The basin was subsiding rapidly because of the instability of the Mosul Block. This subsiding and instability supports the idea that a wider deeper basin, or subduction zone, opened between the Mesopotamian and the area east of the Mediterranean Sea during deposition of the Sargelu Formation

(May, 1991; Ameen, 1992; Beydoun, 1993; Surdashy, 1999). The thickness variations indicate that the entire subsidence attained a few tens of meters, but the presence of oxygenated conditions suggest that the basin did not have considerable depths (Alsharhan and Nairn, 2003).

The basin's depositional center during the Middle Jurassic time was located in the northwest at Mosul near the Butma and Ain Zala oil fields (Al-Omari and Sadiq, 1977). The thickness of the Sargelu Formation at the northwestern Tigris River near Mosul is high and contains marine fauna (Fig. 2.3). This setting reflects the ramp depositional system. In this system, the deeper ramp receives less sediment with a higher percentage of preserved organic matter.

During the Middle Jurassic Period, the carbonate ramp existed as a part of an enormous marine platform. The southern and western parts of the shallow sea received detrital sediments and were laterally graded into carbonates (Alsharhan and Magara, 1994).

Overall the Sargelu Formation deposited in a marine basin and represents deeper ramp (Balaky, 2004). The organic-rich sediments of the Sargelu Formation indicate euxinic (anoxic) condition. The preservation of siliceous and lipid-rich organic material requires such an anoxic environment (Ormiston, 1993; Wever and Baudin, 1996).

2.3   Paleogeography

During the Jurassic time, shallow seas that showed cyclic fluctuations in level covered most parts of the Middle East region (Fig. 2.4). The major variations in the sedimentological facies occurred because of transgressions and regressions that were comparatively small in terms of absolute sea level change (Alsharhan and Nairn, 2003).

Near the end of the Late Toarcian time, moist climate caused the disappearance of evaporites as a transgression covered isolated basins and created more consistent basins (Murris, 1980; Buday, 1980; Jassim and Buday, 2006b).

During the Doggerian time, the Neo-Tethys attained maximum width (Numan, 1997). However, the renewed rifting next to the northeastern boundary of the Arabian

Plate within the Neo-Tethyan Ocean affected the region (Jassim and Buday, 2006b). Moreover, the existence of a ridge area, in the farthest northeast, during this time frame affected the distribution of sedimentological facies (Buday, 1980). The Mid-Late Jurassic Megasequence was deposited during such a segregation period (Jassim and Buday, 2006b). The Neo-Tethys attained maximum width in the Bajocian-Bathonian time. During this time frame, the sediments were deposited within comparatively deep water basin (Numan, 1997; Jassim and Buday, 2006b).

The neritic Muhaiwir Formation represents the base of the megasequence in the Rutba Subzone of western Iraq and the euxinic Sargelu Formation elsewhere in Iraq. The west side of the Salman Zone represents the edge between the two formations (Jassim and Buday, 2006b).

According to Balaky (2004), the Sargelu Formation is geographically distributed in a northwest-southeast trend. The Sanandaj—Sirjan block in western Iran represents the eastern shoreline of the sea and the edge of Rutba-Jazera zone represents the western shoreline (Jassim and Karim, 1984; Balaky, 2004).

A Late Toarcian-Callovian Sequence is included within a Megasequence of the Late Toarcian-Tithonian (Mid-Late Jurassic) (Buday, 1980; Jassim and Buday, 2006b). The end of this subcycle is represented by a regional regression above the Sargelu Formation (Buday, 1980). The Kimmerian tectonic activity (related to the break-up of Pangea) was occurring in the internal part of the Alpine Geosyncline, which caused the end of this subcycle (Buday, 1980; Alsharhan and Nairn, 2003). This movement has clear influence on the reduced thickness of the Sargelu Formation throughout the north and northeastern parts of Iraq (Fig. 2.3). In the same way, this tectonic activity affected the Doggerian sequence in western Iran and southeastern Turkey, and this succession is missing in both areas (Altinli, 1966; Furst, 1970; Buday, 1980).

During the Late Jurassic time, the tectonic movements preceding the opening of the southern Neo-Tethys controlled the paleogeography (Fig. 2.5). A cyclic segregation of the intra-shelf basin from the Neo-Tethys occurred due to the subsidence variation range. During the Late Kimmeridgian-Early Tithonian time, an evaporitic basin existed (Jassim and Buday, 2006b).
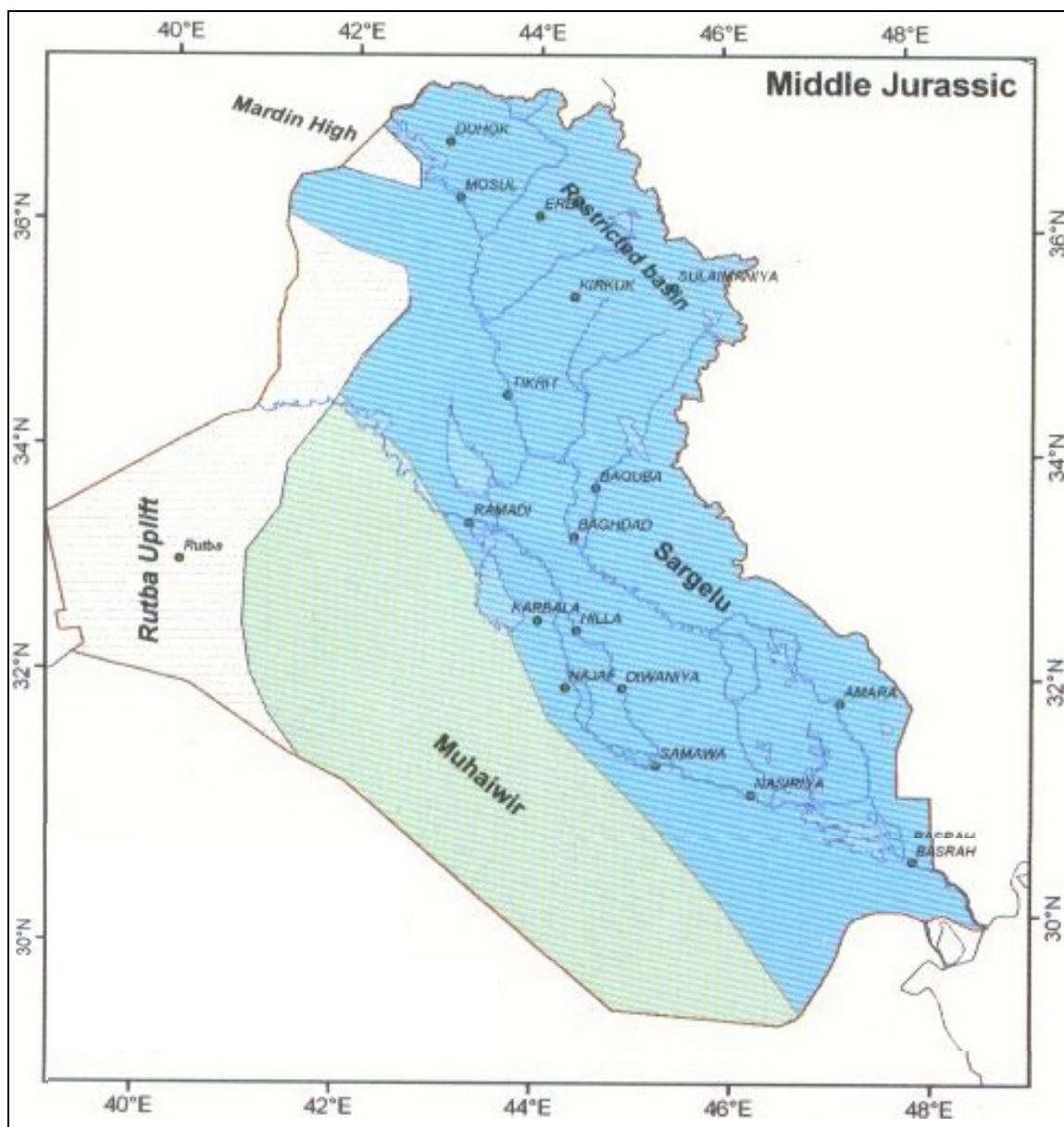
Figure 2.4: Middle Jurassic paleogeography in Iraq (Jassim and Buday, 2006b).
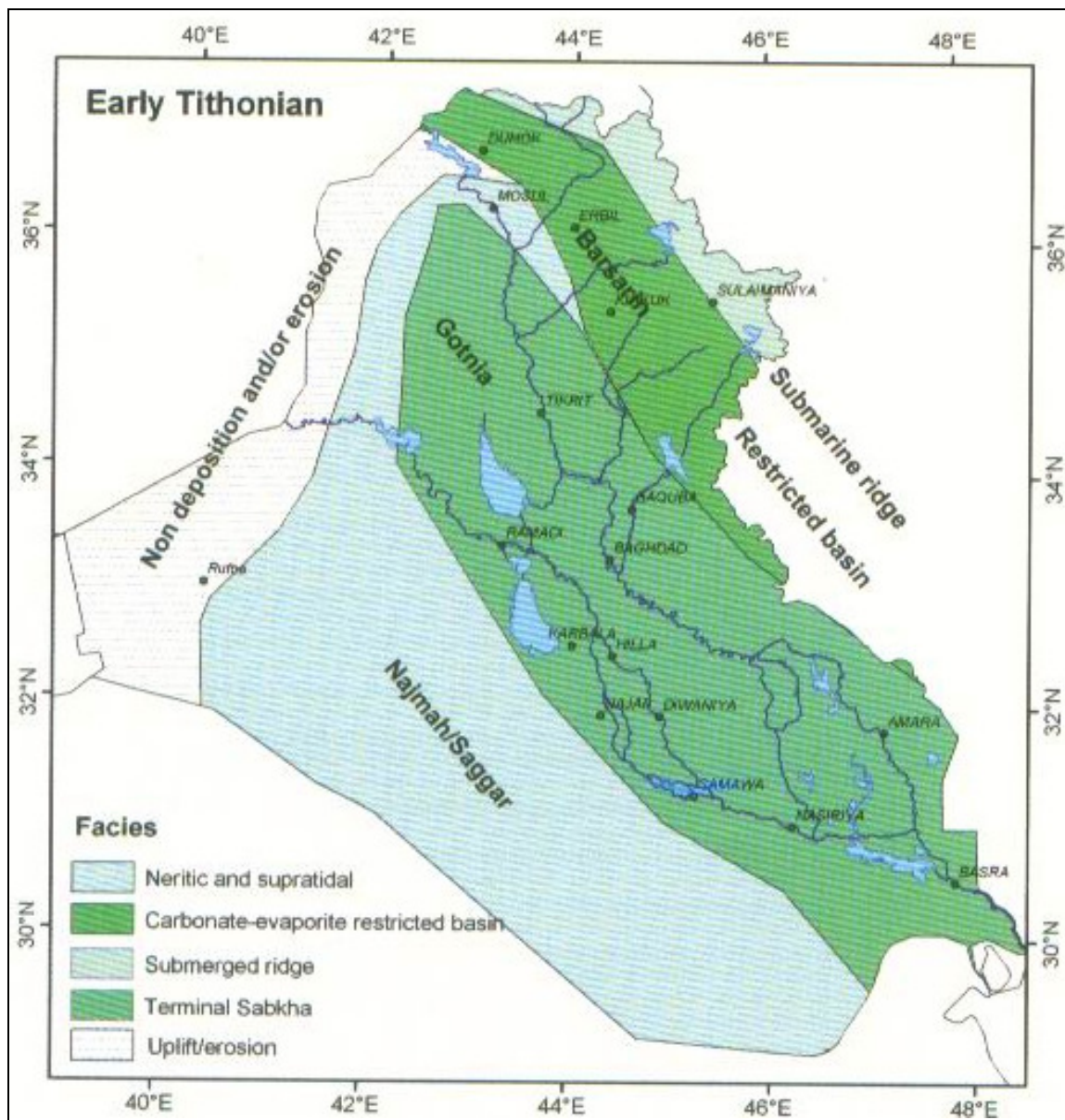
Figure 2.5: Paleogeography of Late Jurassic time (Oxfordian-Early Tithonian) (Jassim and Buday, 2006b).

CHAPTER 3

PYROLYSIS ANALYSIS

A petroleum source rock is any rock that is or was capable of generating petroleum (Tissot and Welte, 1984; Hunt, 1996). The capacity of source rock to generate petroleum depends on quantity (TOC), quality, and thermal maturity of organic matter (Hunt, 1996). Pyrolysis analysis is one of the most accepted and frequently used techniques for recognizing and describing the source rocks (Peters, 1986; Spiro, 1991; Sykes and Snowdon, 2002).

3.1   Total Organic Carbon (TOC)

Total organic carbon includes kerogen and bitumen that may occur together in petroleum source rocks and represents the amount of organic matter in a rock sample (Peters and Cassa, 1994). Generally, source rocks have a minimum of 1.0 wt. percent TOC contents (Bissada, 1982). In order for petroleum be generated, the carbon needs to be associated with hydrogen in a source rock (Demaison and Moore, 1980; Peters, 1986; Dembicki Jr, 2009).

Fifty rock samples, including the 36 samples from the Sargelu Formation, were analyzed to determine their TOC wt. percent (Table 3.1) in order to evaluate the Sargelu Formation quantitatively. Figure 3.1 shows distribution of TOC wt. percent for the Sargelu Formation in northern Iraq. The Sargelu Formation has the highest TOC wt. percent content in the Tawke-15 Well in the northwestern part of Iraq and the lowest TOC wt. percent content in the Hanjeera locality in the eastern part of the study area (Table 3.1). It is observed that the value decreases toward the northeast (Fig. 3.1).

Table 3.1: Total organic carbon and Rock-Eval pyrolysis data on samples selected from the Sargelu Formation at different localities in northern Iraq.

Well or Locality	Formation	Depth (m)	TOC (wt. %)	S1 mg HC/g rock	S2 mg HC/g rock	S3 mg CO2/g rock	Tmax °C	HI mg HC/g rock	OI mg CO2/g rock	GP mg HC/g rock	PI	Calculated Ro %	S2/S3	TOC/S1	PCI=[0.83X(S1+S2)] mg HC/g rock
Sargelu	Barsarin	Surface	0.08	0.08	0.10	0.09	377	125	113	0.18	0.44		1.11	1.00	0.15
Sargelu	Barsarin	Surface	0.44	0.22	0.35	0.11	464	80	25	0.57	0.39		3.18	0.50	0.47
Sargelu	Barsarin	Surface	0.42	0.22	0.34	0.07	474	81	17	0.56	0.39		4.86	0.52	0.47
Sargelu	Naokelekan	Surface	0.17	0.05	0.06	0.04	388	35	24	0.11	0.45		1.50	0.29	0.09
Sargelu	Naokelekan	Surface	1.50	0.18	0.78	0.20	493	52	13	0.96	0.19	1.71	3.90	0.12	0.80
Sargelu	Naokelekan	Surface	0.13	0.06	0.05	0.07	387	38	54	0.11	0.55		0.71	0.46	0.09
Sargelu	Naokelekan	Surface	2.94	0.04	0.17	1.66	522	6	56	0.21	0.19		0.10	0.01	0.17
Sargelu	Naokelekan	Surface	11.25	0.07	0.97	5.08	530	9	45	1.04	0.07		0.19	0.01	0.86
Sargelu	Sargelu	Surface	2.54	0.10	0.52	1.77	496	20	70	0.62	0.16	1.77	0.29	0.04	0.52
Sargelu	Sargelu	Surface	2.15	0.59	1.50	0.27	460	70	13	2.09	0.28	1.12	5.56	0.27	1.74
Sargelu	Sargelu	Surface	0.39	0.16	0.28	0.15	459	72	38	0.44	0.36	1.10	1.87	0.41	0.37
Sargelu	Sargelu	Surface	0.67	0.08	0.25	0.32	492	37	48	0.33	0.24	1.70	0.78	0.12	0.27
Barsarin	Naokelekan	Surface	1.78	0.67	1.30	0.17	478	73	10	1.97	0.34	1.44	7.65	0.38	1.64
Barsarin	Naokelekan	Surface	5.04	0.70	3.59	0.79	467	71	16	4.29	0.16	1.25	4.54	0.14	3.56
Barsarin	Naokelekan	Surface	11.90	2.17	14.34	0.33	462	121	3	16.51	0.13	1.16	43.45	0.18	13.70
Barsarin	Sargelu	Surface	3.37	0.22	1.31	0.80	489	39	24	1.53	0.14	1.64	1.64	0.07	1.27
Barsarin	Sargelu	Surface	2.87	0.09	0.37	1.64	509	13	57	0.46	0.20		0.23	0.03	0.38
Barsarin	Sargelu	Surface	1.60	0.16	0.28	0.77	496	18	48	0.44	0.36		0.36	0.10	0.37
Barsarin	Sargelu	Surface	0.42	0.15	0.18	0.08	355	43	19	0.33	0.45		2.25	0.36	0.27
H-1	Sargelu	3140-3150	0.70	0.39	2.12	0.60	429	303	86	2.51	0.16	0.56	3.53	0.56	2.08
H-1	Sargelu	3160-3170	1.06	0.46	3.45	0.58	432	325	55	3.91	0.12	0.62	5.95	0.43	3.25
H-1	Sargelu	3190-3200	2.04	1.00	8.04	0.84	431	394	41	9.04	0.11	0.60	9.57	0.49	7.50
H-1	Sargelu	3210-3220	1.80	0.81	6.06	0.83	428	337	46	6.87	0.12	0.54	7.30	0.45	5.70
H-1	Sargelu	3250-3260	3.09	1.19	10.94	0.90	432	354	29	12.13	0.10	0.62	12.16	0.39	10.07
Gara	Sargelu	Surface	4.04	0.63	29.38	0.46	435	727	11	30.01	0.02	0.67	63.87	0.16	24.91
Gara	Sargelu	Surface	2.71	0.29	17.66	0.29	436	652	11	17.95	0.02	0.69	60.90	0.11	14.90

Table 3.1: continued. Total organic carbon and Rock-Eval pyrolysis data on samples selected from the Sargelu Formation at different localities in northern Iraq.

Well or Locality	Formation	Depth (m)	TOC (wt %)	S1 mg HC/g rock	S2 mg HC/g rock	S3 mg CO2/g rock	Tmax °C	HI mg HC/g rock	OI mg CO2/g rock	GP mg HC/g rock	PI	Calculated Ro %	S2/S3	TOC/S1	PCI=[0.83X(S1+S2) mg HC/g rock
QC-2	Sargelu	1560-1566	1.18	0.32	5.43	0.24	434	460	20	5.75	0.06	0.65	22.63	0.27	4.73
QC-2	Sargelu	1582-1591	0.88	0.32	3.66	0.25	430	416	28	3.98	0.08	0.58	14.64	0.36	3.30
QC-2	Sargelu	1608-1617	0.98	0.27	4.54	0.18	434	463	18	4.81	0.06	0.65	25.22	0.28	3.99
QC-2	Sargelu	1629-1642	0.88	0.10	4.27	0.14	434	485	16	4.37	0.02	0.65	30.50	0.11	3.63
QC-2	Sargelu	1650-1652	0.80	0.09	3.93	0.14	433	491	18	4.02	0.02	0.63	28.07	0.11	3.34
Qu-2	Sargelu	2158-2165	0.18	0.09	0.38	0.11	439	211	61	0.47	0.19		3.45	0.50	0.39
Qu-2	Sargelu	2241-2250	0.31	0.10	0.82	0.16	440	265	52	0.92	0.11	0.76	5.13	0.32	0.76
Qu-2	Sargelu	2267-2281	0.27	0.07	0.17	0.22	430	63	81	0.24	0.29		0.77	0.26	0.20
Qu-2	Sargelu	2321-2330	1.73	0.47	8.56	0.31	441	495	18	9.03	0.05	0.78	27.61	0.27	7.50
Qu-2	Sargelu	2451-2476	0.34	0.15	0.93	0.24	438	274	71	1.08	0.14	0.72	3.88	0.44	0.90
Qu-2	Sargelu	2559-2573	1.77	0.55	11.18	0.24	441	632	14	11.73	0.05	0.78	46.58	0.31	9.74
Qu-2	Sargelu	2602-2612	2.40	1.23	13.30	0.30	441	554	13	14.53	0.08	0.78	44.33	0.51	12.06
Qu-2	Sargelu	2615-2620	3.43	0.54	19.26	0.21	442	562	6	19.80	0.03	0.80	91.71	0.16	16.43
TA-15	Naokelekan	2830-2840	0.52	0.17	2.29	0.27	425	440	52	2.46	0.07	0.49	8.48	0.33	2.04
TA-15	Sargelu	2860-2870	11.80	5.91	67.45	0.52	440	572	4	73.36	0.08	0.76	129.71	0.50	60.89
TA-15	Sargelu	2880-2890	1.61	0.98	8.02	0.32	436	498	20	9.00	0.11	0.69	25.06	0.61	7.47
TA-15	Sargelu	2890-2900	0.21	0.14	0.52	0.20	435	248	95	0.66	0.21	0.67	2.60	0.67	0.55
TA-15	Sargelu	2900-2910	42.50	36.84	21.59	1.07	392	51	3	58.43	0.63		20.18	0.87	48.50
TA-15	Sargelu	2910-2920	41.20	7.08	108.79	0.41	477	264	1	115.87	0.06		265.34	0.17	96.17
Hanjeera	Naokelekan	Surface	0.12	0.04	0.06	0.06	395	50	50	0.10	0.40		1.00	0.33	0.08
Hanjeera	Naokelekan	Surface	1.07	0.07	0.12	0.41	358	11	38	0.19	0.37		0.29	0.07	0.16
Hanjeera	Sargelu	Surface	0.67	0.05	0.01	0.56	338	1	84	0.06	0.83		0.02	0.07	0.05
Hanjeera	Sargelu	Surface	0.08	0.05	0.04	0.12	388	50	150	0.09	0.56		0.33	0.63	0.08
Hanjeera	Sargelu	Surface	0.17	0.06	0.04	0.17	409	24	100	0.10	0.60		0.24	0.35	0.08
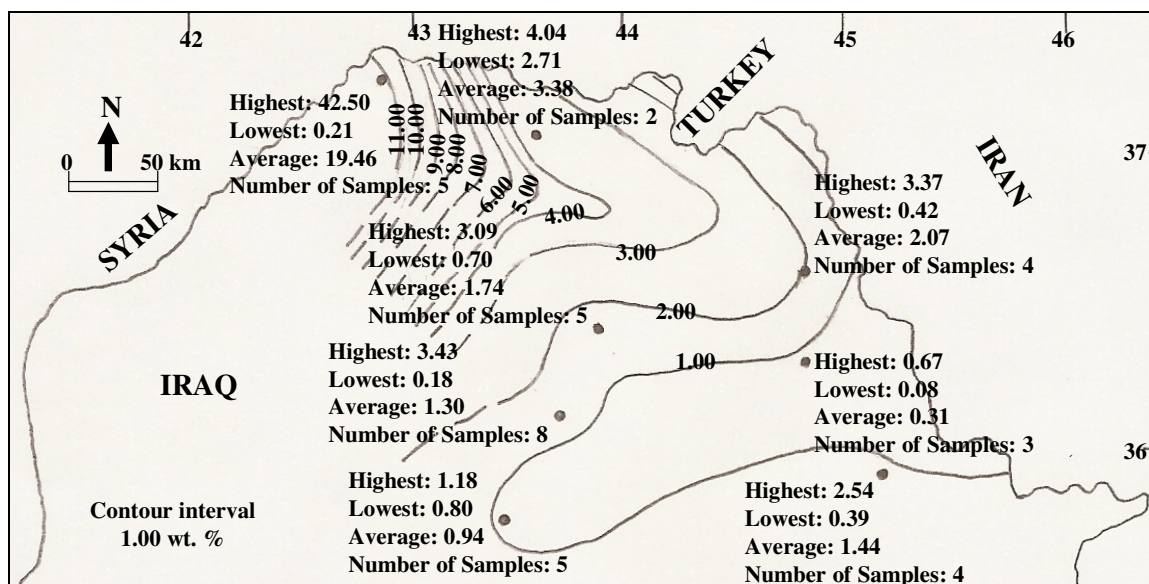
Figure 3.1: Distribution of TOC (wt. percent) for the Sargelu Formation in northern Iraq.

3.2   Rock-Eval Parameters

Pyrolysis analysis provides four important parameters: (1) the total free hydrocarbons (from S_1 peaks); (2) the amount of remaining hydrocarbon or amount of hydrocarbon obtained by heating during pyrolysis (from S_2 peaks); (3) the amount of carbon dioxide (CO_2) released through heating organic matter (from S_3 peaks); and (4) the highest temperature for generating a maximum amount of hydrocarbon during pyrolysis (T_{max}) (Tissot and Welte, 1984). A number of researchers in the United States prefer the use of P_1, P_2, and P_3 instead of S_1, S_2, and S_3 (Peters, 1986). These values are shown in Table 3.1 for organic matter in the Sargelu Formation in northern Iraq.

3.2.1   Hydrogen and Oxygen Indices (HI and OI)

Hydrogen and oxygen indices are comparative to the total hydrogen and oxygen content in the kerogen, respectively. Both are parameters that can be used to describe the origin of organic matter. The potential of a rock to generate oil can be determined by its

hydrogen index. Usually, the oxygen index is not accurate due to the combination of oxygen that was released from organic matter with that from carbonate or that from oxidation of kerogen. These indices are mathematically expressed as $[(100 \times S_2)/TOC]$ and $[(100 \times S_3)/TOC]$ for the hydrogen index and the oxygen index, respectively (Tissot and Welte, 1984; Peters and Cassa, 1994; Hunt 1996).

At early thermal maturity stages:

(1) type I kerogen usually contains HI values >600 mg HC/g TOC and OI values <50 mg CO_2/g TOC;

(2) type II kerogen normally has HI values 300–600 mg HC/g TOC and OI values <50 mg CO_2/g TOC;

(3) a mixture of type II and type III has a low hydrogen index 200–300 mg HC/g TOC;

(4) type III kerogen generally contains HI values 50–200 mg HC/g TOC and OI values of 5–100 mg CO_2/g TOC; and

(5) type IV kerogen commonly has HI values of <50 mg HC/g TOC (Tissot and Welte, 1984; Peters and Cassa, 1994).

It is observed that organic matter in the Sargelu Formation at Gara Mountain has the highest HI, and the lowest HI is at Hanjeera village (Table 3.1). The variations of HI values between both localities are due to organic matter types and their maturity level.

3.2.2   Genetic Potential (GP)

A genetic potential is a summation of the amount of free hydrocarbon that has already been generated from the kerogen (S_1) with the quantity of remaining hydrocarbon which has not yet been converted to hydrocarbons (S_2). This can be mathematically expressed as (S_1+S_2) measured in mg/g of rock (Tissot and Welte, 1984). Genetic potential is not a hydrocarbon type indicator although it can be used to evaluate quality of prospective organic matter (Pitman et al., 1987).

Genetic potential values and their comparable source rock evaluations are shown in Table 3.2. The genetic potential of organic matter in the Sargelu Formation in the Tawke-15 Well is excellent, having an average of 43 mg/g, while the Hanjeera locality

has extremely poor genetic potential, averaging 0.01 mg/g (Table 3.1).

Table 3.2: Genetic potential value and their comparable source rock quality according to Tissot and Welte (1984).

source potential	genetic potential value
poor	<2 mg/g
moderate	2–6 mg/g
good	>6 mg/g

3.2.3   Production Index (PI)

The production index (PI), or transformation ratio, is a proportionality between the hydrocarbons that already generated (S_1) from kerogen and a quantity of whole hydrocarbons that can be obtained from kerogen (Tissot and Welte, 1984). The PI can be mathematically expressed as $[S_1/(S_1+S_2)]$. The PI is related to the type and thermal maturity of organic matter; therefore the PI is not the same for different types of organic matter (Tissot and Welte, 1984; Peters and Cassa, 1994). According to Hunt (1996), the PI value of 0.1 indicates the beginning of a considerable amount of oil generation and 0.4 indicates the termination of oil generation and initiation of gas generation.

The production indices of organic matter in the Sargelu Formation from different localities are shown in Table 3.1.

3.3   Kerogen Type Determined from Pyrolysis

Kerogen is organic matter disseminated in sediments and made of high-molecular-weight compounds (Whelan and Thompson-Rizer, 1993). It is neither soluble in aqueous alkaline solvents nor in common organic solvents (Tissot and Welte, 1984).

The following are the three main kerogen types.

Type I consists of algal material derived from closed basins, lagoons and lakes. It is characterized by having a high H/C ratio, and is able to generate oil. Type II consists of sapropelic organic matter deposited in anoxic marine environments. This kind of kerogen has reasonably high H/C ratios that produce both oil and gas. Type III consists of humic, coaly material derived from continental higher plants. It has a low H/C ratio and high oxygen content and therefore is usually gas prone (Tissot et al., 1974).

Two other types are recognized and can be added to the main types. They are: type IV and IIS. Type IV kerogen has a high atomic O/C ratio and a low atomic H/C ratio. This kind of kerogen is derived from: (1) older sediments by erosion; (2) altered organic material by weathering; (3) thermally combusted deposits; or (4) biologically oxidized organic material before burial (Tissot, 1984). Type IIS kerogen contains high organic sulfur (8–14 wt. percent atomic S/C≥0.04); otherwise, it is similar to type II kerogen in composition (Orr, 1986).

The following are methods to determine kerogen types from pyrolysis data.

3.3.1   HI versus OI

Hydrogen index (HI) versus oxygen index (OI) obtained from Rock-Eval pyrolysis can be plotted on a modified van Krevelen diagram and interpreted (Tissot and Welte, 1984; Peters and Cassa, 1994). It is observed from Figure 3.2 that organic matter in the Sargelu Formation represents type I, II, and III kerogens, assuming that all samples are immature (see following sections and Figure 3.2).

3.3.2   HI versus T_{max}

HI versus T_{max} is commonly used to avoid influence of the OI for determining kerogen type (Hunt, 1996). The majority of the samples from the Sargelu Formation plot within type II and III kerogens with the exception of the samples from Gara Mountain which represent type I kerogen (Fig 3.3).
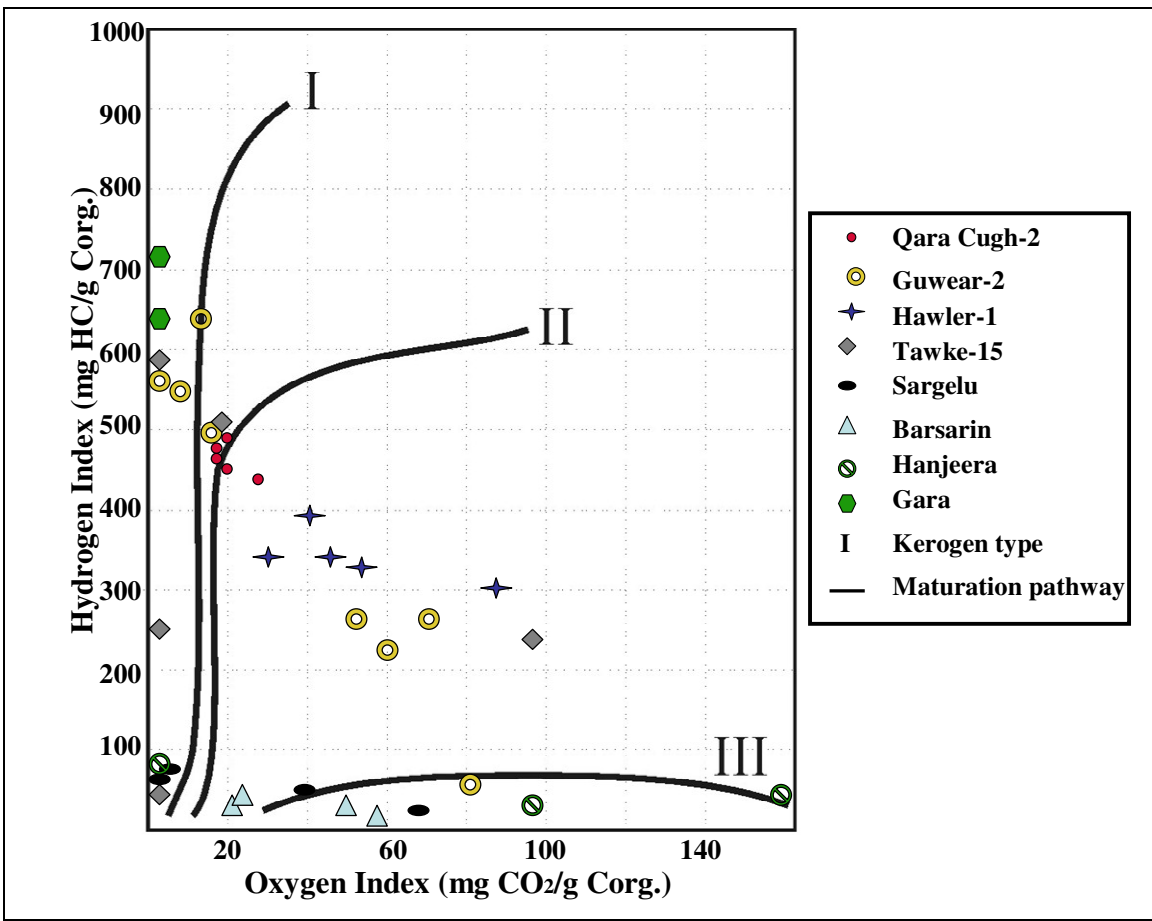
Figure 3.2: HI/OI plot for different kerogen types in the Sargelu Formation analyzed by Rock-Eval pyrolysis (adapted from Espitalié et al., 1977).
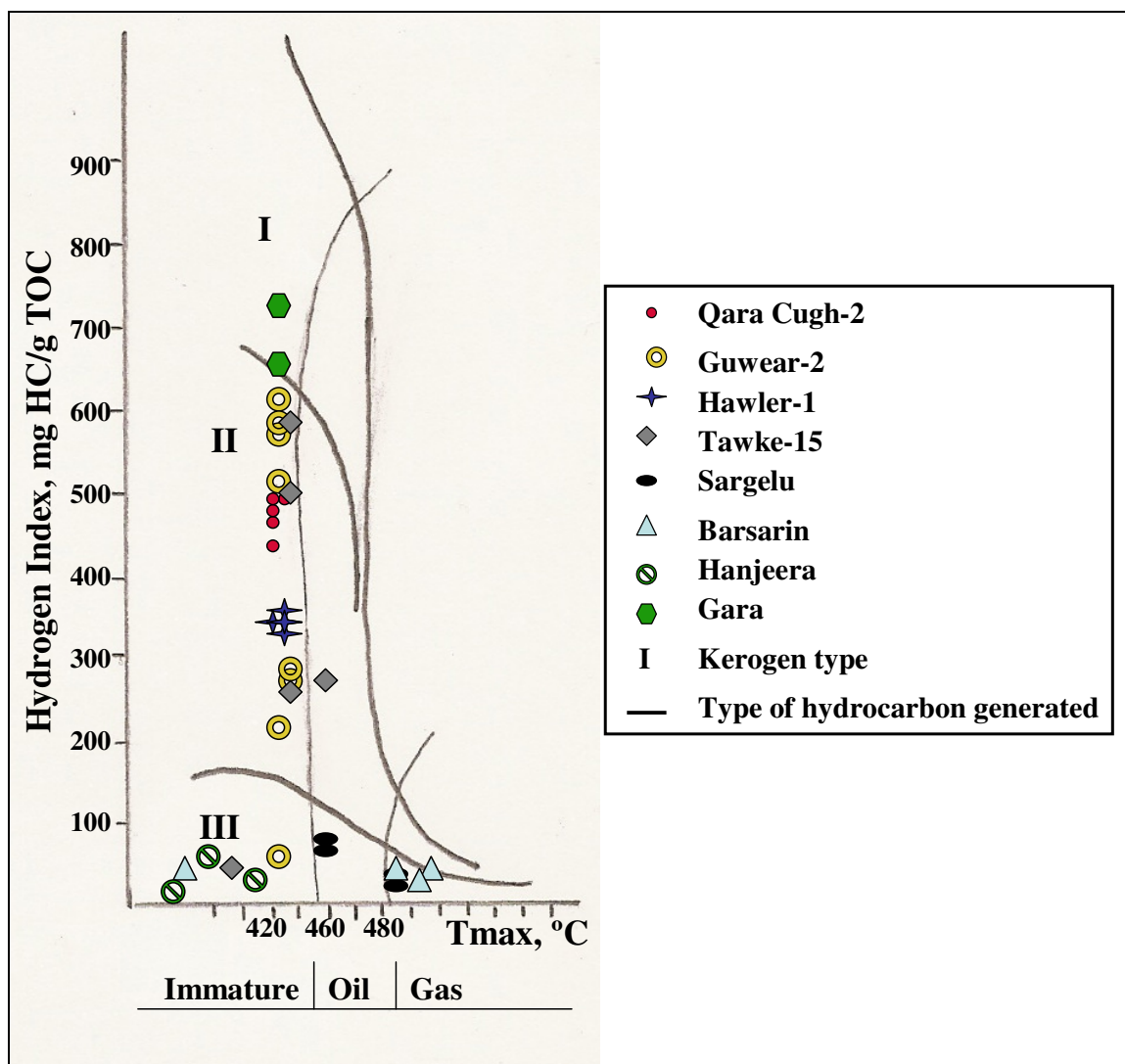
Figure 3.3: Hydrogen index versus T_{max} plot for the Sargelu Formation samples from different localities in northern Iraq (adapted from Espitalié et al., 1985).

3.3.3   Pyrolyzable Carbon Index (PCI)

The pyrolyzable carbon index (PCI) is a maximum amount of hydrocarbon that a sample is able to generate during the analysis, and mathematically, can be expressed as PCI = 0.83 x $(S_1 + S_2)$ (Reed and Ewan, 1986; Geologic Materials Center, 1990; Pimmel and Claypool, 2001; Shaaban et al., 2006).

The PCI can be used to estimate the kerogen type and its hydrocarbon potential (Reed and Ewan, 1986; Shaaban et al., 2006). The PCI values: ≥75 indicates type I; 40–50 represents type II; and <15 indicates type III (Reed and Ewan, 1986) (Fig. 3.4).

In the case of high anomalous value of S_1 due to the presence of nonindigenous hydrocarbons, the value of S_1 should be ignored. The PCI can also be determined according to S_2 only (Reed and Ewan, 1986).
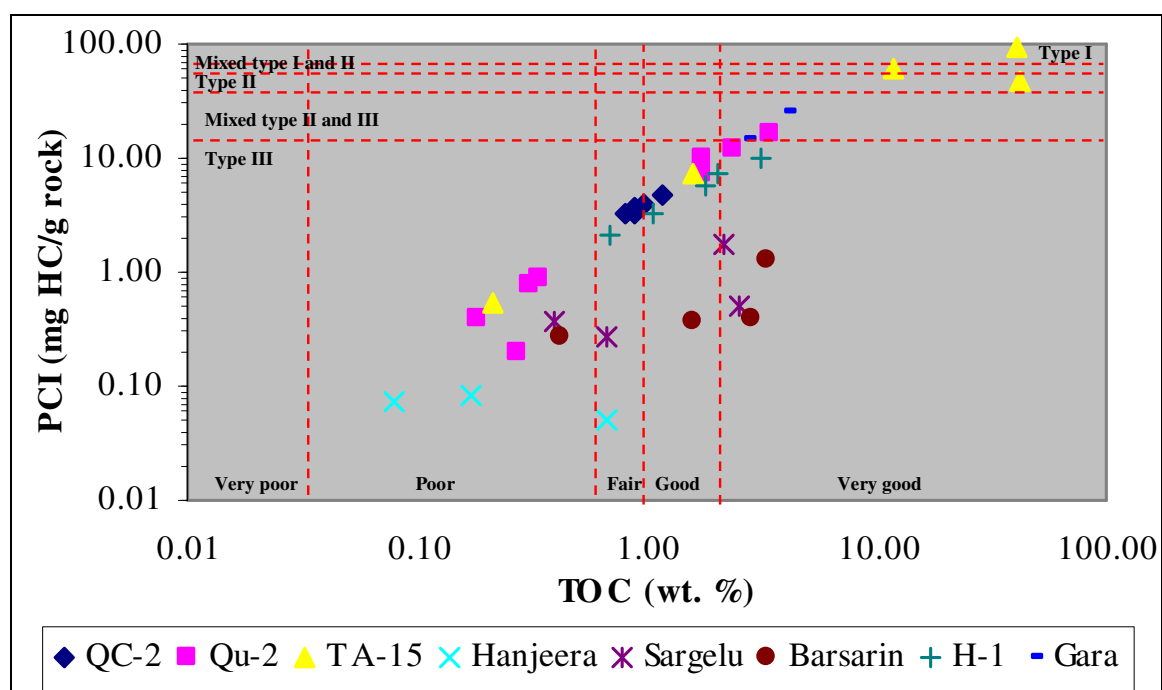
Figure 3.4: TOC wt. percent versus pyrolyzable carbon index (PCI) indicates the quality of the source rock according to TOC wt. percent and kerogen types for samples in studied localities in northern Iraq (adapted from Shaaban et al., 2006).

3.3.4   TOC versus S_2

The plot of TOC versus Rock-Eval pyrolysis S_2 can be used to determine the type of organic matter (Fig. 3.5). The figure shows that samples are mixture of type II and III kerogens.
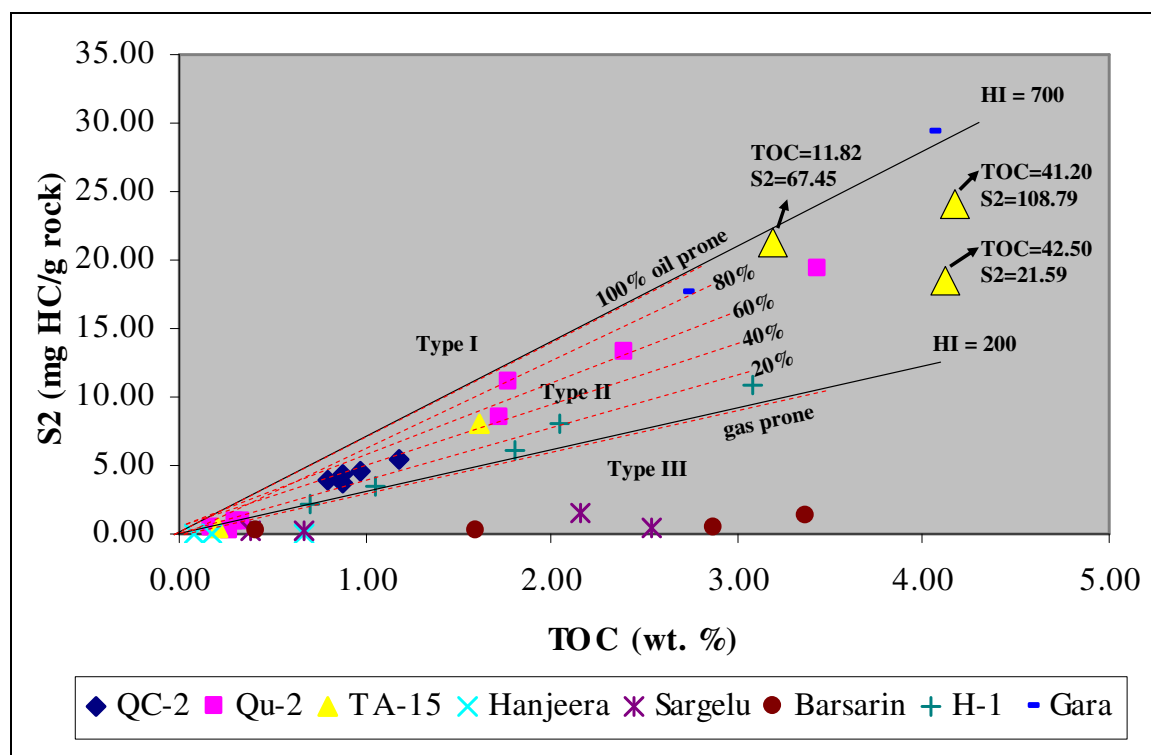
Figure 3.5: Plot of TOC versus Rock-Eval pyrolysis S_2 shows the kerogen type for samples from the Sargelu Formation at eight localities in northern Iraq. Three of five samples from Tawke-15 are off scale (yellow triangles with arrow on top of them). The plot also indicates whether kerogen is oil or gas prone (modified from Dahl et al., 2004; Allen et al., 2008).

3.4   Maturity

The degree of thermal alteration of organic matter due to heating is called maturity (Peters and Cassa, 1994). Organic matter has three different maturity phases: (1) immature, which has not been obviously affected by temperature and may be affected by biological diagenesis processes; (2) mature, which is (or was) within an oil window and

has been converted to petroleum via thermal processes; and (3) postmature, which is in the gas window because it is hydrogen reduced material due to the influence of high temperatures (Peters and Cassa, 1994).

The type and maturity of organic matter in petroleum source rocks was characterized by Rock Eval pyrolysis data. Maturation of the organic matter was estimated by: (1) HI versus OI; (2) T_{max} range; (3) T_{max} versus PI; and (4) vitrinite reflectance.

3.4.1 HI versus OI

The level of thermal maturity can be roughly estimated from the HI versus OI plot (Fig. 3.2). The figure shows that the majority of the samples are mature and immature except for six of them which are postmature.

3.4.2 T_{max} Range

T_{max} is a temperature at which the greatest amount of the S_2 is produced during pyrolysis (Dembicki Jr, 2009). The level of thermal maturity for different types of organic matter may be estimated from the T_{max} range (Peters and Cassa, 1994; Bacon et al., 2000) (Table 3.3). The highest T_{max} value during pyrolysis analysis of organic material was recorded for samples from Barsarin village, Sargelu village and the Tawke-15 Well at a depth of 2910–2920 m below the sea level (Table 3.1). The maturation contour map (T_{max}) of organic matter in the Sargelu Formation in northern Iraq is shown in Figure 3.6. The use of some data was excluded in this figure because they did not correspond to reasonable PI values. These data are: 430 and 442 from Guwear-2; 392 and 477 from Tawke-15; 355 from Barsarin locality; and all T_{max} values from Hanjeera village (Table 3.1 and Fig. 1.1).

Table 3.3: Guidelines for describing stage of thermal maturity (modified from Peters and Cassa, 1994; Bacon et al., 2000).

Stage of Thermal Maturity of Oil		T_{max} for Type I	T_{max} for Type II	T_{max} for Type III	Production Index (PI)
Immature		<440	<435	<445	<0.10
Mature	Early	440	435	445	0.10–0.25
	Peak	445	440	450	0.25–0.40
	Late	450	460	470	>0.40
Postmature		>450	>460	>470	–
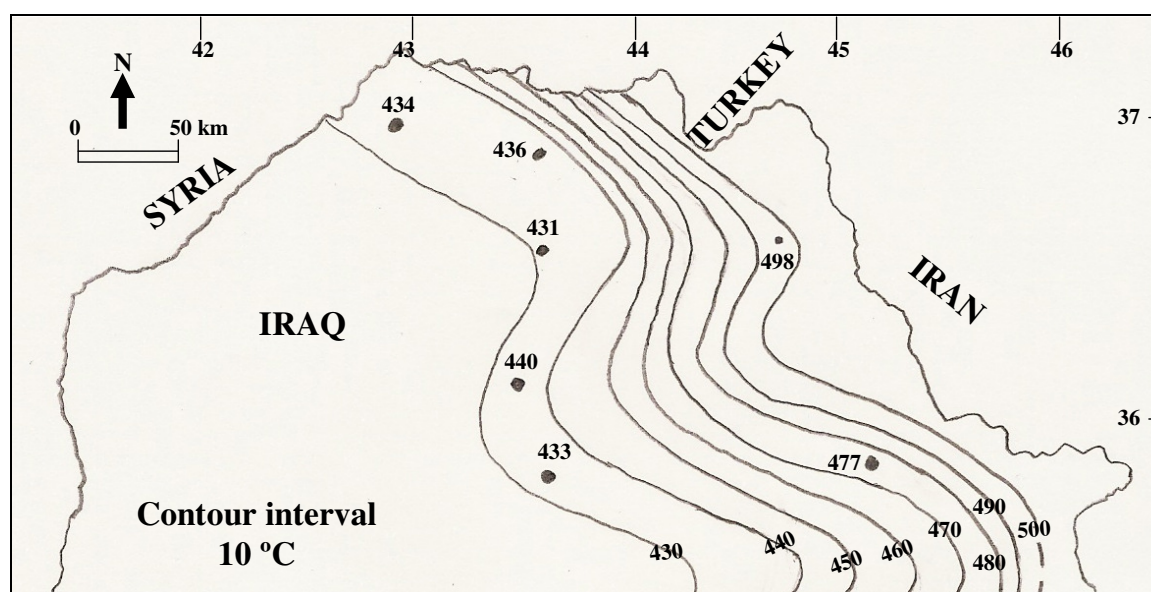
Figure 3.6: Contour map of maturity zones (T_{max}) for the Sargelu Formation's organic matter in northern Iraq.

3.4.3 T_{max} versus PI

Combining and finding relations between the essential Rock-Eval parameter, T_{max}, and calculated Rock-Eval parameter, PI, is a valuable method for indicating the thermal maturity of organic matter. The following relations between T_{max} and PI are observed:

(1) immature organic matter has T_{max} and PI values less than 435°C and 0.10, respectively;

(2) mature organic matter has a range of 0.1–>0.4 PI. At the top of oil window, T_{max} and PI reach 450°C and 0.4, respectively;

(3) mature organic matter within the wet gas-zone has PI values greater than 0.4; and

(4) postmature organic matter usually has a high PI value and may reach 1.0 by the end of the dry-gas zone (Peters, 1986; Peters and Cassa, 1994; Bacon et al., 2000).

As a result of transforming complex organic compounds to simpler compounds with increasing depth, the value of PI progressively increases with depth as well. The values greater than 0.2 and 0.3 PI are thought to be anomalous for T_{max} values of <435°C and T_{max} in the range 435–445°C, respectively (Peters and Cassa, 1994).

The increase of maturity level of organic matter corresponds to an increase in T_{max}. This phenomenon is related to the nature of chemical reactions that occur through thermal cracking. The weaker bonds break in the early stages while the stronger bonds survive until higher temperatures in the late stages break them (Whelan and Thompson-Rizer, 1993).

3.4.4   Vitrinite Reflectance (Ro)

Vitrinite reflectance is an optical method for measuring the source rock maturity (Tissot and Welte, 1984). Vitrinite includes material derived from vascular plants (Hunt, 1996). With increasing maturity of organic matter, the reflectance (Ro) of light also increases (Peters and Cassa, 1994). Since T_{max} obtained from Rock-Eval pyrolysis indicates the level of thermal maturity, it is plausible to convert it to Ro (Dembicki Jr, 2009). The conversion can be mathematically expressed as

Ro (calculated) = (0.018) (T_{max}) – 7.16 (Peters et al., 2005a).

This formula is applicable for type II and type III kerogens as stated by Peters et al. (2005a). To obtain reasonable Ro data, the above formula was not used for samples that have S_2 values smaller than 0.5 mg HC/g rock and samples with T_{max} <420°C or >500°C.

The calculated vitrinite reflectance of samples from the Sargelu Formation in northern Iraq is shown in Table 3.1 and the maturation contour map (Ro) of organic matter in the Sargelu Formation in northern Iraq is shown in Figure 3.7. The figure shows that maturity of source rock (Ro) increase progressively toward the east.
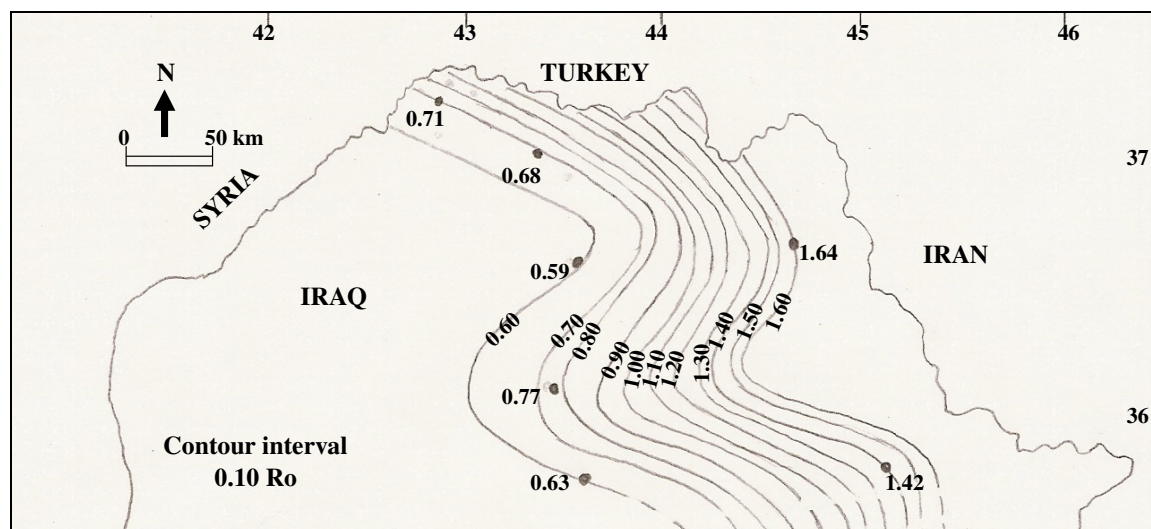
Figure 3.7: Contour map of maturity zones (Ro) for the Sargelu Formation's organic matter in northern Iraq.

3.5   Migrated Hydrocarbons

The comparison of production indices with the thermal maturity stage of samples can be used to identify migrated hydrocarbons (Hunt, 1996). The high S_1 values are either: (1) normal, which indicate prospective source rocks; or (2) abnormal, resulting from a combination with migrated oil, or coming from drilling additives (Peters and Cassa, 1994).

When S_1 is high and the TOC is low, nonindigenous hydrocarbons can be detected (Hunt, 1996). Figure 3.8 separates migrated from non-migrated hydrocarbons for the Sargelu Formation in northern Iraq. The dividing line on the plot is where S_1/TOC = 1.5. Values belonging to nonindigenous hydrocarbons appear above this line while indigenous hydrocarbon values emerge below it (Hunt, 1996). Thus all the samples analyzed indicate indigenous hydrocarbons present.
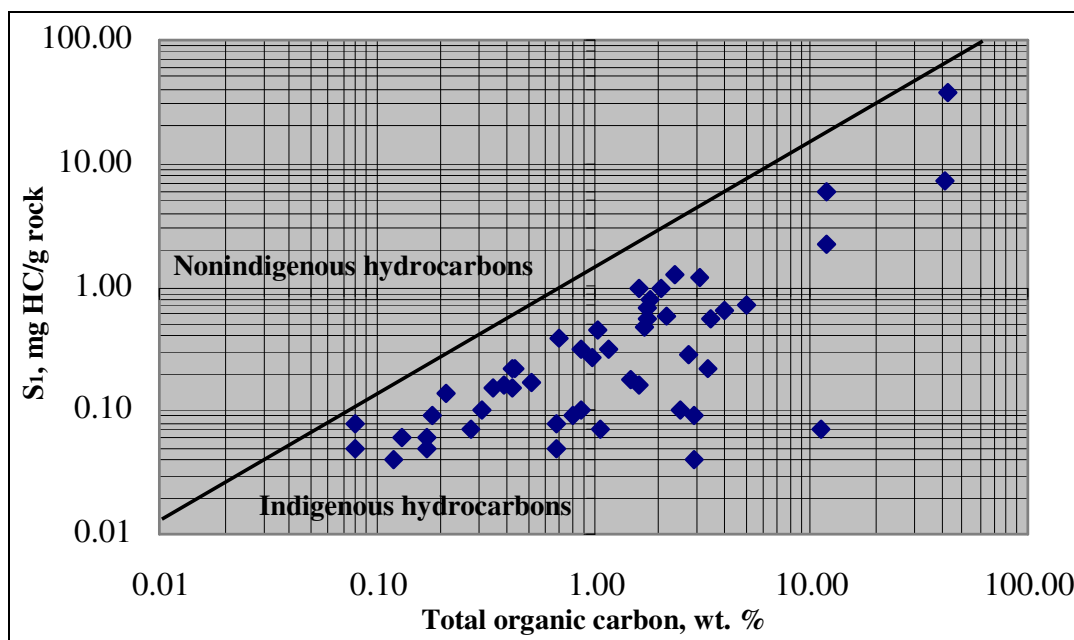
Figure 3.8: S_1 versus TOC for identifying migrated hydrocarbons (adapted from Hunt, 1996).

3.6   Oil or Gas Prone

The Rock-Eval parameters enable one to predict the type of hydrocarbon that could be generated (Peters, 1986). The most useful parameters in this matter are shown in Table 3.4.

The constituents of different organic matter can be identified by plotting S_2 versus TOC (Erik et al., 2006) (Fig. 3.5). This graph may also be used to: (1) determine the kerogen type; (2) measure dissolved organic matter by the surface of rock particles; and (3) make corrections to the hydrogen index (Dahl et al., 2004; Erik et al., 2006).

Table 3.4: Rock-Eval parameters describing type of hydrocarbon generated. Thermal maturation considered to be equal to Ro = 0.6 percent (Peters, 1986).

Type	HI (mg HC/g Corg.)	S_2/S_3
Gas	0–150	0–3
Gas and oil	150–300	3–5
Oil	300 +	5 +

3.7   Depth of Expelled Oil

Primary migration, or expulsion from fine-grained organic rich shales to the migration pathways, is the first migration phase for organic material following conversion to petroleum (Durand, 1988). The depth at which a source rock starts to expel oil can be determined by plotting depth against S_1/TOC (Hunt, 1996). According to Smith (1994) and Hunt (1996), the expulsion of oil starts when the ratio of S_1 to TOC ranges between 0.1 and 0.2.

A plot of depth versus S_1/TOC for samples from the Sargelu Formation in four subsurface localities in northern Iraq indicates that the oil expelled in a depth of: 1629–1650 m below the sea level in Qara Chugh-2 Well, 2615 m below the sea level in Guwear-2 Well, and 2910 m below the sea level in Tawke-15 Well (Figs. 3.9, 3.10, and 3.11). In Hawler-1 Well, the depth of oil expulsion is not clear due to lack of geochemical data (Fig. 3.12).
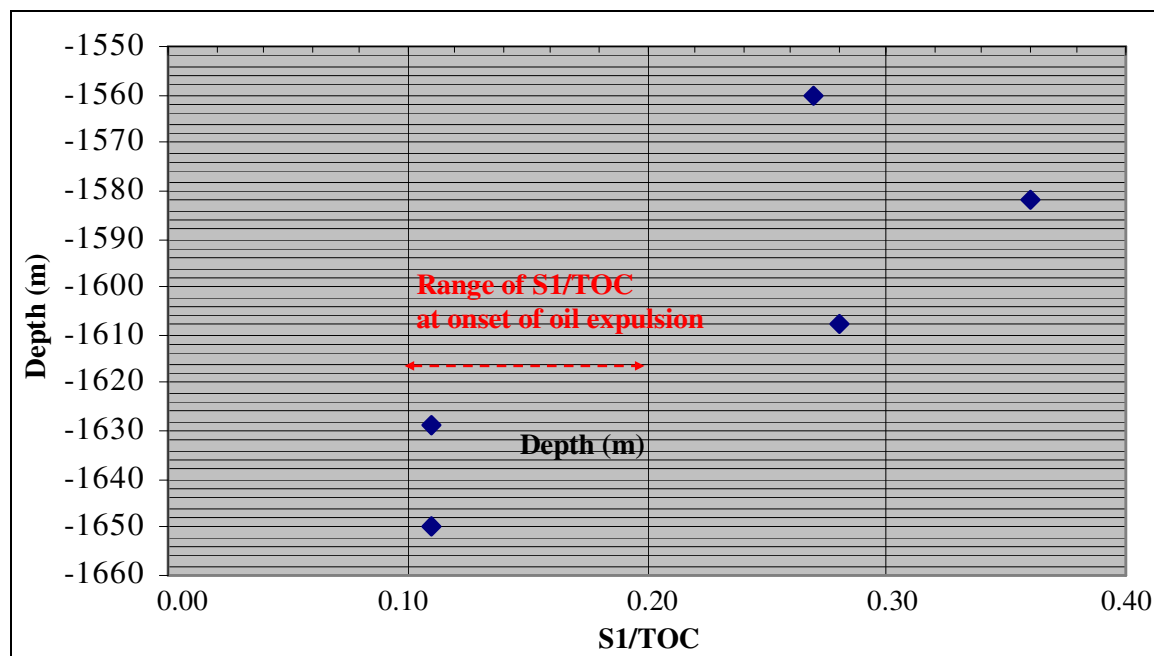
Figure 3.9: Plot of depth-versus-S_1/TOC for organic matter from the Sargelu Formation in Qara Chugh-2 Well northwest of the town of Makhmur in northern Iraq (adapted from Smith, 1994).
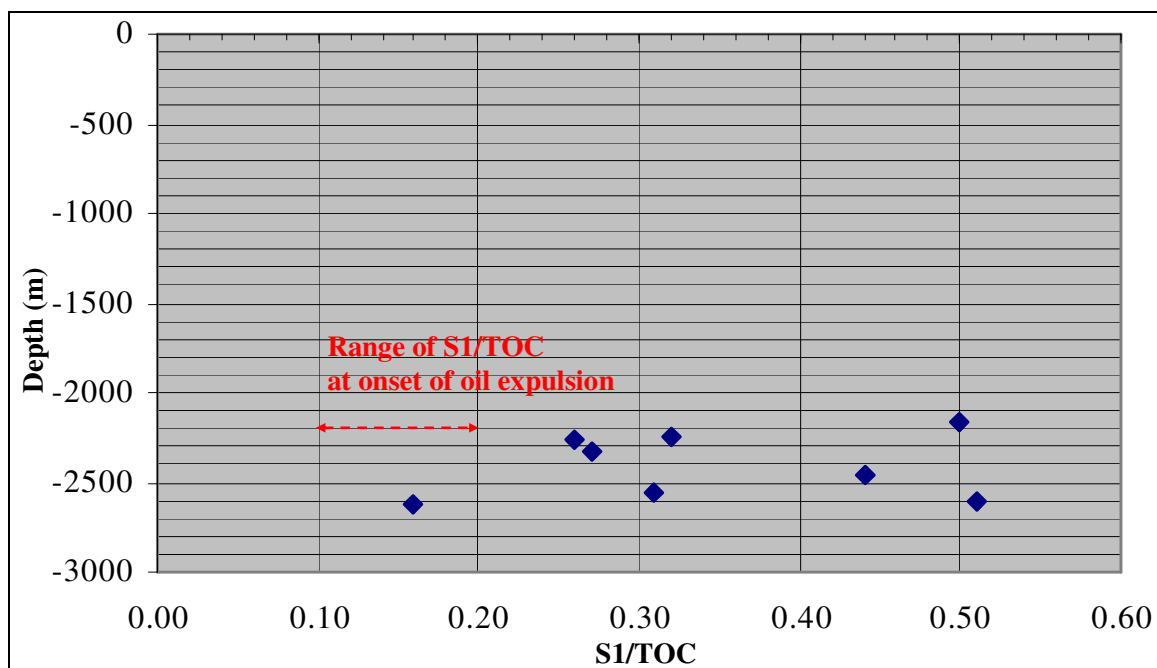
Figure 3.10: Plot of depth-versus-S$_1$/TOC for organic matter from the Sargelu Formation in Guwear-2 Well in the town of Guwear in northern Iraq (adapted from Smith, 1994).
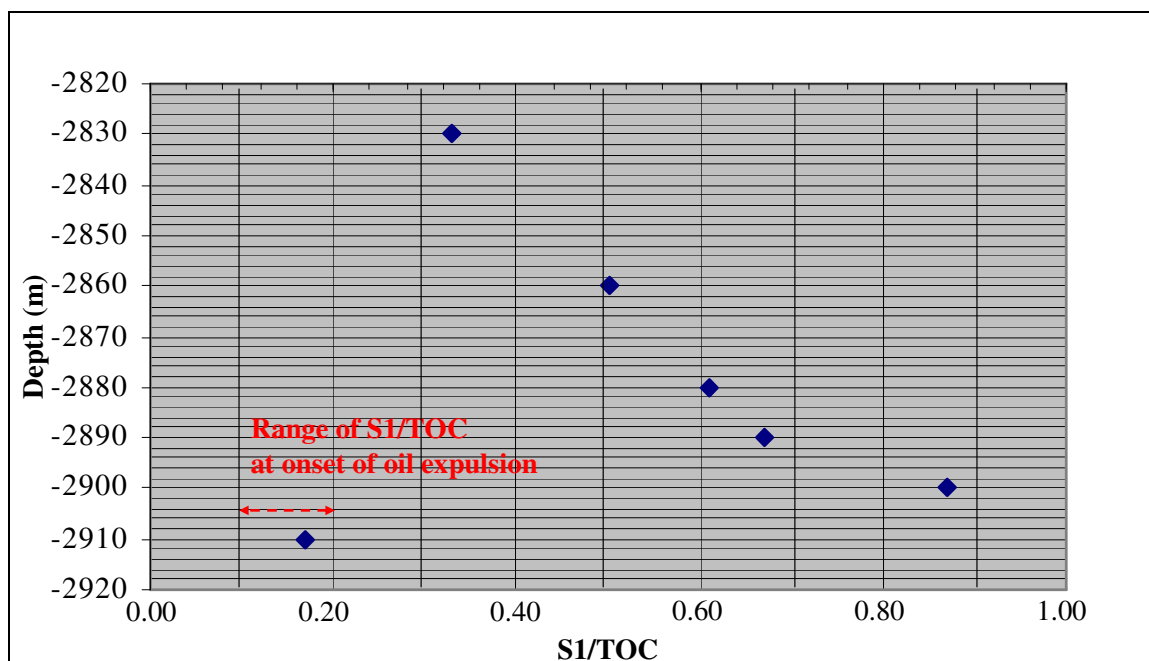
Figure 3.11: Plot of depth-versus-S$_1$/TOC for organic matter from the Naokelekan and Sargelu formations in Tawke-15 Well in Tawke anticline near the town of Zakho in northern Iraq (adapted from Smith, 1994).
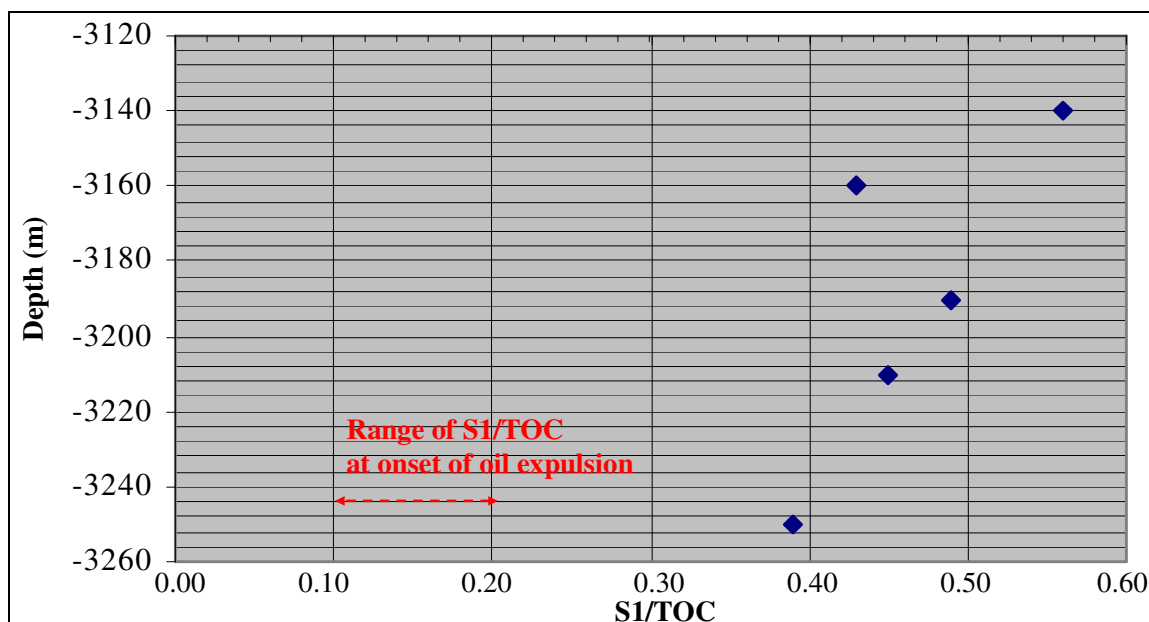
Figure 3.12: Plot of depth-versus-S_1/TOC for organic matter from the Sargelu Formation in Hawler-1 Well in Banenan village in northern Iraq (adapted from Smith, 1994).

3.8   Discussion

In this study, various diagrams and relationships between pyrolysis parameters are used to interpreting the properties and hydrocarbon potential of the studied area of the Sargelu Formation.

It is observed that TOC wt. percent content of the Sargelu Formation decreases to the east and northeast directions (Fig. 3.1). This decrease is due to the change of lithofacies as a result of environmental condition variations. It is clear that land derived organic matter contribution increases toward the northeast (2.2.5 lithology in chapter 2 and Plates II, III, IVa, V, and VI). This increase can be noticed from the TA-15 Well, Gara Mountain, and Qu-2 Well toward H-1 Well, and then Barsarin village, Sargelu village and Hanjeera village (Figs. 3.1, 3.2 and 3.3). The decrease in TOC from the Barsarin locality toward Hanjeera is also seen in the Naokelekan Formation (Fig. 3.13).

The increase in richness towards the west and northwest parts of the study area is due to the change of sedimentary facies and distance from the land. As noted, the facies becomes more sandy and silty (with increase in type III and IV) toward the northeast. The
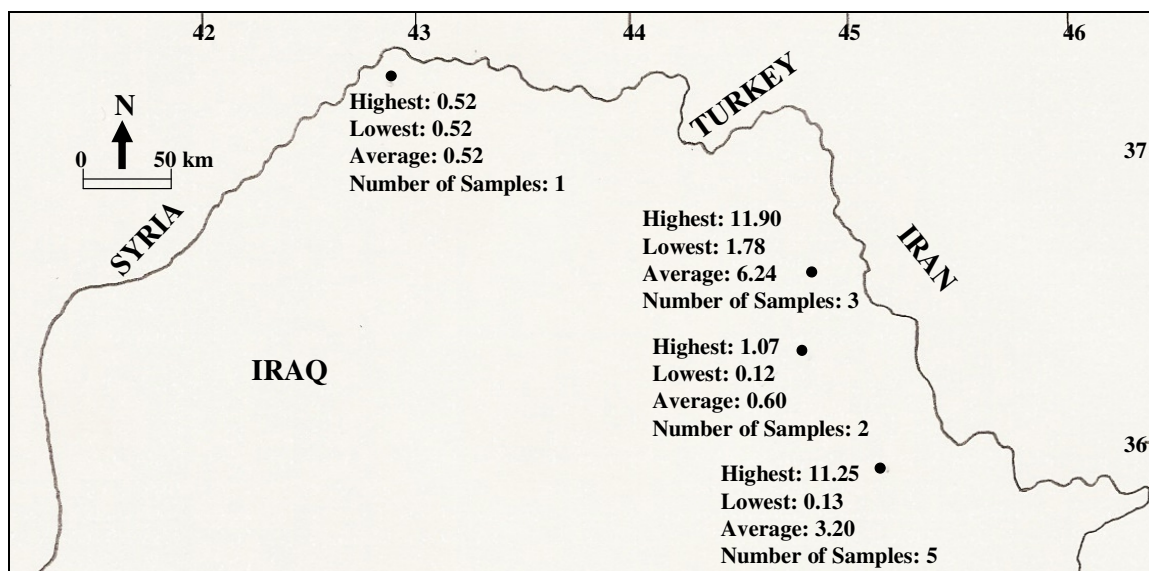
Figure 3.13: Distribution of TOC (wt. percent) for the Naokelekan Formation in northern Iraq.

northwest area represents a marine basin which was deeper. The organic matter may have been better quality originally but the maturity overprint may decreased their quality.

The contour line that passes through the Surdash area in the contour map of TOC wt. percent in northern Iraq which was drawn by Al-Ahmed (2006) has a value of 4 wt. percent. This value is not confirmed by the data that I obtained from samples that I collected from the same area.

Evaluating sediments based on their TOC wt. percent content alone is not enough to satisfy all the requirements of an effective source rock. Accordingly, and depending on Peters' (1986) classification (Table 3.5) and Dembicki's, (2009) classification of TOC wt. percent associated with S_2 (Fig. 3.14), the Sargelu Formation can be considered to be a good source rock.

According to Tissot's and Welte's (1984) evaluation of source rock in general, the genetic potential of samples is: good for 13 samples, moderate for 8 samples, and poor for 15 samples (Table 3.2). It is noticed that samples from Hanjeera village have extremely poor genetic potential, averaging 0.01 mg/g, and samples from Qara Chugh-2 have moderate genetic potential. On the other hand, samples from Gara, lower part of Guwear-2, Tawke-15, and lower part of Hawler-1 have good genetic potential.

Table 3.5: Rock-Eval parameters that indicate quality of different source rocks (Peters, 1986).

Quality	TOC (wt. %)	S_1	S_2
Poor	0–0.50	0–0.50	0–2.50
Fair	0.50–1	0.50–1	2.50–5
Good	1–2	1–2	5–10
Very good	2 +	2 +	10 +
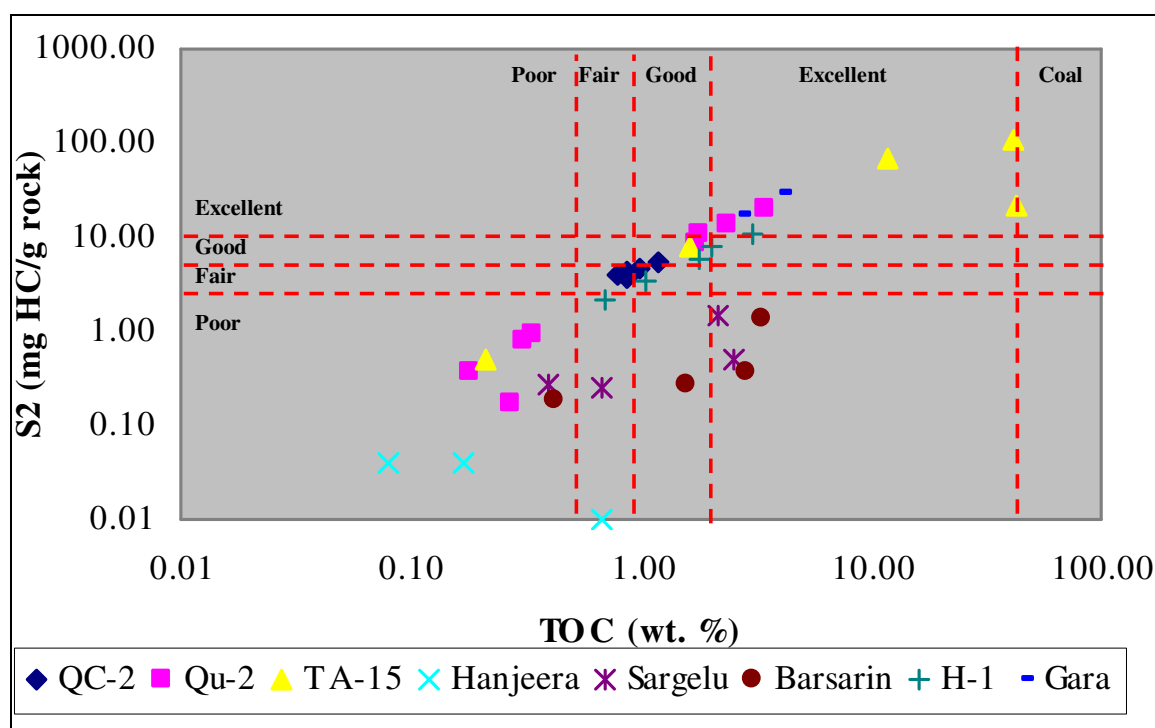
Figure 3.14: Cross plot of TOC wt. percent versus S_2 shows the quality of organic matter in the Sargelu Formation in northern Iraq (adapted from Dembicki Jr, 2009).

Determining kerogen type using T_{max} versus HI appears to be more accurate than OI versus HI. The difference between the results is expected because the Sargelu Formation is dominated by carbonates which affect the OI. It is observed from the T_{max} versus HI plot that: 21 samples appear to be type II, 13 samples are type III, and only 2 samples belong to type I kerogen (Fig. 3.3). The OI versus HI showed different numbers for each type. The latter showed: 5 samples type I, 6 type II, 15 type III, 6 type IV, and 4

located in the lower left corner (Fig. 3.2). The HI values of samples are: greater than 600 mg HC/g Corg. for 3 samples, which means samples are type I; greater than 300 mg HC/g Corg. for 15 samples which is characteristic of type II; greater than 200 mg HC/g Corg. for 5 of them, which means they are a mixture of type II and III; greater than 50 for 5 samples representing type III; and less than 50 for 8 samples, which indicates type IV (Tissot and Welte, 1984; Peters and Cassa, 1994).

The PCI indicates that 30 samples from the Sargelu Formation are type III, which is gas prone. The rest of the samples are: mixed type II and III, type II, mixed type I and II, and type I (Fig. 3.4). The samples from the Naokelekan Formation in Sargelu, Hanjeera, and Barsarin localities represent type III according to their PCI values. The samples from Barsarin Formation in Sargelu village also represent type III based on the PCI values (Table 3.1). The TOC wt. percent versus S_2 diagram shows: 1 sample is type I, 17 samples are type II, 5 samples are mixed type II and III, and the remaining are type III. Each diagram shows different numbers for different types, but all of the diagrams indicate that the majority of samples are type II and III (Table 3.6).

The maturity of source rock based on (T_{max}) and (Ro) (Figs. 3. 6 and 3.7, respectively) increase progressively towards the east. Both contour maps are similar in shape. This increase of maturity toward the east can also be observed from the contour map of maturity zones that is drawn by Al-Ahmed (2006), but the contour line with the value of 0.4 Ro percent which passes the Guwear-2 and Qara Chugh-2 wells were not confirmed by the data that I obtained from Rock-Eval pyrolysis. The contour line with the value of 1.0 Ro percent is also not confirmed by the values of Ro that samples have in TA-15 Well.

The increase of thermal maturity towards the east and northeast of Iraq was also shown by Pitman et al. (2004). The higher Ro values were obtained for some localities that are shown in Pitman et al.'s (2004) map such as in Barsarin, Hanjeera, and Sargalu villages.

This progressive increase of maturity also can be observed from the OI versus HI plot and a T_{max} versus HI plot (Figs. 3.2 and 3.3). It is clear that samples from Barsarin and Sargelu localities emerge in the left corner in the plot of OI versus HI and in the mature and gas zone area in Figure 3.3. The samples in Hanjeera locality have

comparatively low T_{max} values and high OI (84, 100, and 150), which may be a result of weathering and/or lithology and mineral matrix (Peters, 1986). The presence of siderite, silica, and phosphate minerals as a rock matrix affected the Rock-Eval parameters because of the nature of sedimentary minerals, and the amount associated with organic matter causes deviation in: HI, OI, PI, and T_{max} (Spiro, 1991). The images of these minerals are shown in Plate IVa. In the Hanjeera locality, the HI and OI values are unreliable because of the TOC, S_1, and S_2 values are very small (Table 3.1). These data are meaningless due to dividing one small number by another small number (Peters, 1986).

According to Peters (1986), Peters and Cassa (1994), and Bacon et al. (2000), in their definition for maturity level based on T_{max} and PI, the Sargelu Formation is both mature and immature in TA-15 Well (Fig. 3.15); immature in Gara Mountain, H-1 Well and QC-2 Well; and postmature in Barsarin village. It is within the dry gas zone in the type locality but appears to be within the oil window in Qu-2 Well. The Barsarin Formation at Sargelu village appears to be postmature and within the dry gas zone while the results from the underlying Naokelekan Formation samples at the same locality are anomalous. In addition to samples from the Sargelu village, the sample from TA-15 Well at depths 2900–2910 m appears to have an anomalous T_{max} of 392 ºC.

The data obtained from Hanjeera locality samples appear to be anomalous because they have high PI values: 0.60, 0.56, and 0.83 and T_{max} values 409, 388, and 388, respectively. Additionally, the samples have S_2 values less than 0.2 which is insignificant due to measurement errors (Peters, 1986; Hunt, 1996).

The abnormality of samples is determined by using the following assumptions:
(1) PI should be ≤0.1 when T_{max} is between 390–435ºC;
(2) PI should be ≤0.3 as T_{max} is between 436–445ºC; and
(3) PI should be ≤0.4 when T_{max} is between 445–460ºC (Peters and Cassa, 1994).

The western part of the study area represents an immature zone while the eastern part is postmature (Figs. 3.6 and 3.7). The boundary depth between mature and immature zones for the TA-15 Well can be determined by plotting PI versus depth. From Figure 3.15 it is clear that the boundary is located at 2880 m below the sea level.

By applying guidelines from Table 3.4 on samples from studied localities, the HI

and S_2/S_3 values in Table 3.1, it appears that the Sargelu Formation is oil prone in the QC-2 and Gara. It is mixture of oil and gas prone in TA-15 Well, H-1 Well, and Qu-2 Well while it is gas prone in other localities. This can also be concluded from Figure 3.5.

The values of S_1/TOC increase with depth due to an increase of thermal maturity assuming no facies change. This increase continues to the top of the oil window and then stays roughly steady for a short distance, such as in the case of the QC-2 Well, where the value of S_1/TOC stays the same at depths between 1629–1650 m below the sea level. As goes deeper depths, the value of S_1/TOC decreases with depth as a result of increasing thermal maturity. Such a case may apply for the H-1 Well. Thus, the oil expulsion most likely occurred there in depths shallower than - 3120 m (Smith, 1994). The depth of expelled oil in Qu-2 and TA-15 wells is - 2615 m and - 2910 m, respectively, but the thickness of the zone that generated oil is not shown due to unavailability of geochemical data for the deeper horizons.

The summary of results and conclusions from Rock-Eval pyrolysis data are shown in Table 3.6.
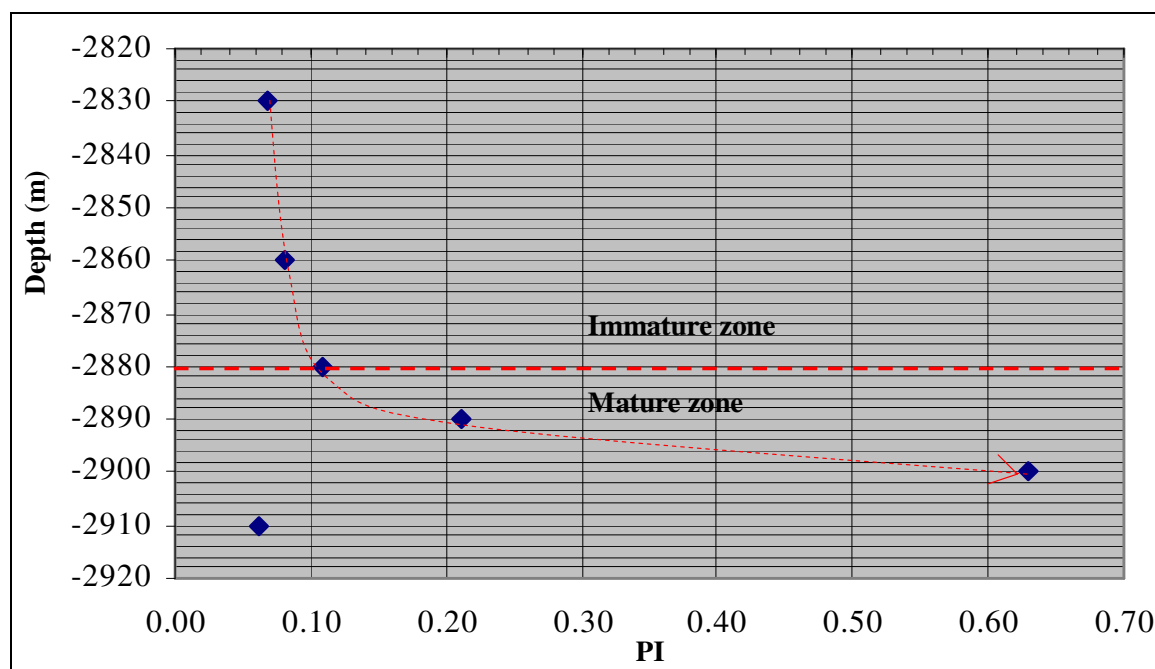
Figure 3.15: Production index versus depth in a Tawke-15 Well in northern Iraq. The discontinuous red line indicates the boundary between the mature zone and the immature zone (adapted from Huc and Hunt, 1980).

Table 3.6 Summary of results and conclusions from Rock-Eval pyrolysis data.

C	coal	G	good	M	moderate	M	mature	NA	not aplicable	O-G	oil and gas	Po	postmature	VP	very poor
F	fair	Im	immature	Ma		O	oil	P	poor	O-G		P		VG	very good

CHAPTER 4

GEOCHEMICAL OIL TYPING

Petroleum is an exceptionally complex mixture (Tables 4.1, 4.2, and 4.3). Crude oil is a liquid phase which is composed of liquid hydrocarbons, dissolved gases, bitumens, and traces of other substances (Levorson, 2001). The geochemical correlations between crude oils from different localities and between oil and extracted source rocks provide useful information regarding the existence and geographic distribution of oil accumulation and production (Peters and Moldowan, 1993; Hunt, 1996; Waples and Curiale, 1999; Peters et al., 2005b). Geochemical correlation can be performed by recognizing compositional similarities or dissimilarities (Tissot and Welte, 1984).

4.1   Classification of Oils

The crude oils from all eight wells can be classified based on their molecular composition (paraffins, aromatics, resins, asphaltenes, and naphthenes) (Fig. 4.1). This figure indicates the Taq Taq oils are paraffinic-naphthenic, except TT-7 which is paraffinic. The aromatic is represented by TA-3, K-247, and K-331, and TA-4 oil is aromatic naphthenic.

4.2   Oil-Oil Correlation

The crude oil correlation method assumes that the same source rock and depositional environment produce oils with similar geochemical characteristics. According to this assumption, genetically related oils can be differentiated from unrelated oils (Philp, 1985; Hunt, 1996). Oil-oil correlation depends on parameters that: (1)

Table 4.1: Bulk properties of oils and extracts from different localities in northern Iraq. The colored values for δ13C are obtained from Sofer's (1984) equation.

Field	Well or Locality	Formation	Age	Depth(m)	API	%S	ppm Ni	ppm V	%Sat	%Aro	%NSO	%Asph	Sat/Aro	P/N	$^{13}C_{sat}$	$^{13}C_{aro}$	CV
Taq Taq	TT-6	Kometan	Creta.	1952		0.94	8.96	5.97	63.97	26.60	7.07	2.36	2.41	0.70	-27.17	-26.61	-1.98
Taq Taq	TT-7	Kometan	Creta.	1925					65.54	26.02	8.19	0.24	2.52	3.90	-27.17	-26.60	-1.96
Taq Taq	TT-8	Kometan	Creta.	1917					65.55	25.71	7.97	0.77	2.55	0.82	-27.15	-26.54	-1.88
Taq Taq	TT-9	Kometan	Creta.	1910					66.67	25.25	7.84	0.25	2.64	1.00	-27.21	-26.48	-1.59
Tawke	TA-3	Qamchuga	Creta.	2545	19.48	3.13	0.00	5.56	37.86	41.14	11.43	9.57	0.92	1.03	-27.51	-27.41	-2.90
Tawke	TA-4	Jeribi	Tertia.	315	24.39	3.51	4.56	1.20	35.24	44.27	9.39	11.10	0.80	0.41	-27.52	-27.34	-2.72
Kirkuk	K-247		Tertia.	740		2.82	5.94	23.64	47.85	33.88	14.41	3.86	1.41	1.73	-27.12	-27.02	-3.02
Kirkuk	K-331		Creta.	1174	25.36	3.53	15.18	38.03	40.06	35.23	16.96	7.75	1.14	0.86	-27.55	-27.73	-3.51
Erbil	QC-2	Sargelu	Jurassic	1560-1566					10.07	11.19	30.97	47.76	0.90	0.75	-28.08	-27.41	-1.46
Erbil	Qu-2	Sargelu	Jurassic	2602-2612					16.23	16.83	31.06	35.87	0.96	0.70	-27.41	-27.40	-3.13
Erbil	H-1	Sargelu	Jurassic	3250-3260					5.83	16.29	18.07	59.82	0.36	0.62	-27.11	-26.91	-2.80
Duhuk	TA-15a	Sargelu	Jurassic	2860-2870					4.96	21.89	9.55	63.60	0.23	2.09	-26.79	-27.15	-4.14
Duhuk	TA-15b	Sargelu	Jurassic	2900-2910					10.37	17.56	4.02	68.05	0.59	0.84	-26.83	-27.22	-4.20
Duhuk	TA-15c	Sargelu	Jurassic	2910-2920					7.70	19.27	10.47	62.56	0.40	2.26	-26.91	-27.04	-3.60
Sulaimani	Sargelu	Naokelekan	Jurassic	Surface					6.98	13.95	37.21	41.86	0.50	0.00	-28.97	-28.12	-0.78
Erbil	Barsarin	Naokelekan	Jurassic	Surface					4.37	23.28	5.79	66.56	0.19	0.61	-24.16	-25.71	-7.60
Duhuk	Gara-a	Sargelu	Jurassic	Surface					3.10	6.20	11.63	79.07	0.50	0.33	-28.77	-27.90	-0.80
Duhuk	Gara-b	Sargelu	Jurassic	Surface					1.11	8.49	15.13	75.28	0.13	3.00	-29.52	-28.73	-0.75

API   API Gravity (15.56 °C)
%S   % Sulfur (Whole Crude)
ppm Ni   ppm Nickel (Whole Crude)
ppm V   ppm Vanadium (Whole Crude)
%Sat   % C_{15+} Saturated Hydrocarbons
%Aro   % C_{15+} Aromatic Hydrocarbons
%NSO   % C_{15+} NSO Compounds

%Asph   % Asphaltenes
Sat/Aro C_{15+} Saturate to Aromatic Hydrocarbons Ratio
P/N C_{15+} n-Paraffin to Branched-Cyclic Hydrocarbons Ratio
$^{13}C_{sat}$ Carbon Isotope Composition: C_{15+} Saturated Hydrocarbons
$^{13}C_{aro}$ Carbon Isotope Composition: C_{15+} Aromatic Hydrocarbons
CV   Canonical Variable: CV = -2.53 δ$^{13}C_{sat}$ + 2.22 δ$^{13}C_{aro}$ - 11.65

Table 4.2: Geochemical characteristics of oils and extracts from different localities in northern Iraq according to GC analysis.

Field	Well	Formation	Depth(m)	15	16	17	Pr	18	Ph	19	20	21	22	23	24	25	26	27	28	29	30	31	32	33	34	35	Pr/Ph	Pr/n-C17	Ph/n-C18	n-C27/n-C17	CPI
Taq Taq	TT-6	Kometan	1952	20.52	16.12	12.72	2.04	10.20	2.07	7.82	6.41	4.78	3.77	2.91	2.32	1.70	1.49	1.09	0.88	0.68	0.63	0.49	0.45	0.33	0.29	0.28	0.98	0.16	0.20	0.09	0.95
Taq Taq	TT-7	Kometan	1925	22.24	17.23	13.48	2.08	10.10	2.11	7.79	6.11	4.56	3.50	2.65	1.98	1.44	1.16	0.81	0.63	0.49	0.38	0.29	0.28	0.23	0.22	0.25	0.99	0.15	0.21	0.06	0.98
Taq Taq	TT-8	Kometan	1917	19.64	15.21	11.96	2.01	9.68	2.06	7.65	6.35	4.80	3.92	3.15	2.67	2.08	1.84	1.38	1.21	0.88	0.79	0.64	0.58	0.50	0.49	0.50	0.98	0.17	0.21	0.12	0.94
Taq Taq	TT-9	Kometan	1910	19.71	15.59	12.39	2.00	9.87	2.03	7.53	6.52	5.00	3.91	2.98	2.50	1.95	1.62	1.25	1.00	0.79	0.73	0.59	0.55	0.48	0.51	0.49	0.99	0.16	0.21	0.10	0.97
Tawke	TA-3	Qamchuqa	2545	16.72	13.18	11.26	2.87	9.04	3.50	7.47	6.70	5.40	4.26	3.51	3.23	2.34	1.90	1.65	1.48	1.21	0.99	0.81	0.82	0.55	0.55	0.41	0.82	0.25	0.39	0.15	0.96
Tawke	TA-4	Jerebi	315	19.85	13.44	10.55	5.91	8.54	7.40	6.17	5.62	3.40	2.98	2.37	2.20	1.87	1.40	1.29	1.07	1.20	0.99	0.81	1.32	0.67	0.52	0.29	0.80	0.56	0.87	0.12	0.97
Kirkuk	K-247		740	16.06	13.28	11.20	2.98	9.46	2.79	7.71	6.80	5.56	4.51	3.71	3.23	2.51	2.07	1.68	1.47	1.13	0.97	0.90	0.75	0.48	0.37	0.29	1.07	0.27	0.30	0.15	0.95
Kirkuk	K-331		1174	17.39	14.30	11.81	2.03	9.69	2.35	7.60	6.72	5.39	4.36	3.56	2.99	2.35	2.29	1.58	1.39	1.09	0.90	0.72	0.65	0.41	0.36	0.19	0.86	0.17	0.24	0.13	0.96
Erbil	QC-2	Sargelu	1560-1566	2.96	8.15	11.79	2.98	12.72	4.28	11.36	9.84	8.02	6.41	4.97	3.90	2.95	2.29	1.73	1.38	1.10	0.90	0.77	0.58	0.42	0.31	0.37	0.70	0.25	0.34	0.15	1.02
Erbil	Qu-2	Sargelu	2602-2612	13.73	19.50	14.09	3.52	10.11	3.26	5.34	4.75	3.50	3.23	2.61	2.36	2.27	1.83	1.68	1.61	1.22	1.24	1.39	0.92	0.88	0.61		1.08	0.25	0.32	0.12	1.07
Erbil	H-1	Sargelu	3250-3260	6.03	13.11	16.82	3.55	15.61	4.08	13.30	10.09	6.89	4.09	2.12	1.18	0.67	0.39	0.26	0.17	0.29	0.13	0.60	0.23	0.20	0.11	0.07	0.87	0.21	0.26	0.02	1.46
Duhuk	TA-15a	Sargelu	2860-2870	10.47	14.15	15.25	3.88	14.17	4.04	11.91	9.59	6.77	4.25	2.28	1.26	0.57	0.39	0.21	0.14	0.17	0.07	0.09	0.13	0.11	0.06	0.04	0.96	0.25	0.29	0.01	1.03
Duhuk	TA-15b	Sargelu	2900-2910	13.48	17.59	18.01	3.78	14.64	3.78	10.84	7.75	4.84	2.69	1.35	0.70	0.36	0.19	0.00	0.00	0.00	0.00	0.00	0.00	0.00	0.00	0.00	1.00	0.21	0.26	0.00	1.15

15   normal alkane series relative%; e.g. n-C15

Pr   Pristane; relative %

Ph   Phytane; relative %

Pr/Ph   pristane to phytane ratio, peak heights from whole crude gas chromatogram

nC27/C17   pristane to phytane ratio, peak heights from whole crude gas chromatogram
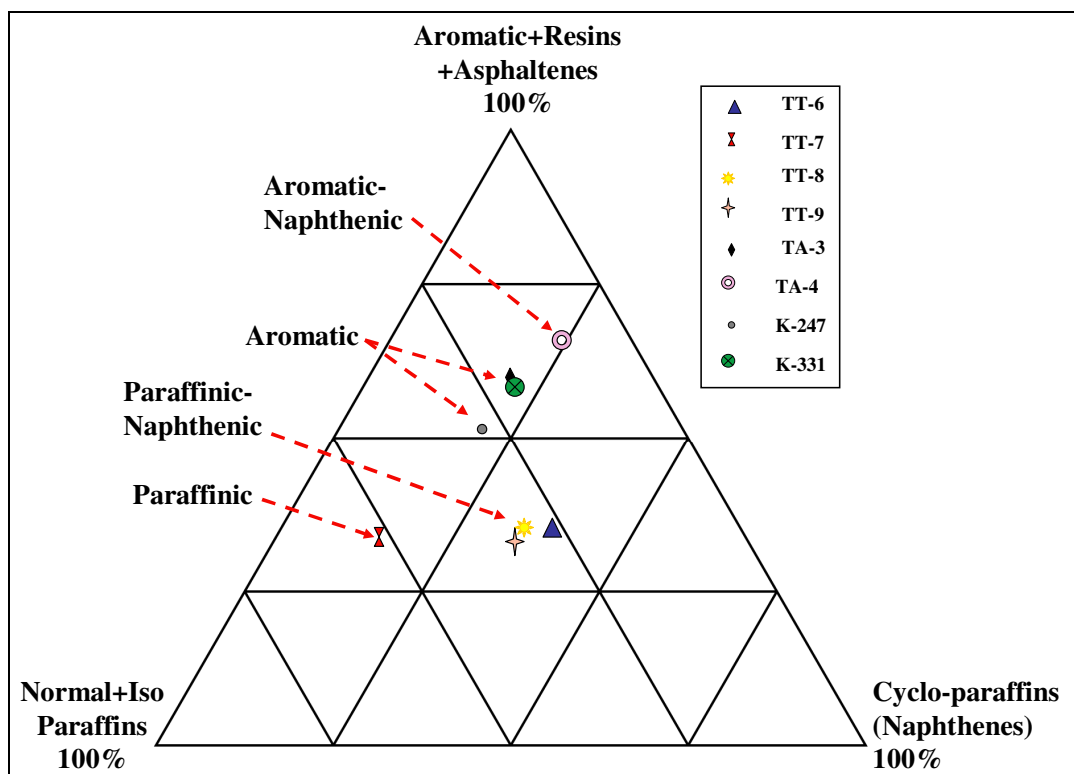
Figure 4.1: Different oil types. The data from: TT-6, TT-7, TT-8, TT-9, TA-3, TA-4, K-247, and K-331 in northern Iraq (adapted from Tissot and Welte, 1984).

discriminate oils from different sources; and (2) are resistant to secondary processes. In general, successful oil-oil correlations can be performed based on a few bulk parameters. Correlations that are based on both molecular ratios and bulk parameters are better because molecular ratios are usually more resistant to secondary alteration processes (Peters and Moldowan, 1993; Peters et al., 2005b).

4.2.1 Bulk Properties

Preliminary grouping of the oils can be obtained by using whole oil properties (Hunt, 1996). Table 4.1 shows various bulk property parameters of oils in the studied area.

American Petroleum Institute (API) gravity is a bulk property of oil and is related inversely to the density of liquid petroleum (Levorsen, 2001; Peters et al., 2005b). The API gravities for the crude oil samples are shown in Table 4.1. Sulfur, nitrogen, and

oxygen content (N, S, O) are also bulk properties of crude oil. Sulfur is the third atomic component of crude oil, after carbon and hydrogen (Tissot and Welte, 1984). Usually, small quantities of nitrogen are present mainly in complex hydrocarbon compounds such as porphyrin. The oxygen content of crude oil is usually more than that of nitrogen, and the oxygen appears as a part of heavy hydrocarbon compounds (Levorsen, 2001). The API gravity is available for only three oils (TA-3, TA-4, and K-331). However, both Tawke oils (TA-3 and TA-4) have different API gravity values, but TA-4 and K-331 have almost similar values. By plotting N+O wt. percent versus sulfur wt. percent, the oils should show whether they are similar or not (Fig. 4.2). The carbon isotope ratios display relationships between oils from: Taq Taq, Tawke, Kirkuk-247, and Kirkuk-331 (Fig. 4.3).
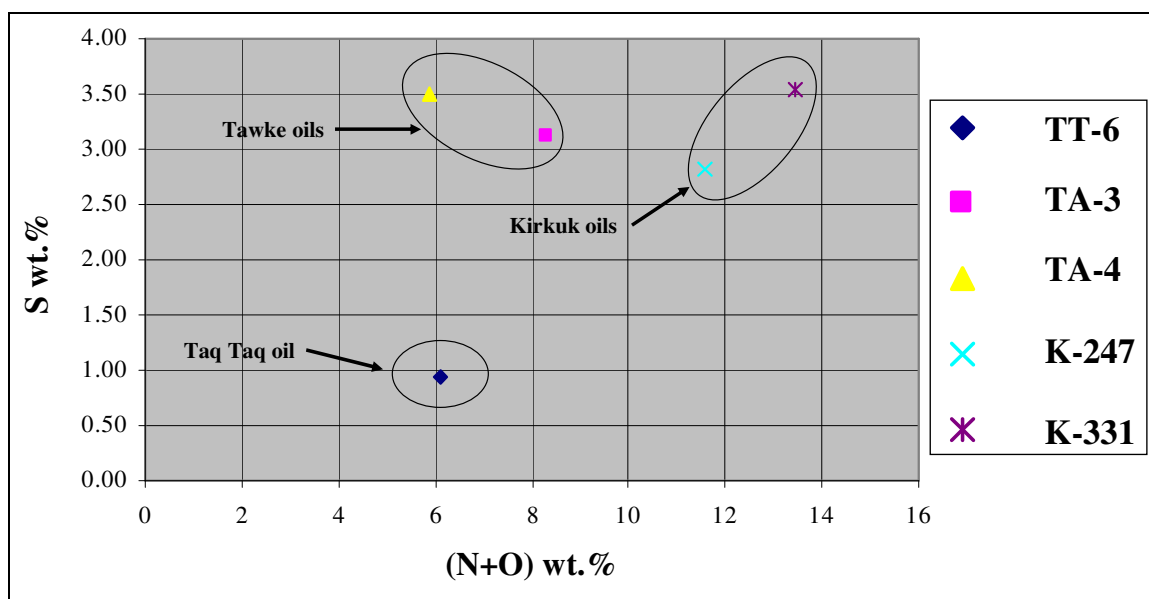
Figure 4.2: Nitrogen (N) and oxygen (O) wt. percent contents versus sulfur (S) wt. percent content for oils from wells: TT-6, TA-3, TA-4, K-247, and K-331 in northern Iraq shows three oil groups: Taq Taq, Tawke, and Kirkuk.

4.2.2   Molecular Ratio or Biomarkers

Biomarkers are molecules derived from organisms that occur in sediments. They are altered slightly, but the carbon skeleton of hydrocarbons or other lipids can be
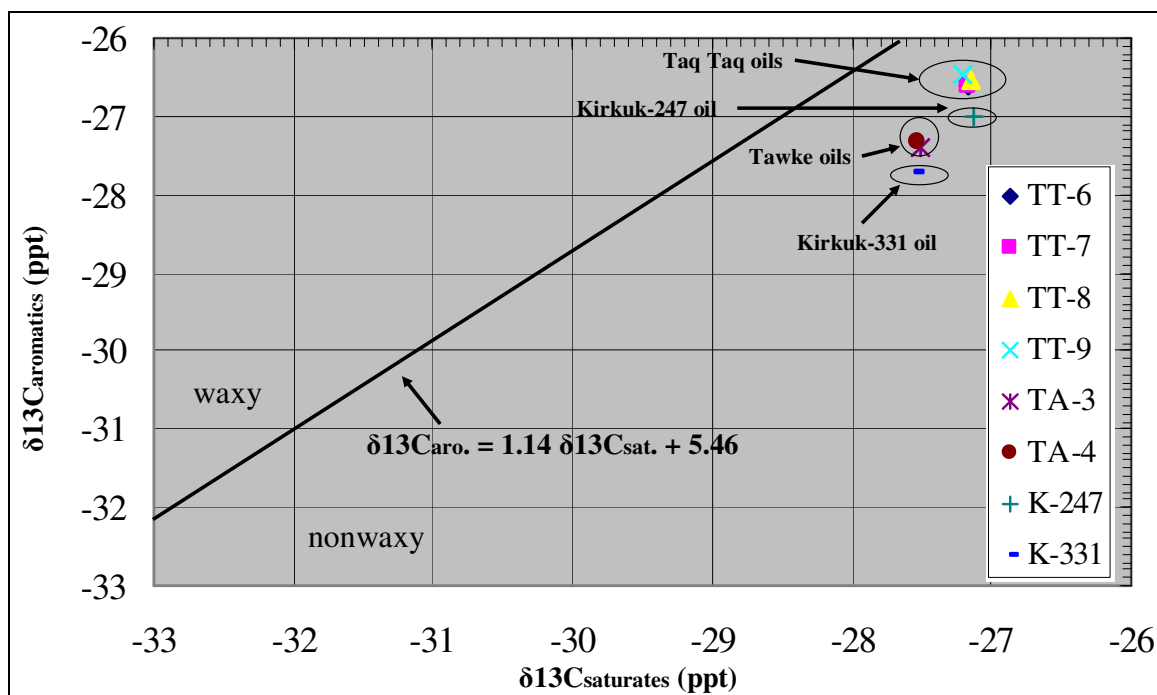
Figure 4.3: Plot of $\delta^{13}C_{saturates}$ versus $\delta^{13}C_{aromatics}$ for oils from: TT-6, TT-7, TT-8, TT-9, TA-3, TA-4, K-247, and K-331 in northern Iraq. The plot reasonably separates Taq Taq, Tawke, Kirkuk-247, and Kirkuk-331 oils (adapted from Sofer, 1984).

recognized (Tissot and Welte, 1984). These molecules have a very low concentration in crude oils (Peters and Moldowan, 1992) (Tables 4.2 and 4.3). They are a valuable tool for description, correlation, and recognition of the depositional environment; this is much the same as geologists use fossils (Tissot and Welte, 1984). The ratio of two biomarkers not affected by degradation and alteration are likely to be the same in oils generated from the same source rock (Philp, 1985; Hunt, 1996).

The biomarker parameters which are resistant and commonly used for correlation are: acyclic isoprenoids (pristane and phytane), C_{27} trisnorhopane, C_{30} diahopane, C_{30} hopane, gammacerane, $C_{31}R$ homohopane, C_{29} norhopane, C_{35} extended hopane (22S), C_{34} extended hopane (22S), C_{24} tricyclic terpane, C_{23} tricyclic terpane, C_{22} tricyclic terpane, C_{21} tricyclic terpane, $C_{31}R$ homohopane (22R), C_{27} steranes (diacholestane and cholestane), steranes (S_1-S_{15}), and C_{27}, C_{28}, and C_{29} sterols (Peters and Moldowan, 1993; Curtis and Lillis, 2008, pers. comm.). Sometimes plotting bulk versus biomarker parameters is useful as well for correlation such as Pr/Ph versus canonical variable CV (Alizadeh et al., 2007). The CV is a statistical parameter and can be mathematically

expressed as

CV = -2.53 $\delta^{13}C_{sat.}$ + 2.22 $\delta^{13}C_{aro.}$ - 11.65 (Sofer, 1984).

Pristane and phytane are branched acyclic isoprenoid hydrocarbons. They contain 19 and 20 carbon atoms, respectively. The pristane peak elutes after the C_{17} n-alkane and the phytane peak elutes directly after the C_{18} n-alkane on most gas chromatographic columns (Peters and Moldowan, 1993; Hughes et al., 1995; Peters et al., 2005b). All samples have a Pr/Ph ratio <1 (0.80–0.99) except for K-247 which has a ratio of 1.07. Figure 4.4 of pristane/phytane (Pr/Ph) ratio versus canonical variable (CV) shows how oils arrange themselves in different groups.

The other biomarker parameters are used in order to differentiate oils from different sources. Figures 4.5, 4.6, 4.7, 4.8, 4.9, 4.10, and 4.11 show the relation between oils from the study area according to similarities or dissimilarities between some biomarker ratios.

The distribution of C_{27}, C_{28}, and C_{29} sterols on a ternary diagram displays a variety of oil groups as well as their source (Riva et al., 1986; Hunt, 1996, Peters et al., 2005b) (Fig. 4.12).
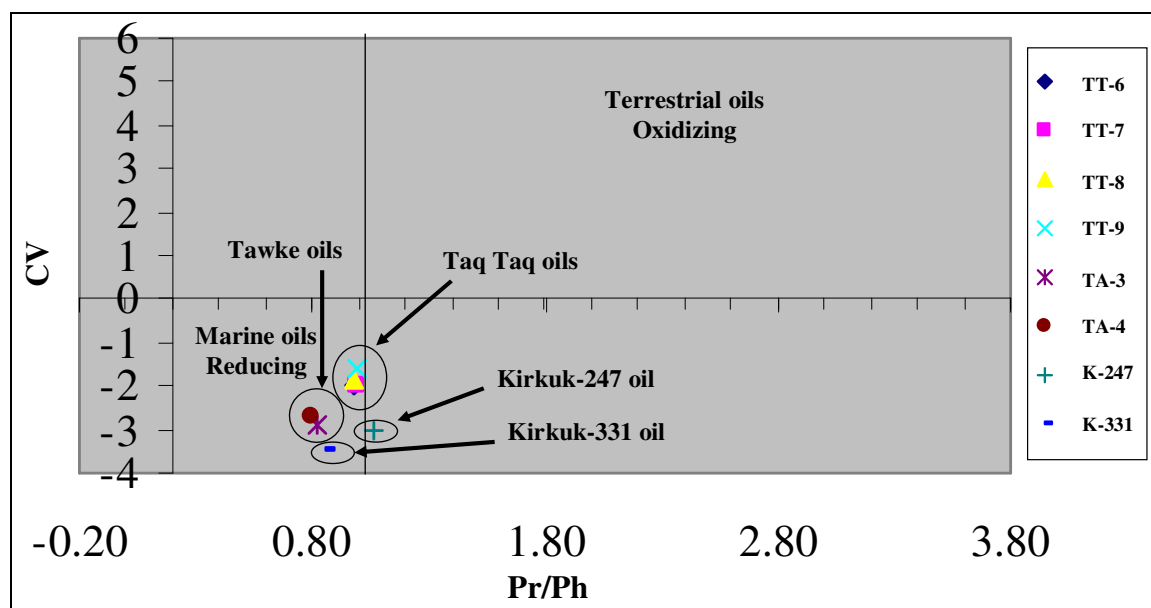
Figure 4.4: Pristane/phytane (Pr/Ph) ratio versus canonical variable (CV) for oils from: TT-6, TT-7, TT-8, TT-9, TA-3, TA-4, K-247, and K-331. The plot shows marine source under reducing condition for oils as well as separates Taq Taq, Tawke, Kirkuk-247, and Kirkuk-331 oils from each other (adapted from Alizadeh et al., 2007).
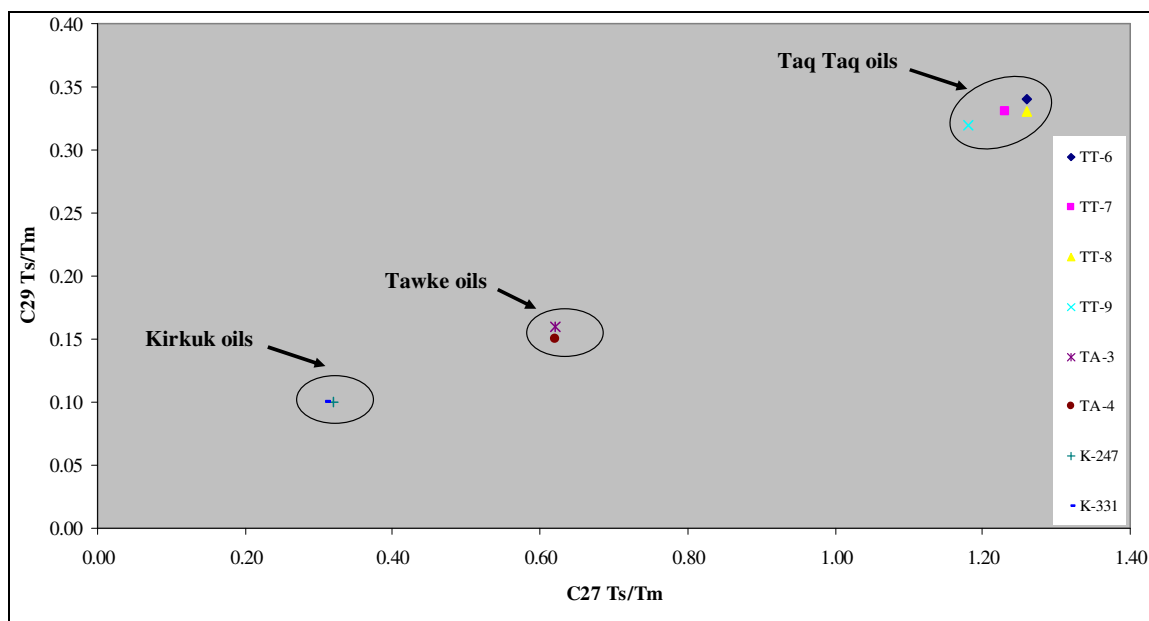
Figure 4.5: Plot of C_{27} Ts/Tm trisnorhopane (17α, 21β-30-norhopane) versus C_{29} Ts/Tm aka C_{29}D/29H (18α-30-norneohopane) for oils from: TT-6, TT-7, TT-8, TT-9, TA-3, TA-4, K-247, and K-331 in northern Iraq. The plot separates Taq Taq, Tawke, and Kirkuk oils.
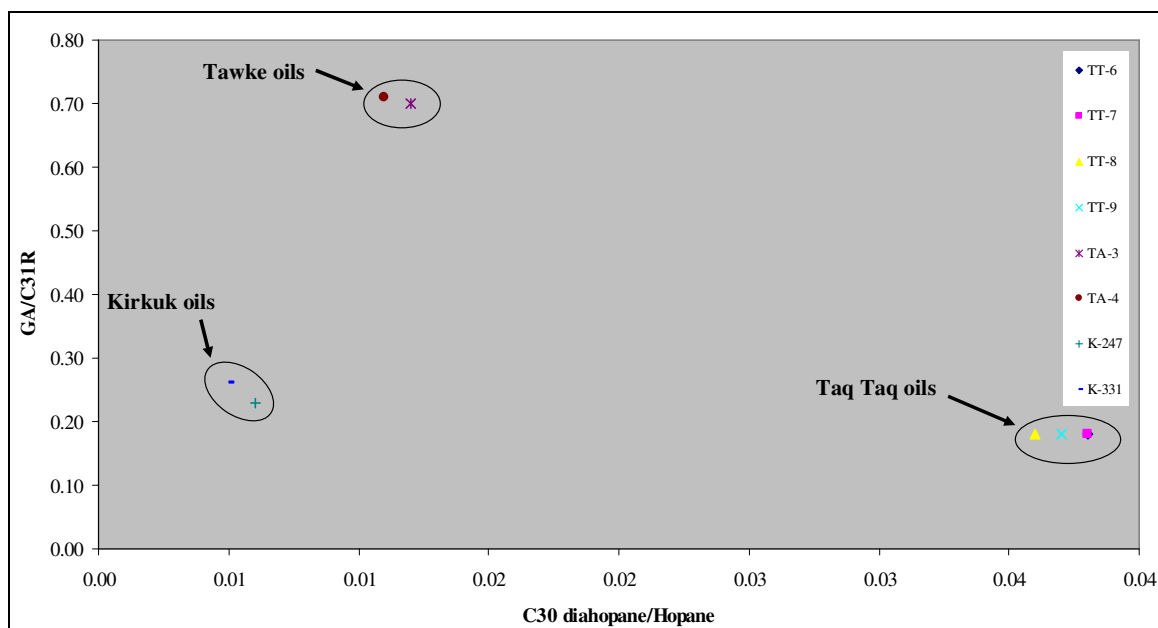
Figure 4.6: Plot of diahopane/C_{30} hopane versus gammacerane/C_{31}R homohopane for oils from: TT-6, TT-7, TT-8, TT-9, TA-3, TA-4, K-247, and K-331 in northern Iraq. The plot separates Taq Taq, Tawke, and Kirkuk oils.
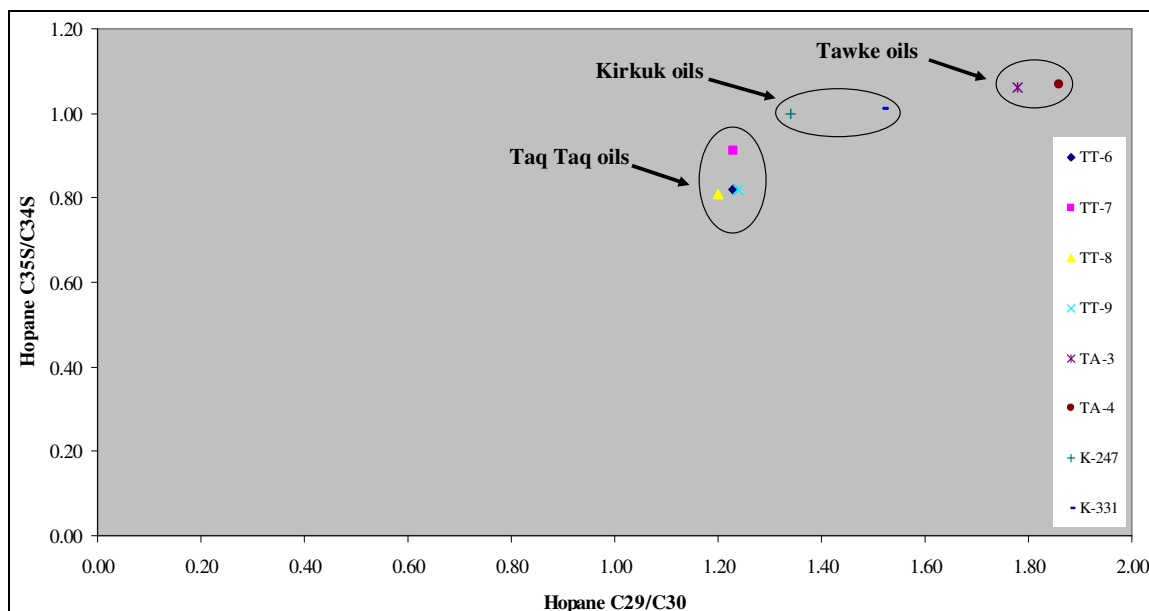
Figure 4.7: Plot of C_{29} norhopane/C_{30} hopane versus C_{35} extended hopane/C_{34} extended hopane (22S) for oils from: TT-6, TT-7, TT-8, TT-9, TA-3, TA-4, K-247, and K-331 in northern Iraq. The plot separates Taq Taq, Tawke, and Kirkuk oils.
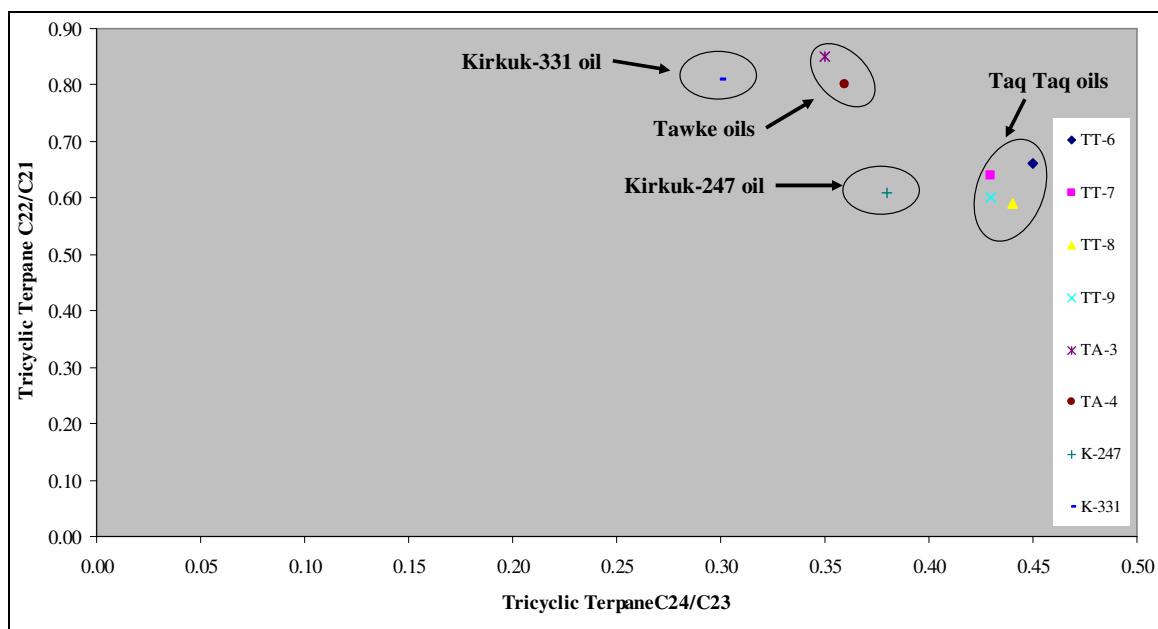
Figure 4.8: Plot of C_{24}/C_{23} tricyclic terpane versus C_{22}/C_{21} tricyclic terpane for oils from: TT-6, TT-7, TT-8, TT-9, TA-3, TA-4, K-247, and K-331 in northern Iraq. The plot separates Taq Taq, Tawke, Kirkuk-247, and Kirkuk-331 oils from each other.
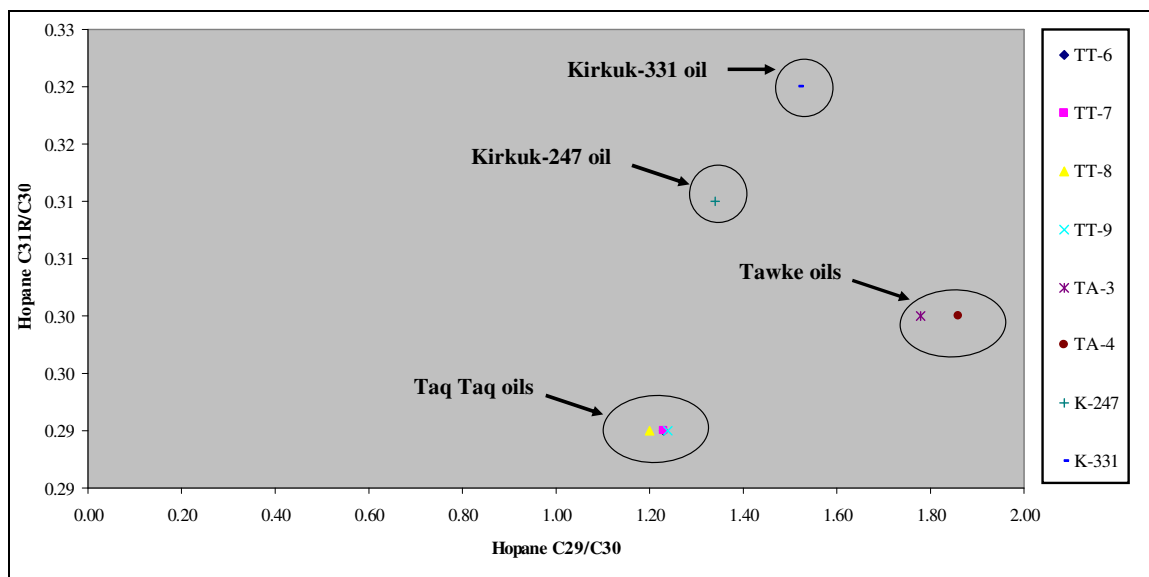
Figure 4.9: Plot of C_{29} norhopane/C_{30} hopane versus $C_{31}R$ homohopane (22R)/C_{30} hopane for oils from: TT-6, TT-7, TT-8, TT-9, TA-3, TA-4, K-247, and K-331 in northern Iraq. The plot separates Taq Taq, Tawke, Kirkuk-247, and Kirkuk-331 oils from each other.
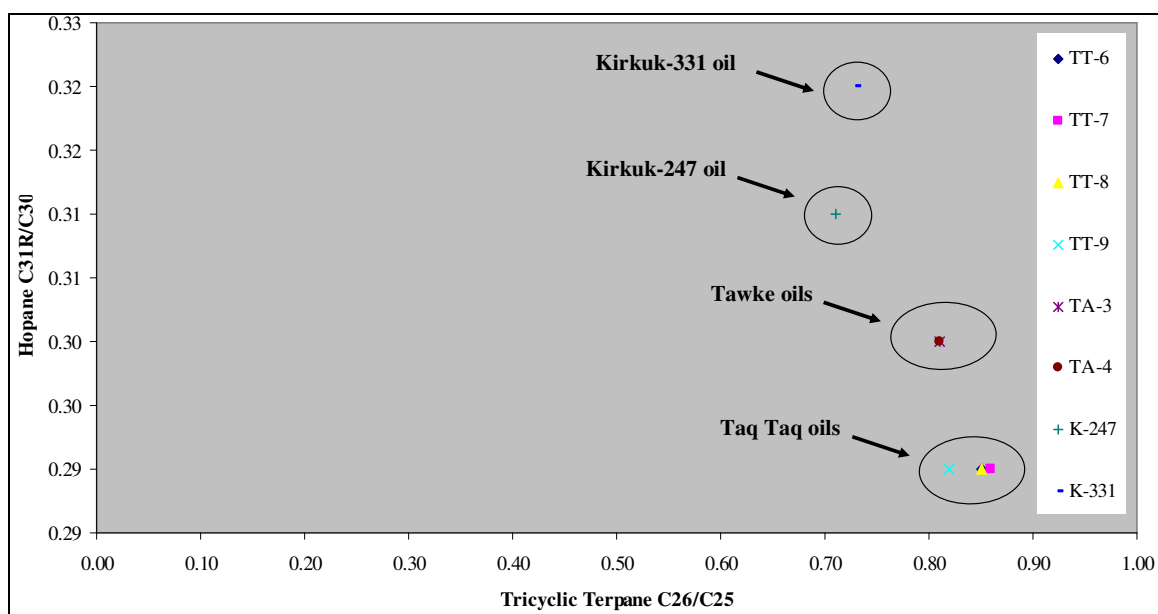
Figure 4.10: Plot of C_{26}/C_{25} tricyclic terpane versus $C_{31}R$ homohopane (22R)/C_{30} hopane for oils from: TT-6, TT-7, TT-8, TT-9, TA-3, TA-4, K-247, and K-331 in northern Iraq. The plot separates Taq Taq, Tawke, Kirkuk-247, and Kirkuk-331 oils from each other.
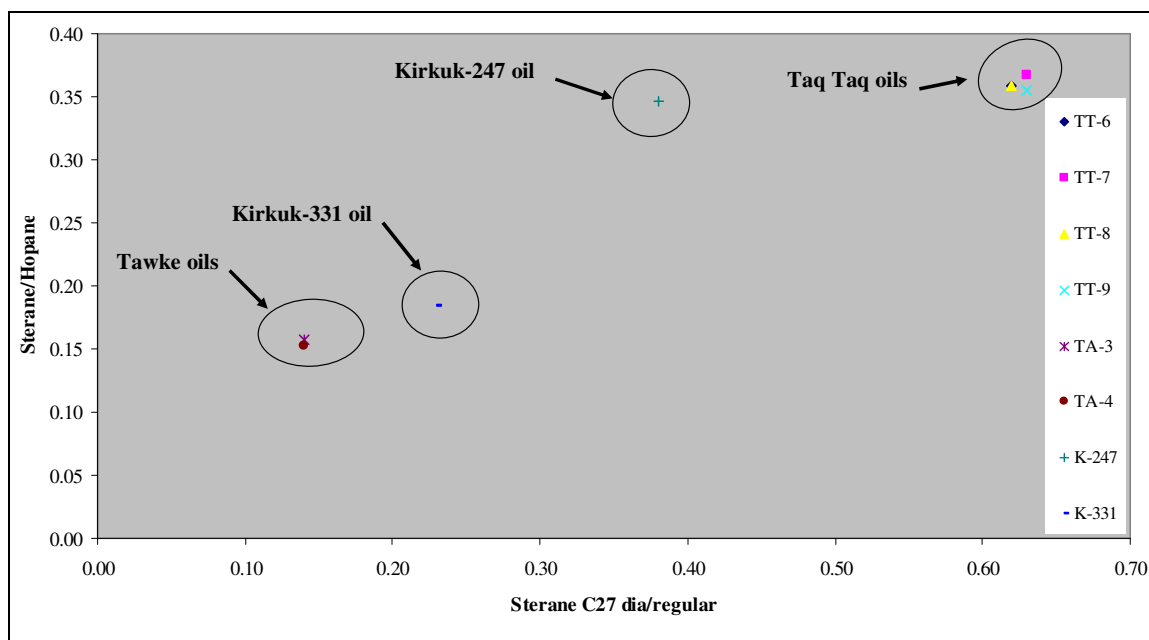
Figure 4.11: Plot of C_{27} rearranged/regular steranes (diacholestane/cholestane) versus steranes/hopanes (S_1-S_{15}/16 hopanes) for oils from: TT-6, TT-7, TT-8, TT-9, TA-3, TA-4, K-247, and K-331 in northern Iraq. The plot separates Taq Taq, Tawke, Kirkuk-247, and Kirkuk-331 oils from each other.

4.2.3   Discussion

The various diagrams and relationships between bulk properties and between biomarkers allow recognition of different oil families in eight oil wells in northern Iraq. It is apparent that there are three different oil families: (1) TT-6, TT-7, TT-8, and TT-9; (2) TA-3 and TA-4; (3) K-247 and K-331 according to C_{27} Ts/Tm trisnorhopane (17α, 21β-30-norhopane) versus C_{29} Ts/Tm aka C_{29}D/29H (18α-30-norneohopane), diahopane/C_{30} hopane versus gammacerane/C_{31}R homohopane, and C_{29} norhopane/C_{30} hopane versus C_{35} extended hopane/C_{34} extended hopane (22S) (Figs. 4.5, 4.6, and 4.7, respectively).

The canonical variable (CV) versus pristane/phytane (Pr/Ph) ratio, C_{24}/C_{23} tricyclic terpane versus C_{22}/C_{21} tricyclic terpane, C_{29} norhopane/C_{30} hopane versus C_{31}R homohopane (22R)/C_{30} hopane, C_{26}/C_{25} tricyclic terpane versus C_{31}R homohopane (22R) /C_{30} hopane, C_{27} rearranged/regular steranes (diacholestane/cholestane) versus steranes/
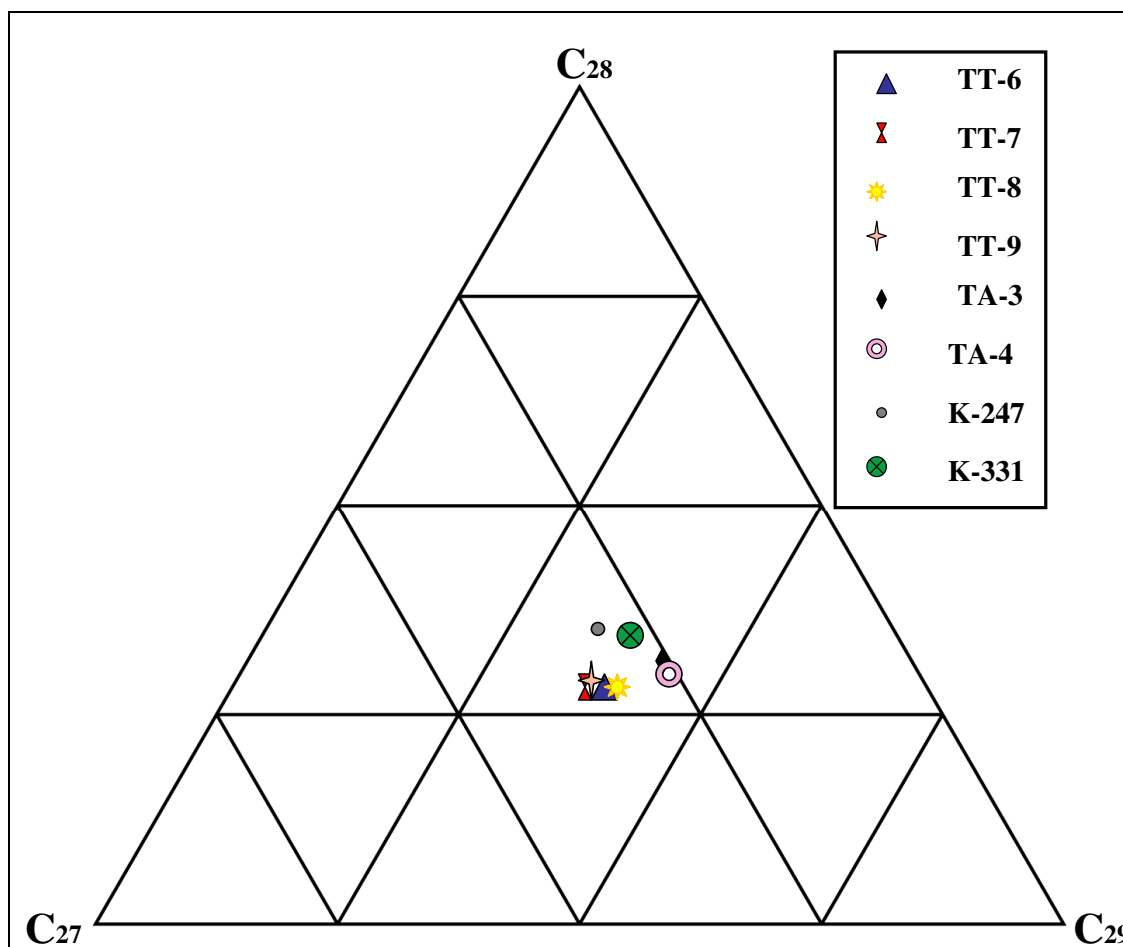
Figure 4.12: Ternary diagram shows the distribution of C_{27}, C_{28}, and C_{29} sterols for oils from: TT-6, TT-7, TT-8, TT-9, TA-3, TA-4, K-247, and K-331 in northern Iraq. The plot separates Taq Taq, Tawke, Kirkuk-247, and Kirkuk-331 oils from each other (adapted from Riva et al., 1986).

hopanes (S_1-S_{15}/16 hopanes), and distribution of C_{27}, C_{28}, and C_{29} sterols in the ternary diagram (Figs. 4.4, 4.8, 4.9, 4.10, 4.11, and 4.12, respectively), indicate that the K-247 and K-331 are not strongly linked together while the two others, the Tawke and Taq Taq oils, keep their affinity within their groups.

Bulk property measurements are not available for all samples. However, API gravity shows the relation between TA-4 and K-331 rather than between TA-3 and TA-4. This can be connected to biodegradation and alteration effects. The TA-4 may be more biodegraded. This can be observed from its asphalt percent content although %S and NSO's are either similar or greater in TA-3. The TA-4 is located at depths much shallower than TA-3 (Tables 4.1, 4.2, and 4.3). The Figure 4.3 shows good relations

between TA-3 and TA-4 and K-331 is close to them while K-247 shows no affinity to them. Nitrogen and oxygen versus sulfur wt. percent show the relation between TA-3 and TA-4 and between K-247 and K-331, but TT-6 is obviously different than the others (Fig. 4.2).

The carbon isotope ratios display good relationships between all Taq Taq oils and between both Tawke oils, but Kirkuk oils are not related to each other (Fig. 4.3). Thus, four oil families seem to exist: (1) TT-6, TT-7, TT-8, and TT-9; (2) TA-3 and TA-4; (3) K-247; and (4) K-331. The distribution of these oil families are shown in Figure 4.13.

These geochemically heterogeneous relationships between oils in the Kirkuk and Taq Taq oil fields are confirmed also through an earlier correlation between oils in the Tertiary Jeribi reservoir in K-156 Well with oil from the Cretaceous reservoir in the TT-1 Well (Ahmed, 2007). The study suggested no relation between these two oils, TT-1 and K-156.
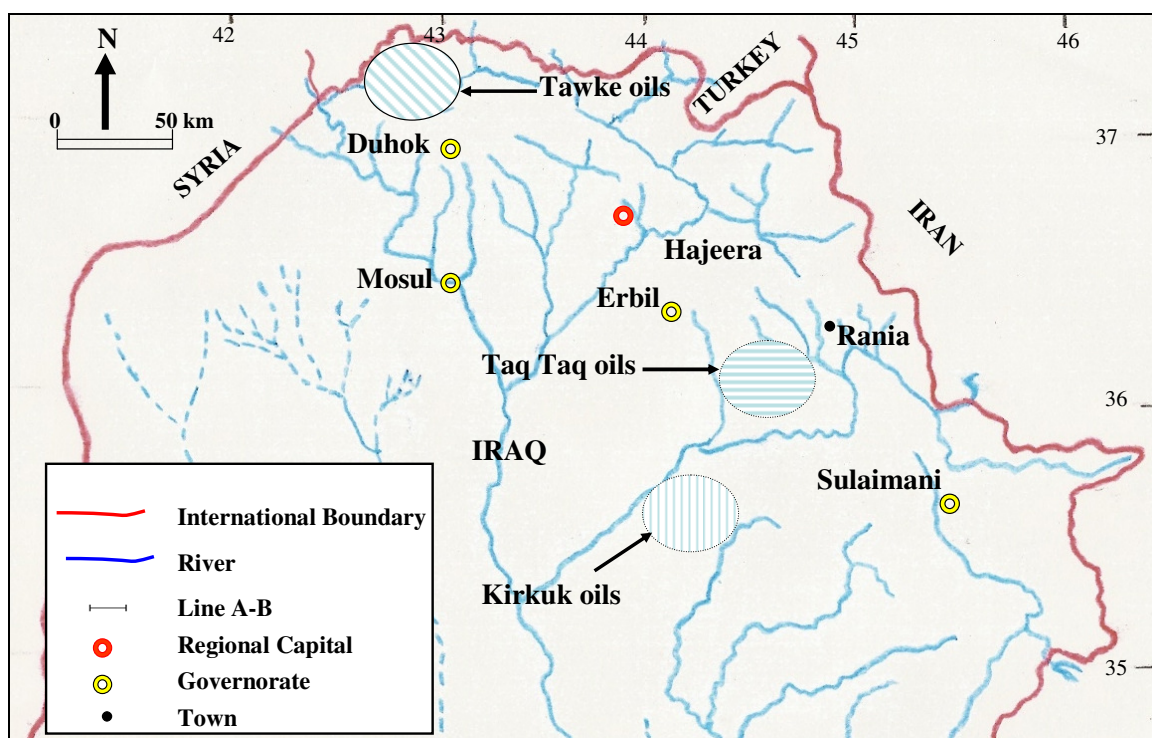
Figure 4.13: Distribution of oil families in northern Iraq according to eight crude oil samples from Taq Taq, Tawke, and Kirkuk oil fields. The map shows different oil families. Both Kirkuk oils, K-247 and K-331, are located within the same geographic region but they occur at different depths (–740m and –1174m for K-247 and K-331, respectively).

4.3   Depositional Environments of the Oils

The paleoenvironment can be determined based on some parameters, such as the stable carbon isotope values, the canonical variable (CV) values, the ratio of nickel to vanadium, and the carbon preference index. The paleoenvironment can also be determined based on the occurrence of some biomarkers since some of them are indicators for a specific ecosystem (Philp, 1985). Among them, acyclic isoprenoids (pristane and phytane), gammacerane, C_{35}/C_{34} hopane, C_{29} norhopane/C_{30} hopane, C_{22}/C_{21} tricyclic terpane, and C_{24}/C_{23} tricyclic terpane are used for determining the depositional environment.

Stable carbon isotope ratios have been used to differentiate sources of petroleum. The δ value for carbon can be used to describe small variations of the ^{13}C concentration in organic matter. A sample rich in heavy isotopes relative to the standard has a positive value while a sample poor in the heavy isotopes relative to the standard has negative δ value (Peters and Moldowan, 1993; Coplen, 1996; Peters et al., 2005a). The isotopic variations between the saturate and aromatic hydrocarbons are due to: (1) the source of the oil; (2) the absolute isotopic value of the oil; and (3) the maturity of the oil (Sofer, 1984).

Oils originated from terrigenous and marine organic matter have a different isotopic relationship between the saturate and aromatic hydrocarbon fractions. The isotopic relationship for oils of a waxy terrigenous organic source is

$$\delta^{13}C_{aro.} = 1.12\ \delta^{13}C_{sat.} + 5.45$$

and for oils of a nonwaxy marine organic source is

$$\delta^{13}C_{aro.} = 1.10\ \delta^{13}C_{sat.} + 3.75\ \text{(Sofer, 1984)}.$$

The canonical variable (CV) is a statistical parameter determined by evaluating the difference between the above equations and can be mathematically expressed as

$$CV = -2.53\ \delta^{13}C_{sat.} + 2.22\ \delta^{13}C_{aro.} - 11.65\ \text{(Sofer, 1984)}.$$

CV values determined by the above equation can be used to differentiate between waxy and nonwaxy oils. The CV values less than 0.47 specify a nonwaxy organic source, while CV values greater than 0.47 signify primarily a waxy organic source for the oil (Sofer, 1984). Table 4.1 shows stable carbon isotope values and CV values for the oil

samples from northern Iraq. It is clear that all CV values for examined oils range between (-3.51 to -1.59) which indicates a nonwaxy source. Figure 4.3 is a plot of $\delta^{13}C_{sat.}$ versus $\delta^{13}C_{aro.}$ for the oil samples which indicates a nonwaxy source for oils.

The ratio of nickel to vanadyl is low (Ni/V <1) for oil from K-331 Well (Table 4.1). This indicates that the oil from this well is derived from marine source rocks deposited under anoxic conditions with low Eh (Lewan, 1984; Barwise, 1990; Peters and Moldowan, 1993; Peters et al., 2005a). However, the ratio of nickel to vanadyl for other oils are not reliable due to precision because of their low concentration (Ni and V <15 ppm) (Zumberge, 2010, pers. comm.).

The carbon preference index is a ratio between a summation of peak heights at 25, 27, 29, 31 and 33 carbon atoms per molecule for the odd-carbon number n-paraffins and a summation of the even-carbon numbers at 24, 26, 28, 30, and 32 carbon atoms per molecule. In order to obtain accurate results, the mean between this value and another value is preferred. The other value can be obtained from the summation of peak heights at 25, 27, 29, 31 and 33 carbon atoms per molecule for the odd-carbon number n-paraffins divided by the summation of the even-carbon numbers at 26, 28, 30, 32, and 34 carbon atoms per molecule (Bray and Evans, 1961). The final ratio can be expressed mathematically as

$$CPI_{25-33} = 0,5*\left(\frac{(C_{25}+C_{27}+C_{29}+C_{31}+C_{33})}{(C_{24}+C_{26}+C_{28}+C_{30}+C_{32})}+\frac{(C_{25}+C_{27}+C_{29}+C_{31}+C_{33})}{(C_{26}+C_{28}+C_{30}+C_{32}+C_{34})}\right).$$

The CPI for samples from all eight wells was calculated. All of them have the CPI value <1 ranging between (0.94–0.97). This CPI range indicates that all oils from the studied wells originated from source rocks that were deposited under reducing conditions (Bray and Evans, 1961). The predominance of even-chain-length n-alkanes in the C_{20}-C_{30} range (22.1 and 19.6 for even and odd, respectively) is known to occur specifically in anoxic carbonate or evaporate sediments as stated by Tissot and Welte (1984).

High pristane/phytane (Pr/Ph) ratios >3.0 indicates a terrigenous organic matter contribution under anoxic conditions, while organic-rich anoxic carbonate rocks generally generate oils with ratios less than 2 (Didyk et al., 1978; Peters and Moldowan, 1993; Hughes et al., 1995; Hunt, 1996; Peters et al., 2005b) (Fig. 4.14). All samples analyzed in this report have a Pr/Ph ratio <1 (0.80–0.99) except K-247 which has a ratio
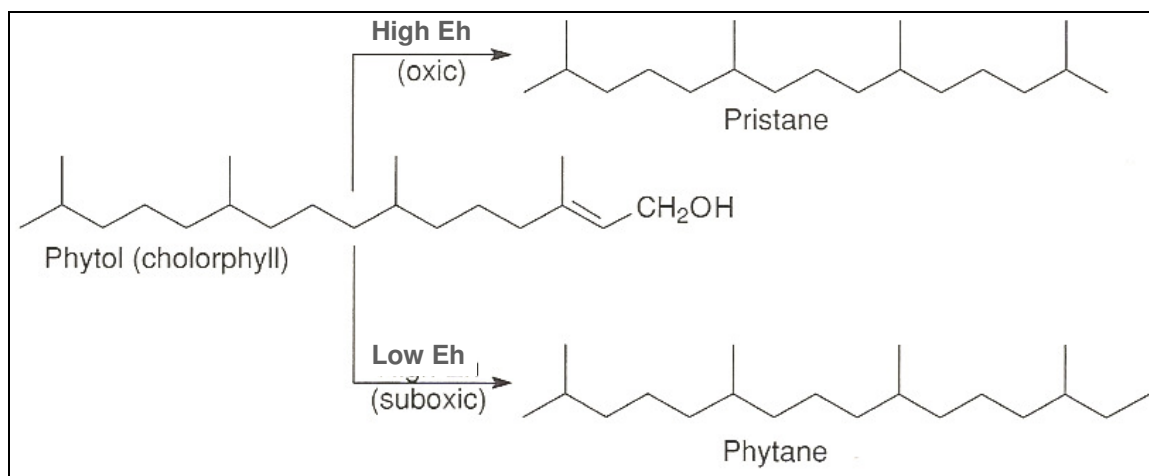
Figure 4.14: Diagenetic origin of pristane and phytane from phytol (modified from Peters and Moldowan, 1993; Peters et al., 2005b).

of 1.07 (Table 4.2). This indicates that all oil samples originated from carbonate source rocks that were deposited under anoxic and low Eh conditions.

The plot of canonical variable (CV) versus pristane/phytane (Pr/Ph) ratio shows the marine environment under reducing condition for oils in TT-6, TT-7, TT-8, TT-9, TA-3, TA-4, and K-331 while oil in K-247 shows slight variation (Fig. 4.4).

Gammacerane is a C_{30} pentacyclic triterpane associated with source rocks deposited under anoxic conditions. Generally, it is a high salinity indicator (Moldowan et al., 1985; Peters and Moldowan, 1993; Hunt, 1996; Peters et al., 2005b). The presence of small quantities of gammacerane in TA-3 and TA-4 indicate that they were deposited under hypersaline conditions, but the others show very small amounts (Table 4.3).

The $C_{35}S/C_{34}S$ hopane ratios are: 0.82, 0.91, 0.81, 0.82, 1.06, 1.07, 1.00, and 1.01; and the C_{29} norhopane/C_{30} hopane ratios are: 1.23, 1.23, 1.20, 1.24, 1.78, 1.86, 1.34, and 1.52 for TT-6, TT-7, TT-8, TT-9, TA-3, TA-4, K-247, and K-331 oils, respectively. The $C_{35}S/C_{34}S$ ratios >0.8 when combined with C_{29} norhopane/C_{30} hopane >0.6 indicate marine carbonate under anoxic conditions (Table 4.3) (Ten Haven et al., 1988; Peters and Moldowan, 1991; Peters et al., 2005b). A marine carbonate source that is under anoxic conditions can also be confirmed by the high C_{22}/C_{21} ratios: 0.66, 0.64, 0.59, 0.60, 0.85, 0.80, 0.61, and 0.81; and low C_{24}/C_{23} ratios: 0.45, 0.43, 0.44, 0.43, 0.35, 0.36, 0.38, and 0.30 tricyclic terpane for oils from TT-6, TT-7, TT-8, TT-9, TA-3, TA-4, K-247, and K-

331, respectively (Peters et al., 2005b; Zumberge, 2010, pers. comm.).

The stable carbon isotope values indicate a nonwaxy marine source for TT-6, TT-7, TT-8, TT-9, TA-3, TA-4, K-247, and K-331 oils. The oil from K-331 is derived from a marine source rock deposited under anoxic conditions with low Eh based on the ratio of nickel to vanadium. The sulfur wt. percent content values are 3.13, 3.51, 2.82, and 3.53 for oils in TA-3, TA-4, K-247, and K-331, respectively which indicate reducing conditions during deposition of the oils' source.

The canonical variable (CV) values, the carbon preference index, and predominance of even-chain-length n-alkanes in the C_{20}–C_{30} range supports the idea that the oils are derived from marine source rocks deposited under anoxic conditions with low Eh. In addition, all of the biomarkers including acyclic isoprenoids (pristane and phytane), gammacerane, $C_{35}S/C_{34}S$ hopane, C_{29} norhopane/C_{30} hopane, C_{22}/C_{21} tricyclic terpane, and C_{24}/C_{23} tricyclic terpane indicate carbonate source rocks that were deposited under anoxic and low Eh conditions.

The Najmah, Barsarin, Naokelekan, and Sargelu formations are carbonate dominant that were deposited under reducing conditions. Thus, the relation exists between oil's source rock depositional system and Lower-Upper Jurassic formations in study area (sections 2.1.1, 2.1.2, 2.2.5, and 2.2.6 in chapter 2).

4.4   Thermal Maturity of the Oils

The degree of thermal alteration of oil over time is called thermal maturity and reflects: (1) expulsion maturity, and (2) cracking after accumulation (Peters and Cassa, 1994; Peters et al., 2005a). The thermal maturity can be determined by a ratio of composition of biomarkers alternating with increasing thermal maturity (Philp, 1985).

The ratio between [$C_{31}S$ {17α, 21β-30-homohopane (22S)}]/[$C_{31}S$ {17α, 21β-30-homohopane (22S)} + $C_{31}R$ {17α, 21β-30-homohopane (22R)}], and the ratio between [$C_{32}S$ {17α, 21β-bishomohopane (22S)}]/[$C_{32}S$ {17α, 21β-bishomohopane (22R)} + $C_{32}R$ {17α, 21β-bishomohopane (22R)}], were used to estimate the thermal maturity. The ratio in the range 0.57–0.62 indicate equilibrium phase (Seifert and

The geochemical properties of oils and extracts from different source rocks are shown in Tables 4.1, 4.2, 4.3, and 4.5.

Oil-source rocks were correlated in this report by using the biomarker ratios: diahopane/C_{30} hopane versus gammacerane/C_{31}R homohopane(22R); C_{29} norhopane/C_{30} hopane versus C_{31}R homohopane (22R)/C_{30} hopane; C_{27} Ts/Tm trisnorhopane (17α, 21β-30-norhopane) versus C_{29} Ts/Tm aka C_{29}D/29H (18α-30-norneohopane); C_{24}/C_{23} tricyclic terpane versus C_{22}/C_{21} tricyclic terpane; C_{26}/C_{25} tricyclic terpane versus C_{31}R homohopane (22R)/C_{30} hopane; C_{27} rearranged/regular steranes (diacholestane/ cholestane) versus steranes/hopanes (S$_1$-S$_{15}$/16 hopanes); C_{27} Ts/Tm trisnorhopane versus C_{35}S extended hopane/C_{34}S extended hopane; C_{29} Ts/Tm trisnorhopane versus C_{35}S extended hopane/C_{34}S extended hopane; C_{31}R homohopane (22R)/C_{30} hopane versus [C_{20}+C_{21}]/[C_{20}-C_{28}] triaromatic sterane (a.k.a. 'cracking ratio') (Figs. 4.15, 4.16, 4.17, 4.18, 4.19, 4.20, 4.21, 4.22, and 4.23, respectively). The distribution of C_{27}, C_{28}, and C_{29} sterols on a ternary diagram for oils and extracts are shown in Figures 4.25 and 4.26. Bulk versus biomarker ratios is useful as well for correlation such as δ^{13}C$_{aromatics}$ versus C_{19}/C_{23} tricyclic terpane and δ^{13}C$_{saturates}$ versus C_{19}/C_{23} tricyclic terpane (Figs. 4.24 and 4.27).

The Taq Taq oils are related to extract from the Barsarin locality (Fig. 4.15). Furthermore, the Figure 4.16 shows affinity between Taq Taq oils and extract from the Sargelu village in addition to extract from the Barsarin locality. These oils have no relation to any extracts from QC-2, Qu-2, H-1, TA-15, and Gara (Figs. 4.15, 4.16, 4.17, 4.18, 4.19, 4.20, 4.21, 4.22, 4.23, 4.24, 4.25, and 4.27). In the same way, these oils show no affinity to extracts from W-3, W-19, W-120, and W-421 (Fig. 4.26). The Taq Taq oils show relation to one of the extracts from K-109 (Fig. 4.27). In addition to K-109, the relation between these oils and extracts from TT-1 and Zb-4 can be observed from Figure 4.26.

The Tawke oils show no relation to extract from the Sargelu locality (Figs. 4.18 and 4.20). These oils also show no link to extract from the Barsarin locality in addition to the extract from the Sargelu locality (Figs. 4.15, 4.16, 4.17, 4.19, 4.23, 4.24, 4.25, and 4.27). The extracts from TT-1, K-109, Zb-4, W-3, W-19, W-120, and W-421 are not correlated with oils from Tawke (Fig. 4.26). Figures 4.20 and 4.22 show a relation

Table 4.5: Geochemical characteristics of 17 extracts from 7 subsurface sections in Iraq and Syria. The data are from Ahmed (2007), Abboud et al. (2005), and Al-Ameri et al. (2009). The colored values for $\delta13C$ are obtained from Sofer's (1984) equation.

Field	Well	Formation	Age	Depth(m)	C_{19}/C_{23}	$\%C_{27}$	$\%C_{28}$	$\%C_{29}$	$Pr/n\text{-}C_{17}$	$Ph/n\text{-}C_{18}$	CPI	$^{13}C_{Sat}$	$^{13}C_{aro}$	CV
Soudieh	W-421	Soukhne	M. Cretace.	1817-1826		46.70	23.40	29.90				-28.56	-27.67	-0.81
Zarba	W-3	Shiranish	M. Cretace.	1378-1396		44.20	14.70	41.00				-27.20	-27.49	-3.86
Rumaila	Zb-4	Zubair	M. Cretace.			33.70	25.40	40.80	0.22	0.33	1.05	-27.20	-27.84	-4.64
Taq Taq	TT-1a	Chia Gara	U. Jura.-L. Creta.	3143	0.26	40.40	24.70	34.90	0.36	0.34	0.75	-27.90	-27.10	-1.23
Taq Taq	TT-1b	Chia Gara	U. Jura.-L. Creta.	3165	0.11	35.80	25.70	38.50	0.28	0.60	0.88	-27.90	-26.94	-0.87
Taq Taq	TT-1c	Chia Gara	U. Jura.-L. Creta.	3200	0.00	36.50	27.40	36.10	0.29	1.07	1.51	-27.80	-26.90	-1.03
Kirkuk	K-109a	Najmah	U. Jurassic	3104					0.25	0.69	0.49	-28.05	-27.10	-0.86
Kirkuk	K-109b	Najmah	U. Jurassic	3143					0.24	1.08	1.40			
Kirkuk	K-109c	Najmah	U. Jurassic	3164					0.23	0.45	0.60	-25.77	-24.60	-1.06
Kirkuk	K-109d	Najmah	U. Jurassic	3188					0.38	3.34	0.69			
Kirkuk	K-109e	Najmah	U. Jurassic	3210	0.21	37.20	24.90	37.90	0.29	2.11	0.37	-27.10	-27.00	-3.03
Kirkuk	K-109f	Najmah	U. Jurassic	3289	0.16	37.20	28.10	34.70	0.33	0.19	1.45	-27.50	-26.80	-1.57
Kirkuk	K-109g	Najmah	U. Jurassic	3299.4	0.14	38.10	27.00	34.90	0.32	0.17	0.79	-27.00	-26.60	-2.39
Kirkuk	K-109h	Najmah	U. Jurassic	3316	0.33	37.60	26.70	35.70	0.29	0.21	0.65	-26.90	-27.40	-4.42
Kirkuk	K-109i	Najmah	U. Jurassic	3364	0.24	39.50	25.90	34.70	0.15	0.31	0.58	-28.05	-27.10	-0.86
Ouda	W-120	Butmah	L. Jurassic	2253-2260		29.40	19.10	51.50				-31.41	-30.98	-0.96
Alhosin	W-19	Amanus	L. Triassic	2420-2430		29.50	30.30	40.10				-30.52	-30.00	-1.03

$C_{19}T$	$C_{19}H_{34}$ tricyclic dierpane	$\%C_{29}$	Relative % $S_{14}B$
$C_{23}T$	$C_{23}H_{42}$ tricyclic terpane	Pr	Pristane; relative %
C_{19}/C_{23}	C_{19}/C_{23}; peak heights from 191m/z	Ph	Phytane; relative %
$\%C_{27}$	Relative % S_5B	%Sat	% C15+ Saturated Hydrocarbons
$\%C_{28}$	Relative % $S_{10}B$	%Aro	% C15+ Aromatic Hydrocarbons

between Tawke oils and extracts from Qu-2 and H-1. The affinity between these oils and extract from QC-2 are shown in Figures 4.18, 4.21, and 4.22. The Tawke oils correlate poorly with one of the extracts from Gara (Fig. 4.15). A better link between these oils and one of the extracts from Gara can be seen in Figure 4.17. Furthermore, the Figures 4.16 and 4.20 displays a relation between both Gara extracts with oils from Tawke. The relation between these oils appears to be obvious with extracts from TA-15 as shown in Figures 4.23, 4.24, 4.16, 4.20, and 4.25.

The Kirkuk oils, K-247 and K-331, have no relation to extracts from W-3, W-19, W-120, and W-421 (Fig. 4.26). Both oils correlate with extracts from K-109 (Fig. 4.27) and extracts from Zb-4 and TT-1 in addition to K-109 (Fig. 4.26). K-247 oil shows a relation to extract from the Sargelu locality (Fig. 4.16) and K-331 has affinity to the same extract (Figs. 4.24 and 4.25). Both Kirkuk oils related to extracts from the Barsarin locality (Figs. 4.16, 4.17, and 4.19). K-247 shows no relation to extract from QC-2 based on all plots while K-331 shows link to this extract (Fig. 4.24). Figure 4.15 shows link between both Kirkuk oils with Qu-2; moreover, Figures 4.18, 4.20, and 4.24 supports this link between Qu-2 and K-331. K-247 related to extract from H-1 (Figs. 4.15 and 4.24) and K-331 related to this extract also (Figs. 4.15, 4.18, and 4.20). K-247 has resemblance to extracts from TA-15 (Figs. 4.15, 4.18, 4.19, and 4.22) and K-331 has affinity to the same extract (Figs. 4.15, 4.19, 4.20, and 4.22). Both Kirkuk oils linked to extracts from Gara (Figs. 4.15, 4.17, 4.21, and 4.22). In addition, Figures 4.18, 4.20, 4.24, and 4.25 supports this link between TA-15 and K-331.

Discussion

The extracts from W-19, W-120, W-421, and W-3 which represent Lower Triassic Amanus, Lower Jurassic Butmah, Middle Cretaceous Soukhne, and Middle Cretaceous Shiranish formations, respectively are clearly different from other extracts and oils (Fig. 4.26).

The extract from Zb-4 which belongs to Middle Cretaceous Zubair Formation appears to be close to Taq Taq oils (Fig. 4.26). These oils have no relation to any extracts

from QC-2, Qu-2, H-1, TA-15, and Gara (Figs. 4.15, 4.16, 4.17, 4.18, 4.19, 4.20, 4.21, 4.22, 4.23, 4.24, 4.25, and 4.27). These extracts belong to the Sargelu Formation. Thus, the Sargelu Formation has no molecular contribution to the Taq Taq oils. The Taq Taq oils are related to extracts from the Barsarin locality (Figs. 4.15 and 4.16), the Sargelu village (Fig. 4.16), K-109 Well (Figs. 4.26 and 4.27), and TT-1 Well (Fig. 4.26). The extracts from Sargelu, Barsarin, K-109, and TT-1 belong to Upper Jurassic formations, Naokelekan and Najmah.

According to Ahmed (2007), the oil in TT-1 correlates poorly with the extracts from the rocks at a depth of 3210–3364 m below the sea level in the K-109 Well and 3143–3200 m below the sea level in the TT-1 Well, while oils from the K-156 Well show no molecular contribution from these rocks. Ahmed (2007) thinks that the rocks at depth of 3210–3364 below the sea level in the K-109 Well belong to the Barsarin Formation, but the presence of this formation cannot be confirmed in the Kirkuk area (Buday, 1980; Jassim and Buday, 2006b). The rocks at a depth of 3210–3364 below the sea level likely belong to the Najmah Formation. Similarly Ahmed (2007) believes that the rocks at depth of 3143–3200 m below the sea level in the TT-1 Well belong to the Barsarin Formation, but this assumption conflicts with the presence of the Chia Gara Formation at the depth of 3112–3203 m below the sea level that were documented by Iraqi Company for Oil Operations (1978). According to this report, the Barsarin Formation with the thickness of 31 m is present at a depth of 3203−3234 m below the sea level. The geologic column of Jurassic succession in northern Iraq is shown in Figure 1.7. The oils in Taq Taq field likely originate from the Upper Jurassic formations, Naokelekan and Najmah. The Upper Jurassic-Lower Cretaceous Chia Gara Formation has molecular contribution as well.

The Tawke oils show no relation to extract from the Sargelu locality (Figs. 4.15, 4.16, 4.17, 4.18, 4.19, 4.20, 4.23, 4.24, 4.25, and 4.27). These oils also show no link to extract from the Barsarin locality (Figs. 4.15, 4.16, 4.17, 4.19, 4.23, 4.24, 4.25, and 4.27). The extracts from TT-1, K-109, and Zb-4 are not correlated with oils from Tawke (Fig. 4.26). The Tawke oils show relation to extracts from: Qu-2 and H-1 (Figs. 4.20 and 4.22); QC-2 (Figs. 4.18, 4.21, and 4.22); Gara (Figs. 4.15, 4.16, 4.17, and 4.20); and TA-15 (Figs. 4.16, 4.20, 4.23, 4.24, and 4.25). These extracts, QC-2, Qu-2, H-1, TA-15, and Gara, belong to the Sargelu Formation. Thus, the Sargelu Formation has molecular

contribution to oils in Tawke. The presence of small quantities of gammacerane in Tawke oils indicates Lower-Middle Jurassic age for oil's source (Peters and Moldowan, 1993; Zumberge, 2010, pers. comm.). This age supports the link between Tawke oils and extracts from the Middle Jurassic Sargelu Formation. In the same way, the relation exists between oil's source rock, carbonate deposited under reducing conditions, with the Sargelu Formation, carbonate dominant deposited under reducing conditions (sections 2.2.5, 2.2.6, and 4.3).

The Kirkuk oils, K-247 and K-331, appear to have various sources. Both oils correlate with extracts from: (1) Middle Cretaceous Zubair Formation in Zb-4 (Fig. 4.26); (2) Upper Jurassic-Lower Cretaceous Chia Gara Formation in TT-1 (Fig. 4.26); (3) Upper Jurassic formations: Najmah in K-109 (Figs. 4.26 and 4.27); K-247 oil with Naokelekan in the Sargelu locality (Fig. 4.16) and K-331 with same formation in the same locality (Figs. 4.24 and 4.25); Naokelekan in the Barsarin locality (Figs. 4.16, 4.17, and 4.19); and (4) Middle Jurassic Sargelu Formation in: Qu-2, K-247 (Fig. 4.15) and K-331 (Figs. 4.18, 4.20, and 4.24); H-1, K-247 (Figs. 4.15 and 4.24) and K-331 (Figs. 4.15, 4.18, and 4.20); TA-15, K-247 (Figs 4.15, 4.18, 4.19, and 4.22) and K-331 (Figs. 4.15, 4.19, 4.20, and 4.22); Gara, K-247 (Figs. 4.15, 4.17, 4.21, and 4.22) and K-331 (Figs. 4.15, 4.17, 4.18, 4.20, 4.21, 4.22, 4.24, and 4.25); and QC-2, only K-331 (Fig. 4.24).

Therefore, the Kirkuk oils have originated from different source rocks. The relation between Kirkuk oils and extracts from the Sargelu Formation was confirmed by Al-Ameri et al. (2006).The oils in two wells in Kirkuk field correlate with extracts from the Sargelu Formation in MK-2, Aj-8, and QC-1 (Ameri et al., 2006).

The oil in K-247 contains oleanane, which means its source may be Cretaceous or younger rocks or a mixture of Jurassic and Paleocene–Eocene. Zumberge (2010, pers. comm.) thinks that the oil in K-247 is likely from the Eocene Pabdeh shale. But the presence of this formation cannot be confirmed in Iraq. The purple shales of the Lower Pabdeh and the upper part of Amiran formations in southwestern Iran are comparable to the Kolosh Formation (James and Wynd, 1965; Furst, 1970; Buday, 1980; Jassim and Buday, 2006c). Therefore, the source of the oil in K-247 is probably from the Middle Paleocene-Early Eocene Kolosh Formation.
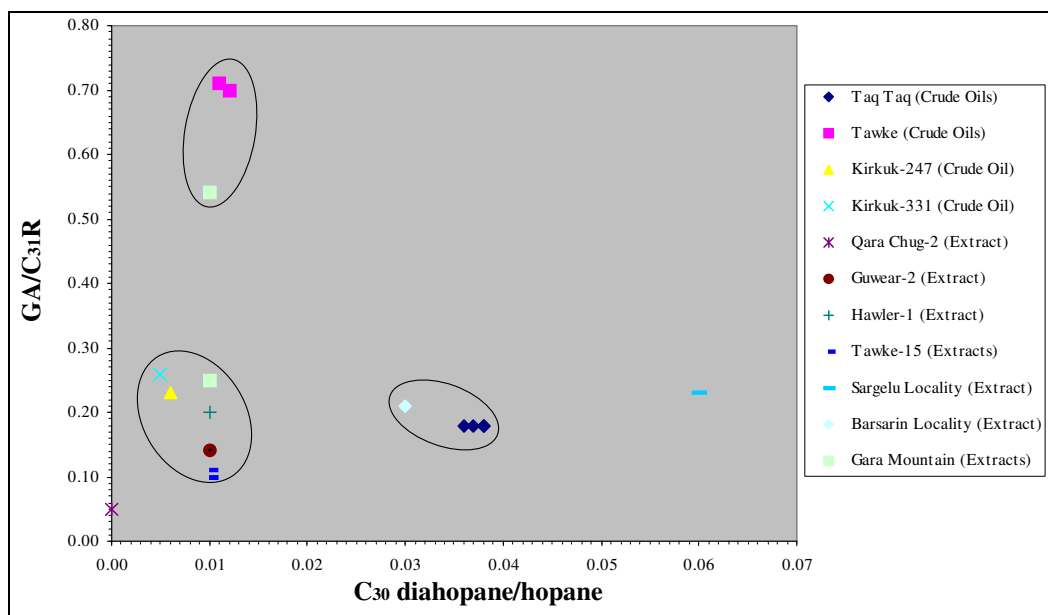
Figure 4.15: Plot of diahopane/C_{30} hopane versus gammacerane/C_{31}R homohopane (22R) for oils from: TT-6, TT-7, TT-8, TT-9, TA-3, TA-4, K-247, and K-331; and extracts from Qara Chug-2, Guwear-2, Hawler-1, Tawke-15, Sargelu, Barsarin, and Gara in northern Iraq. The plot shows a relation between: Taq Taq oils with extract from Barsarin village; Tawke oils with one of the extracts from Gara; K-247 with one of the extracts from Gara, Hawler-1, Guwear-2, and Tawke-15; and K-331 with one of the extracts from Gara, Hawler-1, Guwear-2, and Tawke-15.
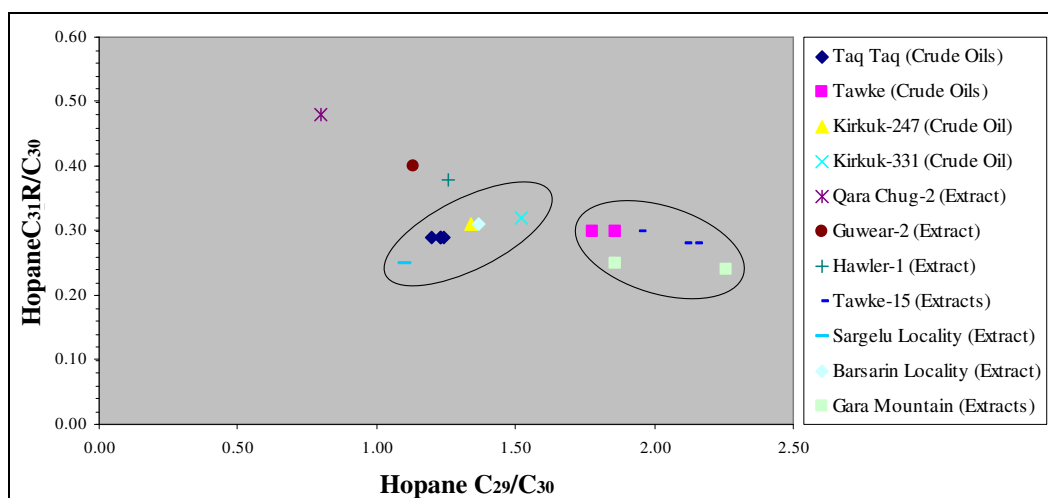
Figure 4.16: Plot of C_{29} norhopane/C_{30} hopane versus C_{31}R homohopane (22R)/C_{30} hopane for oils from: TT-6, TT-7, TT-8, TT-9, TA-3, TA-4, K-247, and K-331; and extracts from Qara Chug-2, Guwear-2, Hawler-1, Tawke-15, Sargelu, Barsarin, and Gara in northern Iraq. The plot shows a relation between: Taq Taq oils with extracts from Sargelu and Barsarin localities; Tawke oils with Gara and Tawke-15; K-247 with Barsarin and Sargelu; K-331 with Barsarin.
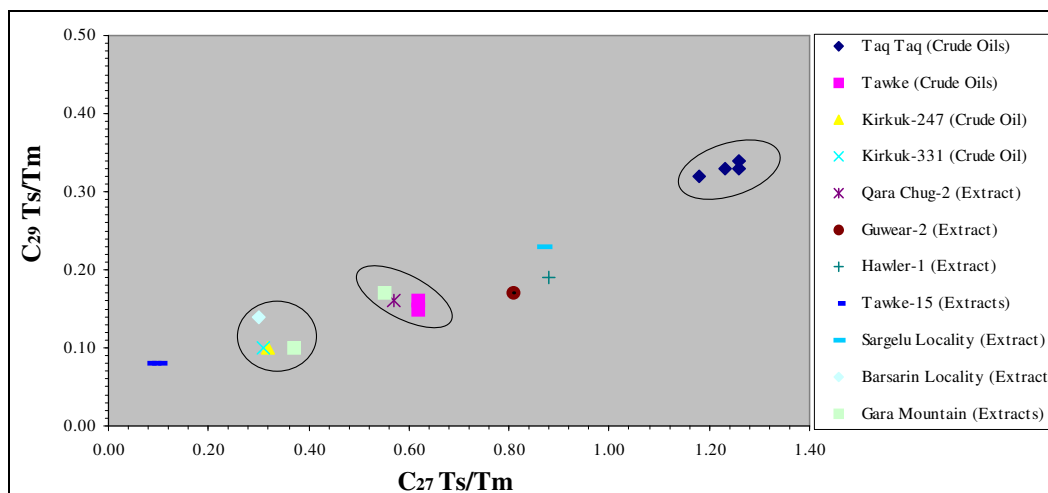
Figure 4.17: Plot of C_{27} Ts/Tm trisnorhopane (17α, 21β-30-norhopane) versus C_{29} Ts/Tm aka C_{29}D/29H (18α-30-norneohopane) for oils from: TT-6, TT-7, TT-8, TT-9, TA-3, TA-4, K-247, and K-331; and extracts from Qara Chug-2, Guwear-2, Hawler-1, Tawke-15, Sargelu, Barsarin, and Gara in northern Iraq. The plot shows no relation between Taq Taq oils with any of the extracts but shows a relation between: Tawke oils with extracts from Qara Chug-2 and one of the extracts from Gara; K-247 with one of the extracts from Gara and Barsarin; and K-331 with Gara and Barsarin.
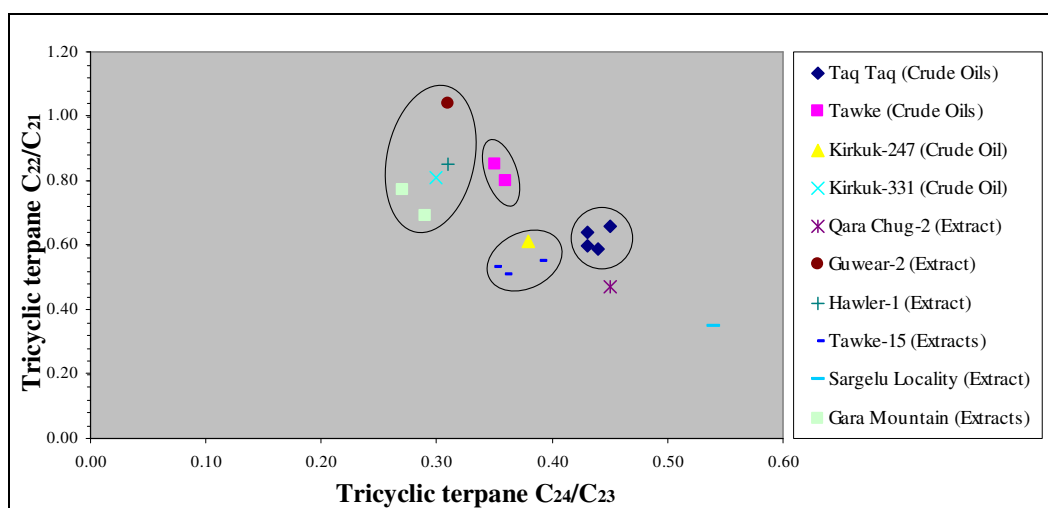
Figure 4.18: Plot of C_{24}/C_{23} tricyclic terpane versus C_{22}/C_{21} tricyclic terpane for oils from: TT-6, TT-7, TT-8, TT-9, TA-3, TA-4, K-247, and K-331; and extracts from Qara Chug-2, Guwear-2, Hawler-1, Tawke-15, Sargelu, and Gara in northern Iraq. The plot shows no relation between Taq Taq and Tawke oils with any of the extracts but shows a relation between: K-247 with Tawke-15; and K-331 with Gara, Hawler-1, and Guwear-2.
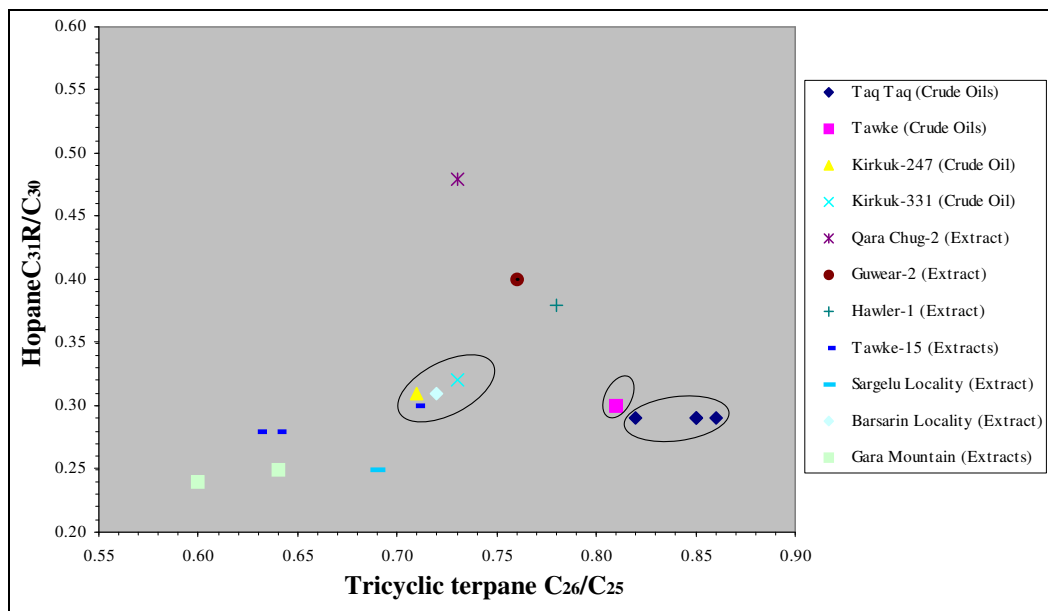
Figure 4.19: Plot of C_{26}/C_{25} tricyclic terpane versus $C_{31}R$ homohopane (22R)/C_{30} hopane for oils from: TT-6, TT-7, TT-8, TT-9, TA-3, TA-4, K-247, and K-331; and extracts from Qara Chug-2, Guwear-2, Hawler-1, Tawke-15, Sargelu, Barsarin, and Gara in northern Iraq. The plot shows no relation between Taq Taq and Tawke oils with any of the extracts but shows a relation between: K-247 with one of the extracts from Tawke-15, and Barsarin; and K-331 with one of the extracts from Tawke-15, and Barsarin.
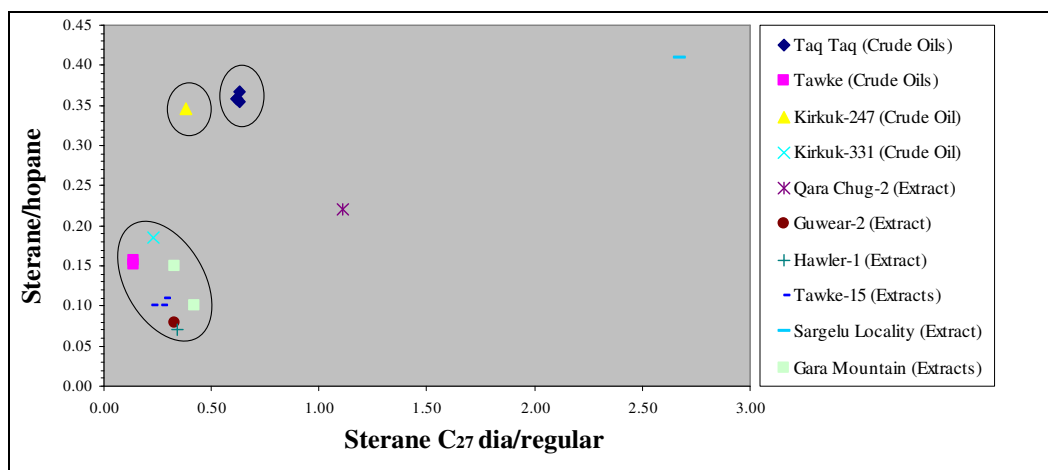
Figure 4.20: Plot of C_{27} rearranged/regular steranes (diacholestane/cholestane) versus steranes/hopanes (S_1-S_{15}/16 hopanes) for oils from: TT-6, TT-7, TT-8, TT-9, TA-3, TA-4, K-247, and K-331; and extracts from Qara Chug-2, Guwear-2, Hawler-1, Tawke-15, Sargelu, and Gara in northern Iraq. The plot shows no relation between Taq Taq and K-247 with any of the extracts but shows a relation between: Tawke oils with extracts from Guwear-2, Gara, Tawke-15, and Hawler-1; and K-331 with Guwear-2, Gara, Tawke-15, and Hawler-1.
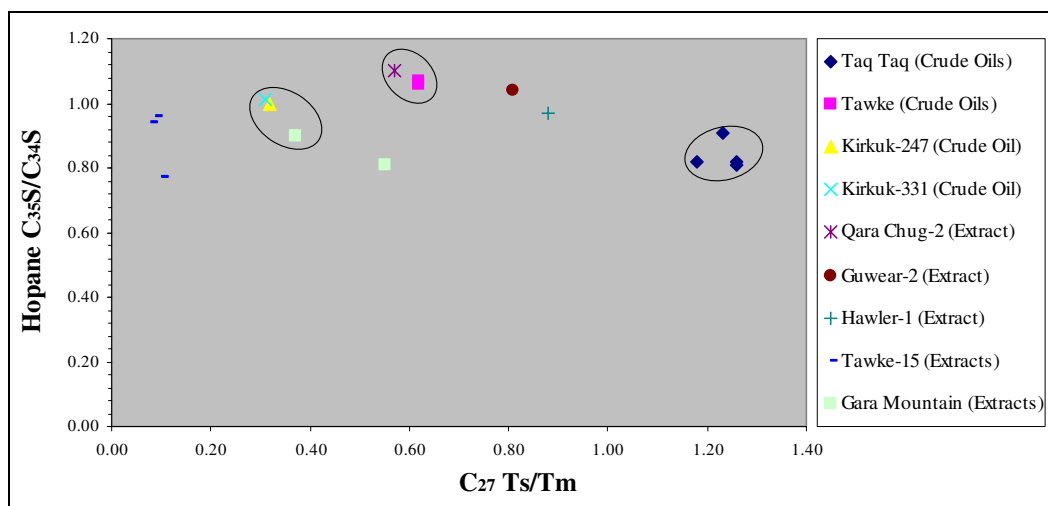
Figure 4.21: Plot of C_{27} Ts/Tm trisnorhopane versus $C_{35}S/C_{34}S$ extended hopane for oils from: TT-6, TT-7, TT-8, TT-9, TA-3, TA-4, K-247, and K-331; and extracts from Qara Chug-2, Guwear-2, Hawler-1, Tawke-15, and Gara in northern Iraq. The plot shows no relation between Taq Taq oils with any of the extracts but shows a relation between: Tawke oils with extract from Qara Chug-2; K-247 with one of the extracts from Gara; and K-331 with one of the extracts from Gara.
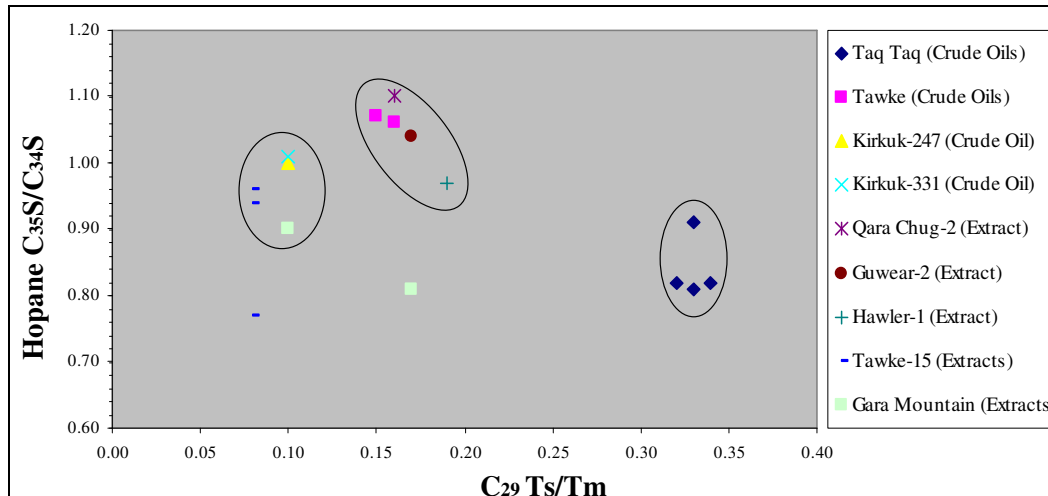
Figure 4.22: Plot of C_{29} Ts/Tm trisnorhopane versus $C_{35}S/C_{34}S$ extended hopane for oils from: TT-6, TT-7, TT-8, TT-9, TA-3, TA-4, K-247, and K-331; and extracts from Qara Chug-2, Guwear-2, Hawler-1, Tawke-15, and Gara in northern Iraq. The plot shows no relation between Taq Taq oils with any of the extracts but shows a relation between: Tawke oils with extracts from Qara Chug-2, Guwear-2, and Hawler-1; K-247 with one of the extracts from Gara and Tawke-15; and K-331 with one of the extracts from Gara and Tawke-15.
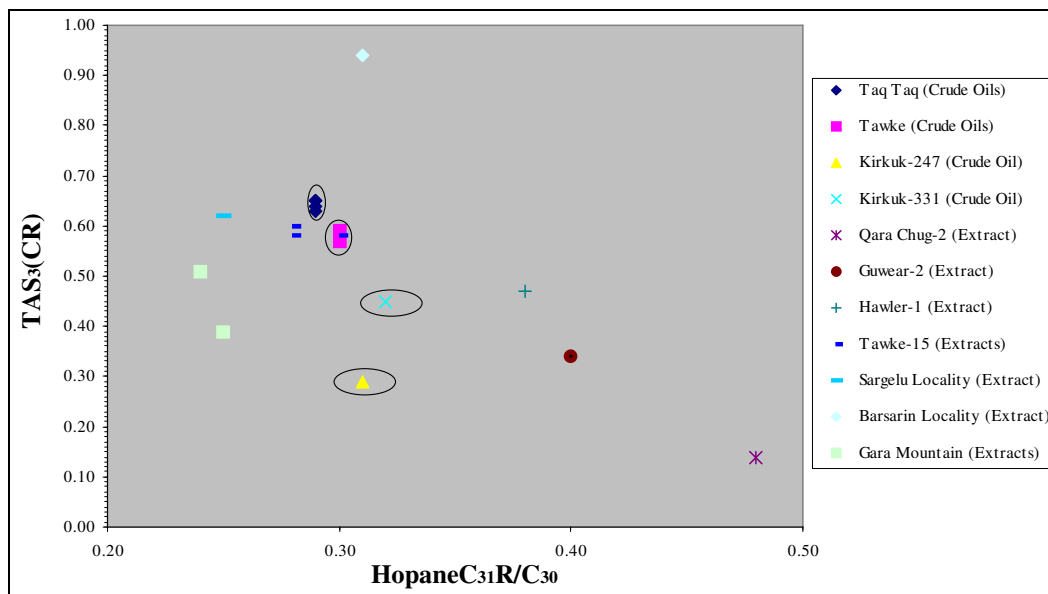
Figure 4.23: Plot of $C_{31}R$ homohopane (22R)/C_{30} hopane versus $[(C_{20}+C_{21})/(C_{20}-C_{28})]$ triaromatic sterane (a.k.a. 'cracking ratio') for oils from: TT-6, TT-7, TT-8, TT-9, TA-3, TA-4, K-247, and K-331; and extracts from Qara Chug-2, Guwear-2, Hawler-1, Tawke-15, Sargelu, Barsarin, and Gara in northern Iraq. The plot shows no relation between Taq Taq, K-247, and K-331 oils with any of the extracts but shows a relation between Tawke oils with one of the extracts from Tawke-15.
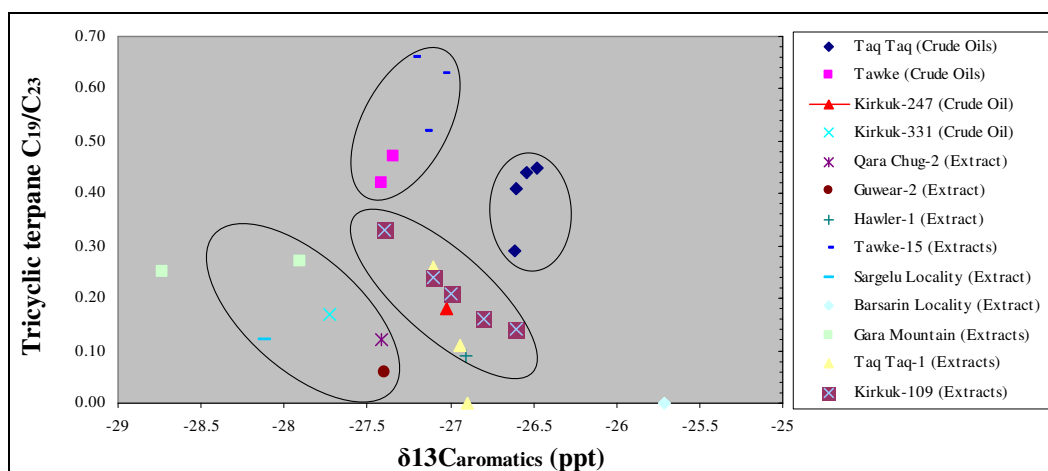
Figure 4.24: Plot of $\delta^{13}C_{aromatics}$ (ppt) versus C_{19}/C_{23} tricyclic terpane for oils from: TT-6, TT-7, TT-8, TT-9, TA-3, TA-4, K-247, and K-331; and extracts from Qara Chug-2, Guwear-2, Hawler-1, Tawke-15, Sargelu, Barsarin, Gara, Taq Taq-1, and Kirkuk-109 in northern Iraq. The plot shows no relation between Taq Taq oils to any of the extracts but shows a relation between: Tawke oils with extracts from Tawke-15; K-247 with Hawler-1, Taq Taq-1, and Kirkuk-109; and K-331 with Gara, Guwear-2, Qara Chug-2, and Sargelu.
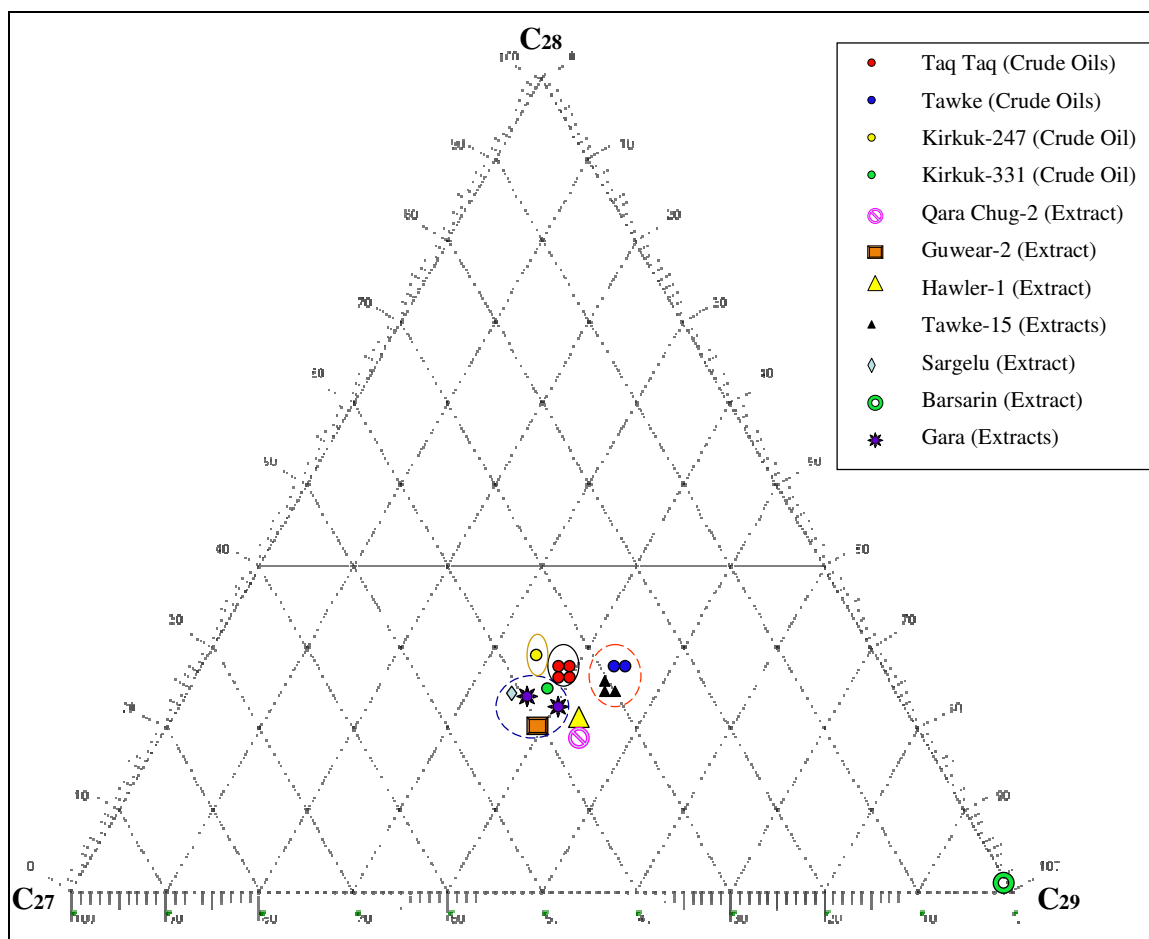
Figure 4.25: Ternary diagram shows the distribution of C_{27}, C_{28}, and C_{29} sterols for oils from: TT-6, TT-7, TT-8, TT-9, TA-3, TA-4, K-247, and K-331; and extracts from Qara Chug-2, Guwear-2, Hawler-1, Tawke-15, Sargelu, Barsarin, and Gara in northern Iraq. The diagram shows no relation between Taq Taq and K-247 oils to any of the extracts but shows a relation between: Tawke oils with extracts from TA-15a, TA-15b, and TA-15c; K-331 with Gara, Guwear-2, and Sargelu (adapted from Riva et al., 1986).
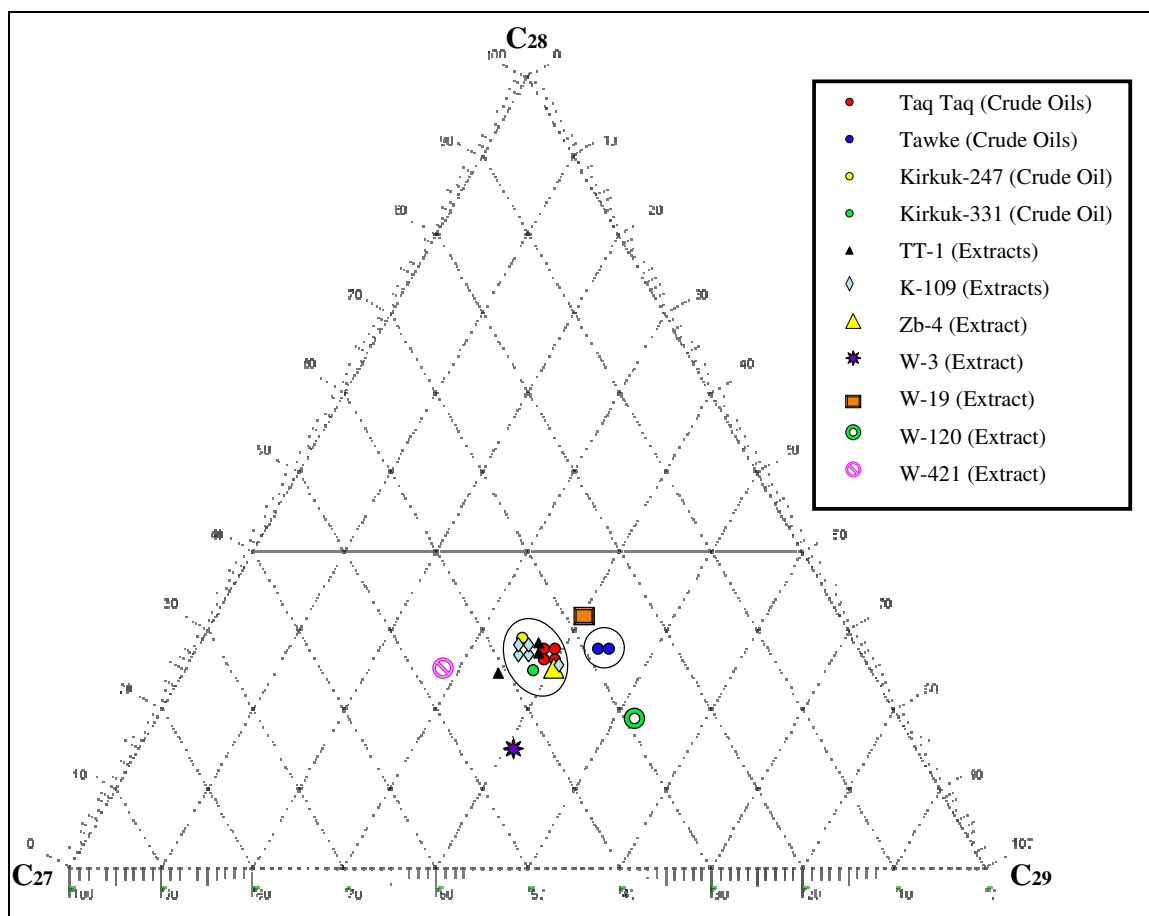
Figure 4.26: Ternary diagram shows the distribution of C_{27}, C_{28}, and C_{29} sterols for oils from: TT-6, TT-7, TT-8, TT-9, TA-3, TA-4, K-247, and K-331; and extracts from: W-3, W-19, W-120, and W-421 in Syria; TT-1 and K-109 in northern Iraq; and Zb-4 in southern Iraq. The diagram shows no relation between Tawke oils to any of the extracts but shows a relation between: Taq Taq oils with extracts from Taq Taq-1, Kirkuk-109, and Zubair-4; K-247 with extracts from Taq Taq-1, Kirkuk-109, and Zubair-4; and K-331 with Taq Taq-1, Kirkuk-109, and Zubair-4 (adapted from Riva et al., 1986).
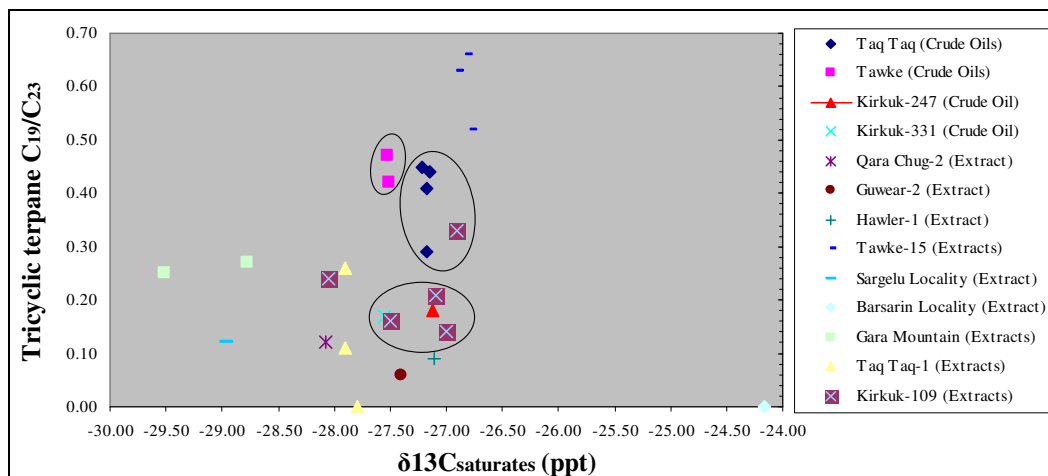
Figure 4.27: Plot of $\delta^{13}C_{saturates}$ (ppt) versus C_{19}/C_{23} tricyclic terpane for oils from: TT-6, TT-7, TT-8, TT-9, TA-3, TA-4, K-247, and K-331; and extracts from Qara Chug-2, Guwear-2, Hawler-1, Tawke-15, Sargelu, Barsarin, Gara, Taq Taq-1, and Kirkuk-109 in northern Iraq. The plot shows no relation between Tawke oils with any of the extracts but shows a relation between: Taq Taq oils with K-109; K-247 with Kirkuk-109; and K-331 with Kirkuk-109.

4.6   Oil Migration Path

The Sargelu Formation initially entered the oil generation phase at the end of Eocene Epoch (Beydoun et al., 1993). In the Kirkuk Embayment, the Jurassic source started to generate oil during the Oligocene Epoch (Pitman et al., 2004). In the fold belt, the Jurassic source reached peak oil generation in the Late Miocene and Pliocene time (Pitman et al., 2004).

This migration was in response to regional structural dips by sediment loading in the northeastern part of Iraq (Pitman et al., 2004). The structure map on the top Middle Jurassic at Middle Miocene is shown in Plate Ib and Figure 4.28 shows the thickness and geometry of Upper Miocene (Lower Fars Formation) and Pliocene (Bakhtiari Formation) oil container.

According to Pitman et al. (2004), the oil from the Foothills Zone migrated westward and southward towards the Salman Zone, the Mosul High, and the Euphrates River regions (Fig. 4.29). The Mosul High region also received migrated oil from fold belt in northern Iraq (Fig. 4.29). In the fold belt, faults became a main migration path for
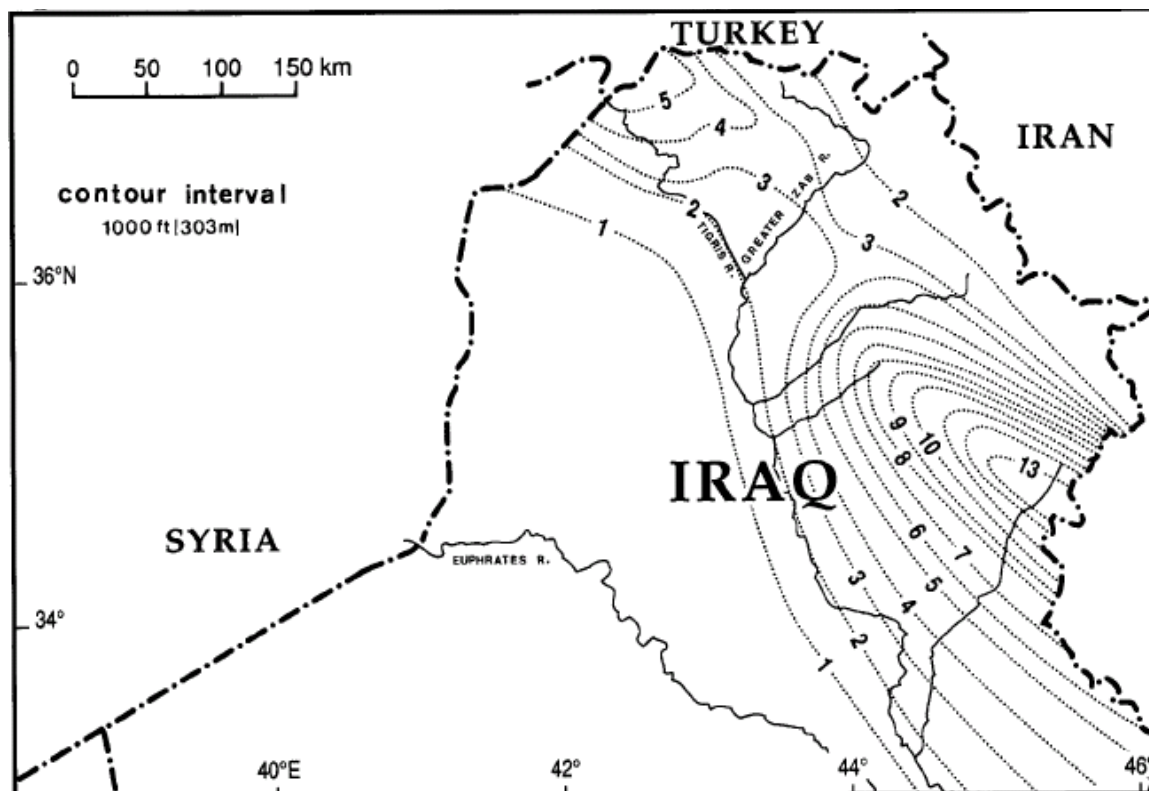
Figure 4.28: Isopach map of the Upper Miocene and Pliocene in northern Iraq (Ameen, 1992).

petroleum from the Jurassic source to younger reservoir beds (Pitman et al., 2004) (Fig. 1.6). The oil from the Foothill Zone migrated towards the central Mesopotamia Zone and then towards the Euphrates River region (Pitman et al., 2004). In the Kirkuk Oil Field, the V and Ni concentrations in the oil from the productive unit of Tertiary age is clearly different from oils in the Cretaceous (Al-Shahristani and Al-Atyia, 1973).

According to samples that were collected and analyzed for this study, there is no molecular contribution to oils found in Taq Taq from the Sargelu Formation. The Sargelu Formation may have molecular contribution to other oils in other localities or to oils in other horizons. The present distribution of Jurassic formations in Iraq is shown in the tectonic map of Iraq (Plate Ia). On the other hand, the molecular contribution from the Sargelu Formation to oils in Tawke and Kirkuk supports the idea that the oils that were generated from the Sargelu Formation were migrated from eastern part of the study area towards the west and southwestern. This molecular contribution from the Sargelu Formation to oils in western part of the studied area is shown by Al-Ameri et al. (2006).

The oil in Demir Dagh Oil Field (36º 12′ 36″ N and 43º 44′ 3″ E) correlates well with extracts from the Sargelu Formation in Makhul-2 Well at a depth of 2263.4 m below the sea level (Al-Ameri et al., 2006).
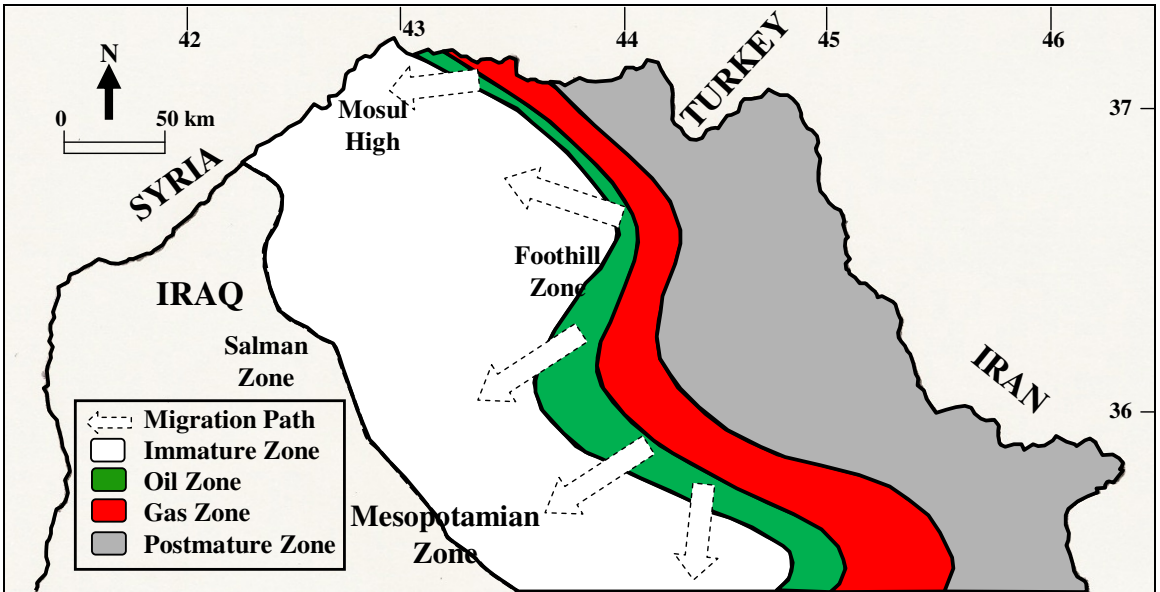
Figure 4.29: Map of northern Iraq shows the extent of oil and gas zones (highlighted in green and red), and the area of postmature and immature zones (highlighted in gray and white). The figure shows the migration pathways (arrows). My schematic arrows based on Pitman et al. (2004).

CHAPTER 5

CONCLUSIONS AND RECOMMENDATIONS

5.1   Conclusions

The main conclusions from this study are:

(1) Thickness

- The thickness progressively decreases from about 485 m west of the Tigris River in the Mosul area toward north where it is 20-30 m thick and northeastern Iraq where it is 49 m thick.

- This change in thickness is due to influence of the Kimmerian tectonic activity by causing the subsidence in the western part and uplift in the eastern part.

(2) Environment

- Position in overall marine basin represent deeper ramp.

- The organic-rich sediments of the Sargelu Formation indicate euxinic (anoxic).

(3) Richness (TOC)

- The TOC wt. percent of the sampled Sargelu Formation decreases toward the north and northeastern parts of Iraq. The mean of TOC wt. percent is 11.1 in northwestern part in Tawke-15 and it is only 0.5 in eastern part in Hanjeera locality.

- Land-derived organic matter contribution increases toward the northeast. The quality of organic matter also affected by high maturity especially toward the east and northeast.

(4) Kerogen type

- The organic material is characterized by type II and III kerogens.

(5) Maturity

- The thermal maturity increases to the east of the studied area from 431 ℃ T_{max} in

western part to 498 ℃ T_{max} in Barsarin village.

- Organic matter is within the dry gas zone in the eastern part, within oil window in the central portion, and marginally mature and immature further to the west and northwest.

(6) Oil types

- Four different oil families in northern Iraq are recognized. They are: (1) the Upper Jurassic Taq Taq; (2) the Lower–Middle Jurassic Tawke; (3) the Upper Jurassic Kirkuk; and (4) the Tertiary Kirkuk. Some of the plotted parameters do not separate Kirkuk oils and only distinguish three families.

(7) Oil-to-rock typing

- The geochemical parameters show a carbonate source for oils in a reducing environment.
- The biomarker parameters show no evidence of molecular contribution from the Sargelu Formation to the oils in Taq Taq, but the Tawke and Kirkuk oils show a molecular contribution from the Sargelu Formation.

(8) Migration pathways

- The oils that were generated from the Sargelu Formation were migrated from eastern part of the studied area toward western and southwestern parts.

5.2   Recommendations

The Sargelu Formation is considered to be a good source rock in the eastern part of the studied area. This formation has no molecular contribution to oils found in Taq Taq Oil Field. This may be due to isolation of its organically rich layers from good reservoirs or due to oil migration; however, further sampling may be required to quantify. It is recommended to provide researchers the seismic lines in order to discover structural traps, stratigraphic traps, and indicate active faulting in the area. Consequently, this helps to find the reason for no molecular contribution by the Sargelu Formation to the oils found in Taq Taq.

Triassic source rock data do not exist, and Paleozoic source rocks data are only

available for the Rutba area. Further study should include the main hydrocarbon source rocks, Paleozoic, Mesozoic, and Cenozoic. Additionally, the wider area than that covered by this study should be included in any future study to redraw the paleogeography map during different geologic times. This study indicates that the quantity (TOC wt. percent) and quality (hydrogen content) of organic matter decreases toward the north and northeastern part of the studied area. This phenomenon reflects facies change due to change in depositional environment and perhaps preservation or hydrocarbon generation. Thus, additional investigation is needed to indicate the location of shorelines, presence of ridges, or islands during Mesozoic time. Further study needs data through a broader area and may include parts of northwestern Iran, southeastern Turkey, central Iraq, and northeastern Syria. Regional correlation due to nomenclature is a problematic issue throughout the Middle East. This problem should be solved in order to obtain a successful correlation all through the area and to redraw paleogeographic map and indicate facies change vertically and laterally.

The Naokelekan Formation appears to be an important Jurassic source rock. More detailed study needed to quantify that. The role of this formation in the generated oils from whole Jurassic source rocks should be clarified.

The Triassic source rocks are present in the area and deeper drilling is required to penetrate them. Among these formations, the Upper Triassic (Rhaetic) Baluti Shale Formation is known to be a good source rock. The oils may be present in more than one pay zone. Therefore, the drilling to deeper horizons to penetrate older formations with broader seismic surveys should be performed to obtain better understanding of the area and find petroleum distribution and accumulation.

REFERENCES CITED

Abboud, M., R.P. Philp, and J. Allen, 2005, Geochemical correlation of oils and source rocks from central and NE Syria: Journal of Petroleum Geology, v. 28, issue 2, p. 203-216.

Abdullah, F.H.A., 2001, A preliminary evaluation of Jurassic source rock potential in Kuwait: Journal of Petroleum Geology, v. 24, issue 3, p. 361-378.

Ahlbrandt, T.S, R.M. Pollastro, T.R. Klett, C.J. Schenk, S.J. Lindquist, and J.E. Fox, 2000, Region 2 assessment summary—Middle East and North Africa: U.S. Geological Survey Digital Data Series 60, chapter R2, 39p. <http://energy.cr.usgs.gov/WEcont/regions/reg2/R2chap.pdf> Accessed March 3, 2010.

Ahmed, M.A., 1997, Sedimentary facies and depositional environments of Jurassic rocks, NW Iraq: Ph.D. dissertation (unpublished), Science College, University of Mosul, Mosul, Iraq, 170 p. (in Arabic).

Ahmed, S.M., 2007, Source rock evaluation of Naokelekan and Barsarin formations (Upper Jurassic) Kurdistan Region/N. Iraq: Master's thesis (unpublished), Science College, University of Sulaimani, Sulaimani, Iraq, 174 p.

Al-Ahmed, A.A.N., 2001, Palynofacies indications of depositional environment and source potential for hydrocarbon-Middle Jurassic (Sargelu Formation) northern Iraq: Master's thesis (unpublished), Science College, University of Baghdad, Baghdad, Iraq, 103 p. (in Arabic).

Al-Ahmed, A.A.N., 2006, Organic geochemistry, palynofacies and hydrocarbon potential of Sargelu Formation (Middle Jurassic) northern Iraq: Ph.D. dissertation (unpublished), Science College, University of Baghdad, Baghdad, Iraq, 120 p.

Al-Ameri, T.K., A. Al-Ahmed, J. Zumberge, J.K. Pitman, 2009, Hydrocarbon potential of the Middle Jurassic Sargelu Formation, Zagros Fold Belt, northern Iraq: AAPG Search and Discovery Article, no. 90090, Annual Convention and Exhibition, Denver, Colorado.

Al-Ameri, T.K., A.A. Najaf, J. Zumberge, and S. Brown, 2006, Petroleum potential and oil correlation of the Middle Jurassic Sargelu Formation, Iraq: AAPG Annual Convention and Exhibition, Houston, Texas, April 9-12, 2006.

Al-Ameri, T.K., A.J Al-Khafaji, J. Zumberge, 2009, Petroleum system analysis of the Mishrif reservoir in the Ratawi, Zubair, north and south Rumaila oil fields, southern Iraq: GeoArabia, Gulf PetroLink, Bahrain, v. 14, no. 4, p. 91-108.

Al-Ameri, T.K., Z.M. Markarian, and M.A. Naser, 2008, Middle Miocene Jeribe Formation hydrocarbon sources and accumulations, Diala District, northeastern Iraq: AAPG Search and Discovery Article, no. 90077, Middle East Conference and Exhibition, Manama, Bahrain.

Al-Barzanji, S.T.M., 1989, Facies analysis for Muhaiwir Formation-W. Iraq: Master's thesis (unpublished), Science College, University of Baghdad, Baghdad, Iraq, 86 p. (in Arabic).

Al-Dujaily, L.S., 1994, Stratigraphy section of Middle-Upper Jurassic system and Lower Cretaceous, northern Iraq: Master's thesis (unpublished), Science College, University of Baghdad, Baghdad, Iraq, 98 p. (in Arabic).

Al-Habba, Y.Q., and M.B. Abdullah, 1989, A geochemical study of hydrocarbon source rocks in northwestern Iraq: Oil and Arab Cooperation Journal, v. 15, p. 11-51 (in Arabic).

Al-Hadithi, J.N.A., 1989, Ostracods of Muhaiwir Formation (Middle Jurassic) in Iraqi Western Desert: Master's thesis (unpublished), Science College, University of Baghdad, Baghdad, Iraq, 103 p. (in Arabic).

Alizadeh, B., M.H. Adabi, and F. Tezheh, 2007, Oil-oil correlation of Asmari and Bangestan reservoirs using gas chromatography and stable isotopes in Marun Oilfield, SW Iran: Iranian Journal of Science & Technology, Transaction A, v. 31, no. A3, p. 241-253.

Al-Juboury, A.I., 2009, Palygorskite in Miocene rocks of northern Iraq-environmental and geochemical indicators: Acta Geologica Polonica, v. 59, no. 2, p 269-282.

Al-Kadhimi, J.A.M., and V.K., Sissakian (compiled), F.A. Ibrahim, and V.K., Sissakian (editing and cartographic completion), R.M. Al-Jumaily, and H.Kh. Mahmoud (approved), E.I. Ibrahim, and N.M. Al-Ali (cartographic execution), 1996, 2nd Edition, Tectonic map of Iraq: Ministry of Industry and Minerals-State Establishment of Geological Survey and Mining, series of geological maps of Iraq, sheet no. 2, National Library Legal Deposit no. 10/1996.

Al-Kubaisy, B.F.L., 2001, Analysis of depositional basin and petroleum evaluation of Middle-Upper Jurassic succession, northern Iraq: Ph.D. dissertation (unpublished), Science College, University of Baghdad, Baghdad, Iraq, 189 p. (in Arabic).

Allen, T.L., T.A. Fraser, and K.G. Osadetz, 2008, Rock-Eval/TOC data for 18 wells, Peel Plateau and Plain, Yukon Territory (65º 50' to 67º 00' N; 133º 45' to 135º 15' W): Yukon Geological Survey, Open File 2008-1, 14 p. plus spreadsheet(s): <http://ygsftp.gov.yk.ca/publications/openfile/2008/of2008_1.pdf> Accessed 2/8/2010.

Al-Omari, F.S., and A. Sadiq, 1977, Geology of northern Iraq: Mosul, Iraq, Mosul University Press, 198 p. (in Arabic).

Al-Mashhadani, A.M., 1986, Paleogeographic evolution of Mesopotamian sedimentary basin during Mesozoic and Cenozoic and relationship with the geological system of Arabia: Iraqi Geological Society Journal, v. 19, no. 3, p. 29-43.

Al-Sayyab, A., N. Al-Ansari, D. Al-Rawi, J. Al-Jassim, F. Al-Omari, and Z. Al-Shaikh, 1982, Geology of Iraq: Mosul, Iraq, Mosul University Press, 280 p. (in Arabic).

Al-Shahristani, H., and M.J. Al-Atyia, 1973, Determination and geochemical significance of trace elements in Iraqi crude oils using instrumental neutron activation analysis: Journal of Radioanalytical Chemistry, v. 14, p. 401-413.

Alsharhan, A.S., and K.H. Habib, 2005, Geological setting and hydrocarbon potential in the Mesopotamian Basin, Iraq: AAPG Search and Discovery Article, no. 90039, Annual Meeting (June 19-22), Calgary, Alberta, Canada.

Alsharhan, A.S., and A.E.M. Nairn, 2003, Sedimentary basins and petroleum geology of the Middle East: Amsterdam, Netherlands, Elsevier Science B. V., 843 p.

Alsharhan, A.S., and K. Magara, 1994, The Jurassic of the Arabian Gulf Basin-facies, depositional setting and hydrocarbon habitat, in Embry, A.F., B. Beauchamp, and D.J. Glass, eds., Pangea-global environments and resources: Canadian Society of Petroleum Geologists, Memoir 17, p. 397-412.

Altinli, I.E., 1966, Geology of eastern and southeastern Anatolia, Turkey: Bulletin of Mineral Research Exploration Institute of Turkey, Foreign Edition, Ankara, no. 60, p. 35-76.

Al-Zubaidi, A.A., and Al-Zebari, A.Y., 1998, Prospects for production and marketing of Iraq's heavy oil: Ministry of Oil, State Oil Marketing, Baghdad, Iraq, no. 1998. 221, 10 p.

Ameen, M.S., 1992, Effect of basement tectonics on hydrocarbon generation, migration, and accumulation in northern Iraq: AAPG Bulletin, v. 76, no. 3, p. 356-370.

Bacon, C.A., C.R. Calver, C.J. Boreham, D.E. Leaman, K.C. Morrison, A.T. Revill, and J.K. Volkman, 2000, The petroleum potential of onshore Tasmania-a review: Geological Survey Bulletin, 71, 93 p.

Balaky, S.M.H., 2004, Stratigraphy and sedimentology of Sargelu Formation (Middle Jurassic) in selected sections in Erbil and Duhuk Governorates–Iraqi Kurdistan: Master's thesis (unpublished), Science College, University of Salahaddin, Erbil, Iraq, 109 p.

Barwise, A.J.G., 1990, Role of nickel and vanadium in petroleum classification: Energy & Fuels, v. 4, p. 467-652.

Bellen, R.C. van, H.V. Dunnington, R. Wetzel, and D.M. Morton, eds., 1959, Lexique stratigraphic international: Paris, v. III, Asie, Fascicule 10a Iraq, 333 p.

Beydoun, Z.R., 1986, The petroleum resources of the Middle East-a review: Journal of Petroleum Geology, v. 9, issue 1, p. 5-28.

Beydoun, Z.R., M.W.H. Clarke, and R. Stoneley, 1992, Petroleum in the Zagros Basin-a Late Tertiary foreland basin overprinted onto the outer edge of a vast hydrocarbon-rich Paleozoic-Mesozoic passive-margin shelf, in MacQueen, R.W., and D.A. Leckie, eds. Foreland basins and fold belts: AAPG Memoir 55, p. 309-339.

Beydoun, Z.R., 1991, Arabian plate hydrocarbon geology and potential—a plate tectonic approach: AAPG studies in geology, no. 33, 77 p.

Beydoun, Z.R., 1993, Evolution of the northeastern Arabian plate margin and shelf-hydrocarbon habitat and conceptual future potential: Revue De L'institut Français Du Pétrole (IFP), v. 48, no. 4, p. 311-345.

Bissada, K.K., 1982, Geochemical constraints on petroleum generation and migration-a review, in Proceeding from the Association of South East Asian Nations Council on Petroleum 81, Manila, Philippine, October, 1981, p. 69-87.

Bordenave, M.L., and R. Burwood, 1990, Source rock distribution and maturation in the Zagros Orogenic Belt-provenance of the Asmari and Bangestan Reservoir oil accumulations, in Durand, B., and F. Bihar, eds., Proceedings of the 14th International Meeting on Organic Geochemistry, Paris, France (18-22 September 1989): Organic Geochemistry, v. 16, nos. 1-3, p. 369-387.

Bray, E.E., and E.D. Evans, 1961, Distribution of n-paraffins as a clue to recognition of source beds: Geochimica et Cosmochimica Acta, v. 22, no. 1, p. 2-15.

Buday, T., 1980, The regional geology of Iraq, v. 1, stratigraphy and paleogeography: Mosul, Iraq, Dar Al-Kutub Publishing House, University of Mosul, 445 p.

Coplen, T.B., 1996, New guidelines for reporting stable hydrogen, carbon, and oxygen isotope-ratio data: Geochimica et Cosmochimica Acta, v. 60, no. 17, p. 3359-3360.

Curtis, J.B., and P.G. Lillis, 2008, pers. comm.

Dahl, B., J. Bojesen-Koefoed, A. Holm, H. Justwan, E. Rasmussen, and E. Thomsen, 2004, A new approach to interpreting Rock-Eval S_2 and TOC data for kerogen quality assessment: Organic Geochemistry, Elsevier Ltd., v. 35, p. 1461-1477.

Demaison, G.J., and G. Moore, 1980, Anoxic environments and oil source bed genesis: AAPG Bulletin, v. 64, no. 8, p. 1179-1209.

Dembicki Jr, H., 2009, Three common source rock evaluation errors made by geologists during prospect or play appraisals: AAPG Bulletin, v. 93, no. 3, p. 341-356.

Didyk, B.M., B.RT. Simoneit, S.C. Brassell, and G. Eglinton, 1978, Organic geochemical indicators of paleoenvironmental conditions of sedimentation: Nature, v. 272, p. 216-222.

Ditmar, V. and Iraqi-Soviet Team, 1971, Geological conditions and hydrocarbon prospects of the Republic of Iraq (northern and central parts) (manuscript report): Iraq National Oil Company, Baghdad, Iraq.

Dubertret, B., 1966, Liban, Syrie et bordure des pays voisins: Notes and Memoires Meyen Orient, v. VIII, Paris.

Dunnington, H.V., 1953a, Alan Anhydrite Formation, in Bellen, R.C. van, H.V. Dunnington, R. Wetzel, and D.M. Morton, eds., Lexique stratigraphic international: Paris, v. III, Asie, Fascicule 10a Iraq, p. 34-35.

Dunnington, H.V., 1953b, Gotnia Anhydrite Formation, in Bellen, R.C. van, H.V. Dunnington, R. Wetzel, and D.M. Morton, eds., Lexique stratigraphic international: Paris, v. III, Asie, Fascicule 10a Iraq, p. 117-120.

Dunnington, H.V., 1953c, Najmah Limestone Formation, in Bellen, R.C. van, H.V. Dunnington, R. Wetzel, and D.M. Morton, eds., Lexique stratigraphic international: Paris, v. III, Asie, Fascicule 10a Iraq, p. 207-211.

Dunnington, H.V., 1955, Generation, migration, accumulation and dissipation of oil in northern Iraq, in Weeks, L.G., ed., Habitat of oil: AAPG Symposium, p. 1194-1251.

Durand, B., 1988, Understanding of HC migration in sedimentary basins (present state of knowledge): Organic Geochemistry, v. 13, no. 1-3, p. 445-459.

Erik, N.Y., O. Özçelik, and M. Altunsoy, 2006, Interpreting Rock–Eval pyrolysis data using graphs of S_2 vs. TOC, Middle Triassic–Lower Jurassic units, eastern part of SE Turkey: Journal of Petroleum Science and Engineering, v. 53, issues 1-2, p. 34-46.

Erik, N.Y., O. Özçelik, M. Altunsoy, and H.I. Illeez, 2005, Source-rock hydrocarbon potential of the Middle Triassic—Lower Jurassic Cudi Group Units, eastern southeast Turkey: International Geology Review, v. 47, no. 4, p. 398-419.

Espitalié, J., J.L. Laporte, M. Madec, F. Marquis, P. Leplat, J. Paulet, and A. Boutefeu, 1977, Rapid method for source rocks characterization and for determination of petroleum potential and degree of evolution: Revue De L'institut Français Du Pétrole (IFP), v. 32, no. 1, p. 23-42.

Espitalié, J., G. Deroo, and F. Marquis, 1985, Rock-Eval pyrolysis and its applications: Revue De L'institut Français Du Pétrole (IFP), v. 40, no. 5, p. 563-579.

Fox, J.E., and T.S. Ahlbrandt, 2002, Petroleum geology and total petroleum systems of the Widyan Basin and interior platform of Saudi Arabia and Iraq: USGS Bulletin 2202-E, version 1.0, 26 p.

Furst, M., 1970, Stratigraphie und Werdegang der oestlichen Zagrosketten (Iran): Erlanger Geology Abhandlungen, v. 80, 50 p.

Geologic Materials Center, 1990, Total organic carbon, Rock-Eval pyrolysis, and whole oil gas chromatograms of core from the Standard Alaska Production Co. Sag Delta 34633 No. 4 well (11,637–12,129) and from the Shell Oil Co. OCS Y-0197 (Tern No. 3) well (12,978-13,131): State of Alaska Geologic Materials Center Data Report no. 157, total of 4 pages in report. <http://www.dggs.dnr.state.ak.us/webpubs/dggs/gmc/text/gmc157.PDF> Accessed 2/14/2010.

Haq, B.U. and A. Al-Qahtani, 2005, Phanerozoic cycles of sea-level change on the Arabian platform: GeoArabia, Gulf PetroLink, Bahrain, v. 10, no. 2, p. 127-160.

Hill, K.C., and S. Shane, 2009, Bayou Bend signs agreements for three highly prospective blocks in Kurdistan: Bayou Bend Petroleum Ltd., <http://www.marketwire.com/press-release/Bayou-Bend-Signs-Agreements-for-Three-Highly-Prospective-Blocks-in-Kurdistan-TSX-VENTURE-BBP-1037441.htm> Accessed January 23, 2010.

Huc, A.Y., and J.M. Hunt, 1980, Generation and migration of hydrocarbons in offshore south Texas Gulf Coast sediments: Geochemica et Cosmochimica Acta, printed in Great Britain, v. 44, p. 1081-1089.

Hughes, W.B., A.G. Holba, and L.I.P. Dzou, 1995, The ratios of dibenzothiophene to phenanthrene and pristane to phytane as indicators of depositional environment and lithology of petroleum source rocks: Geochimica et Cosmochimica Acta, v. 59, no.17, p. 3581-3598.

Hunt, J.M., 1996, Petroleum geochemistry and geology, second edition: New York, W. H. Freeman, and Company, 743 p.

Ibrahim, M.W., 1984, Geothermal gradients and geothermal oil generation in southern Iraq-a preliminary investigation: Journal of Petroleum Geology, v. 7, issue 1, p. 77-86.

Iraqi Company for Oil Operations-deepening program, 1978, Taq Taq-1 final report, 5 p.

James, G.A., and J.G. Wynd, 1965, Stratigraphic nomenclature of Iranian oil consortium agreement area: AAPG Bulletin, v. 49, no. 12, p. 2182-2245.

Jassim, S.Z., and T. Buday, 2006a, Units of the Unstable Shelf and the Zagros Suture, chapter 6, in Jassim, S.Z., and J.C. Goff, eds., Geology of Iraq, first edition: Brno, Czech Republic, Prague and Moravian Museum, p. 71-83.

Jassim, S.Z., and T. Buday, 2006b, Late Toarcian-Early Tithonian (Mid-Late Jurassic) Megasequence AP7, chapter 10, in Jassim, S.Z., and J.C. Goff, eds., Geology of Iraq, first edition: Brno, Czech Republic, Prague and Moravian Museum, p. 117-123.

Jassim, S.Z., and T. Buday, 2006c, Middle Paleocene-Eocene Megasequence AP10, chapter 13, in Jassim, S.Z., and J.C. Goff, eds., Geology of Iraq, first edition: Brno, Czech Republic, Prague and Moravian Museum, p. 155-168.

Jassim, S.Z., T. Buday, I. Cicha, and V. Prouza, 2006, Late Permian-Liassic MegasequenceAP6, chapter 9, in Jassim, S.Z., and J.C. Goff, eds., Geology of Iraq, first edition: Brno, Czech Republic, Prague and Moravian Museum, p. 104-116.

Jassim, S.Z., and M. Al-Gailani, 2006, Hydrocarbons, chapter 18, in Jassim, S.Z., and J.C. Goff, eds., Geology of Iraq, first edition: Brno, Czech Republic, Prague and Moravian Museum, p. 232-250.

Jassim, S.Z., and S.A. Karim, 1984, Final report on regional geology survey of Iraq: Paleogeography, State Organization for Mineral, Baghdad, Iraq, v.4, 69 p.

Karim, H.K., 2009, pers. comm.

Khan, B., H. Abu-Habbiel, H. Al-Ammar, M. Qidwai, A. Al Enezi, and A. Al-Ajmi, 2009, Integrated fracture characterization of Najmah-Sargelu, tight carbonate reservoirs, Sabriyah Structure, Kuwait-its implications from hydrocarbon exploration: AAPG Search and Discovery Article, no. 90090, Annual Convention and Exhibition (June 7-10), Denver, Colorado.

Konyuhov, A.I., and B. Maleki, 2006, The Persian Gulf Basin: geological history, sedimentary formations, and petroleum potential: Lithology and Mineral Resources, Pleiades Publishing, Inc., v. 41, no. 4, p. 344-361.

Levorsen, A.I., 2001, Geology of petroleum, second edition: Tulsa, Oklahoma, AAPG Foundation, 724 p.

Lewan, M.D., and T.E. Ruble, 2002, Comparison of petroleum generation kinetics by isothermal hydrous and nonisothermal open-system pyrolysis: Organic Geochemistry, v. 33, p. 1457-1475.

Lewan, M.D., 1984, Factors controlling the proportionality of vanadium to nickel in crude oils: Geochimica et Cosmochimica Acta, v. 48, p. 2231-2238.

Marouf, N.Z., 1999, Dynamic evolution of the sedimentary basins in northern Iraq and hydrocarbon formation, migration and entrapment: Ph.D. dissertation (unpublished), Science College, University of Baghdad, Baghdad, Iraq, 236 p.

May, P.R., 1991, The eastern Mediterranean Mesozoic Basin-evolution and oil habitat: AAPG Bulletin, v. 75, p. 1215-1232.

Mohyaldin, I.M.J., 2008, Source rock appraisal and oil/source correlation for the Chia Gara Formation, Kurdistan-north Iraq: Ph.D. dissertation (unpublished), Science College, University of Sulaimani, Sulaimani, Iraq, 140 p.

Mohyaldin, I.M.J., and F.M. Al-Beyati, 2007, Sedimentology and hydrocarbon generation potential of Middle Tithonian-Berriassian Chia Gara Formation, Well K-109, Kirkuk Oil Field, NE Iraq: Journal of Kirkuk University-Scientific Studies, v. 2, no. 1, p. 27-43.

Moldowan, J.M., W.K. Seifert, and E.J. Gallegos, 1985, Relationship between petroleum composition and depositional environment of petroleum source rocks: AAPG Bulletin, v. 69, p. 1255-1268.

Moshrif, M.A., 1987, Sedimentary history and paleogeography of Lower and Middle Jurassic rocks, central Saudi Arabia: Journal of Petroleum Geology, v. 10, issue 3, p. 335-350.

Murris, R.J., 1980, Middle East-stratigraphic evolution and oil habitat: AAPG Bulletin, v. 64, no. 5, p. 597-618.

Muttoni, G., M. Gaetani, D.V. Kent, D. Sciunnach, L. Angiolini, F. Berra, E. Garzanti, M. Mattei, and A. Zanchi, 2009, Opening of the Neo-Tethys Ocean and the Pangea B to Pangea A transformation during the Permian: GeoArabia, Gulf PetroLink, Bahrain, v. 14, no. 4, p. 17-48.

North Oil Company, 1953, Final report of Well K-109 (unpublished report): Kirkuk, Iraq.

Numan, N.M.S., 1997, A plate tectonic scenario for the Phanerozoic succession in Iraq: Iraqi Geological Society Journal, v. 30, no. 2, p. 85-110.

Numan, N.M.S., 2000, Major Cretaceous tectonic events in Iraq: Rafidain Journal Society, v. 11, no. 3, p. 32-54.

Ormiston, A.R, 1993, The association of radiolarians with hydrocarbon source rocks, in J.R. Blueford, and Murchey, eds., Radiolaria of giant and subgiant fields in Asia: New York, Micropaleontology Press, Nazarov memorial volume, p. 9-16.

Orr, W.L., 1986, Kerogen/asphaltene/sulfur relationships in sulfur-rich Monterey oils: Organic Geochemistry, Great Britain, v. 10, p. 499-516.

Outhman, R.S., 1990, Generation, migration and maturation of the hydrocarbons in northern Iraq (Upper Jurassic-Lower Cretaceous): Master's thesis (unpublished), Science College, University of Salahaddin, Erbil, Iraq, 208 p. (in Arabic).

Peters, K.E., and J.M. Moldowan, 1991, Effects of source, thermal maturity, and biodegradation on the distribution and isomerization of homohopanes in petroleum: Organic Geochemistry, v. 17, no.1, p. 47-61.

Peters, K.E., and M.R. Cassa, 1994, Applied source rock geochemistry, chapter 5, in Magoon, L.B., and W.G. Dow, eds., The petroleum system—from source to trap: AAPG Memoir 60, p. 93–120.

Peters, K.E., C.C. Walters, and J.M. Moldowan, 2005a, The biomarker guide, second edition, volume I, biomarkers and isotopes in petroleum systems and human history: United Kingdom, Cambridge University Press, 476 p.

Peters, K.E., C.C. Walters, and J.M. Moldowan, 2005b, The biomarker guide, second edition, volume II, biomarkers and isotopes in petroleum systems and earth history: United Kingdom, Cambridge University Press, 679 p.

Peters, K.E., 1986, Guidelines for evaluating petroleum source rock using programmed pyrolysis: AAPG Bulletin, v. 70, no. 3, p. 318-329.

Peters, K.E., and J.M. Moldowan, 1993, The Biomarker Guide-interpreting molecular fossils in petroleum and ancient sediments: New Jersey, Prentice-Hall, Englewood Cliffs, 363 p.

Peters, K.E., and J.M. Moldowan, 1992, The Biomarker Guide-interpreting molecular fossils in petroleum and ancient sediments: New Jersey, Prentice-Hall, Englewood Cliffs, 320 p.

Petroleum Geological Analysis LTD., 2000, Source rock potential and maturity of the Sargelu and Naokelekan formations in Iraq. Petroleum Geological Analysis LTD., Quantock and saker geological Services, University of Reading, 69 High Street West Glossop, Derbyshire SK138AZ, England <www.pgal.co.uk> Accessed 4/14/2010.

Philp, R.P., 1985, Fossil fuel biomarkers: Amsterdam-Oxford-New-York Tokyo, Elsevier Science Publishing Company Inc., 294 p.

Pimmel, A., and G. Claypool, 2001, Introduction to shipboard organic geochemistry on the JOIDES Resolution: ODP Tech. Note, 30 [Online]: Available from World Wide Web: <http://www-odp.tamu.edu/publications/tnotes/tn30/INDEX.HTM> Accessed 2/14/2010.

Pitman, J.K., K.J. Franczyk, and D.E. Andres, 1987, Marine and non marine gas-bearing rocks in Upper Cretaceous Blackhawk and Nelson formations, eastern Uinta Basin, Utah-sedimentology, diagenesis, and source rock potential: AAPG Bulletin, v. 71, no. 1, p. 76-94.

Pitman, J.K., D.W. Steinshouer, and M.D. Lewan, 2003, Generation and migration of petroleum in Iraq, A 21/2D and 3D modeling study of Jurassic source rocks: AAPG international meeting in Cairo, Egypt, compiled power point slides, open-file report 03-192.

Pitman, J.K., D. Steinshouer, and M. D. Lewan, 2004, Petroleum generation and migration in the Mesopotamian Basin and Zagros Fold Belt of Iraq, results from a basin-modeling study: GeoArabia, Gulf PetroLink, Bahrain, v. 9, no. 4, p. 41-72.

Qaddouri, A.K.N., 1972, Jurassic formations in northern Iraq (Benavi area) (unpublished report): State Organization for Mineral, Baghdad, Iraq.

Qaddouri, A.K.N., 1986, Triassic-Jurassic sediments in Iraq: Iraqi Geological Society journal, v. 19, no. 3, p. 43-76.

Rabbani, A.R., and M.R. Kamali, 2005, Source rock evaluation and petroleum geochemistry; offshore SW Iran: Journal of Petroleum Geology, v. 28, issue 4, p. 413-428.

Rasoul Sorkhabi, Iraq: resource base, University of Utah's Energy & Geoscience Institute <http://images.google.com/imgres?imgurl=http://www.geoexpro.com/sfiles/85/61/2/picture/figure3.jpg&imgrefurl=http://www.geoexpro.com/hydrocarbo/theresourcebase/&usg=__eQoEass3BxbT72d16erfa444e4A=&h=665&w=464&sz=70&hl=en&start=1&um=1&itbs=1&tbnid=j-kJQE0b0noYyM:&tbnh=138&tbnw=96&prev=/images%3Fq%3DIraq%2BTectonic%2BZones%26um%3D1%26hl%3Den%26sa%3DN%26tbs%3Disch:1> Accessed March 22, 2010.

Read, J., 1985, Carbonate platform facies models: AAPG Bulletin, v. 69, no. 1, p. 1-21.

Reed, S., and H.M. Ewan, 1986, Geochemical report, Norse Hydro A/S, 6407/7-1, <http://www.npd.no/engelsk/cwi/pbl/geochemical_pdfs/474_7.pdf> Accessed February 8, 2010.

Riva, A., T. Salvatori, R. Cavaliere, T. Ricchiuto, and L. Novelli, 1986, Origin of oils in Po Basin, northern Italy: Organic Geochemistry, v.10, p. 391-400.

Sadooni, F.N., and A.S. Alsharhan, 2004, Stratigraphy, lithofacies distribution, and petroleum potential of the Triassic strata of the northern Arabian plate: AAPG Bulletin, v. 88, no. 4, p. 515-538.

Sadooni, F.N., 1997, Stratigraphy and petroleum prospects of Upper Jurassic carbonates in Iraq: Petroleum Geoscience, v. 3, no. 3, p. 233-243.

Salae, A.T.S., 2001, Stratigraphy and sedimentology of the Upper Jurassic succession northern Iraq: Master's thesis (unpublished), Science College, University of Baghdad, Baghdad, Iraq, 95 p.

Scotese, C.R. Paleomap project <http://www.paleoportal.org/kiosk/sample_site/period_9.html> Accessed January 19, 2010.

Seifert, W.K., and J.M. Moldowan, 1980, The effect of thermal stress on source-rock quality as measured by hopane stereochemistry: Physics and Chemistry of the Earth, v. 12, p. 229-237.

Setudehnia, A., 1978, The Mesozoic sequence in south-west Iran and adjacent areas: Journal of Petroleum Geology, v. 1, issue 1, p. 3-42.

Shaaban, F., R. Lutz, R. Littke, C. Bueker, and K. Odisho, 2006, Source-rock evaluation and basin modelling in NE Egypt (NE Nile Delta and northern Sinai): Journal of Petroleum Geology, v. 29, issue 2, p. 103-124.

Sharief, F.A., 1981, Permian and Triassic geological history and tectonics of the Middle East: Journal of Petroleum Geology, v. 6, issue 1, p. 95-102.

Smith, J.T., 1994, Petroleum system logic as an exploration tool in a frontier setting, chapter 2, in Magoon, L.B., and W.G. Dow, eds., The petroleum system—from source to trap: AAPG Memoir 60, Tulsa, p. 25-49.

Sofer, Z., 1984, Stable carbon isotope compositions of crude oils-application to source depositional environments and petroleum alteration: AAPG Bulletin, v. 68, no. 1, p. 31-49.

Spiro, B., 1991, Effects of minerals on Rock Eval pyrolysis of kerogen: Journal of Thermal Analysis, v. 37, p. 1513-1552.

Sykes, R., and L.R. Snowdon, 2002, Guidelines for assessing the petroleum potential of coaly source rocks using Rock-Eval pyrolysis: Organic Geochemistry, v. 33, p. 1441-1455.

Surdashy, A.M., 1999, Sequence stratigraphic analysis of the Early-Jurassic central and northern Iraq: Ph.D. dissertation (unpublished), Science College, University of Baghdad, Baghdad, Iraq, 145 p.

Ten Haven, H.L., and J. Rullkötter, 1988, The diagenetic fate of taraxer-14-ene and oleanene isomers: Geochimica et Cosmochimica Acta, v. 52, p. 2543-2548.

Tissot, B., B. Durand, J. Espitalié, and A. Combaz, 1974, Influence of nature and diagenesis of organic matter in formation of petroleum: AAPG Bulletin, v. 58, no. 3, p. 499-506.

Tissot, B.P., and D.H. Welte, 1984, Petroleum formation and occurrence, 2nd revised and enlarged edition: Berlin Heidelberg New York Tokyo, Springer-Verlag, 699 p.

Tissot, B.P., 1984, Recent advances in petroleum geochemistry applied to hydrocarbon exploration: AAPG Bulletin, v. 68, no. 5, p. 545-563.

Waples, D.W., and J.A. Curiale, 1999, Oil-oil and oil-source rock correlations, chapter 8, in Beaumont, E.A., and N.H. Foster, eds., Exploring for oil and gas traps: AAPG, Tulsa, p. 8-1 to 8-71.

Whelan, J.K., and C.L. Thompson-Rizer, 1993, Chemical methods for assessing kerogen and protokerogen types and maturity, chapter 14, in Engel, M.H., and S.A. Macko, eds., Principles and applications: Organic Geochemistry, Plenum Press, New York, p. 289-353.

Wetzel, R., 1948, Sargelu Formation, in Bellen, R.C. van, H.V. Dunnington, R. Wetzel, and D.M. Morton, eds., Lexique stratigraphic international: Paris, v. III, Asie, Fascicule 10a Iraq, p. 250-253.

Wetzel, R., and D.M. Morton, 1950a, Naokelekan Formation, in Bellen, R.C. van, H.V. Dunnington, R. Wetzel, and D.M. Morton, eds., Lexique stratigraphic international: Paris, v. III, Asie, Fascicule 10a Iraq, p. 211-215.

Wetzel, R., and D.M. Morton, 1950b, Sehkaniyan Formation, in Bellen, R.C. van, H.V. Dunnington, R. Wetzel, and D.M. Morton, eds., Lexique stratigraphic international: Paris, v. III, Asie, Fascicule 10a Iraq, p. 261-264.

Wetzel, R., 1951, Muhaiwir Formation, in Bellen, R.C. van, H.V. Dunnington, R. Wetzel, and D.M. Morton, eds., Lexique stratigraphic international: Paris, v. III, Asie, Fascicule 10a Iraq, p. 192-194.

Wever, P.De., and F. Baudin, 1996, Paleogeography of radiolarite and organic-rich deposits in Mesozoic Tethys: Geologische Rundschau, v. 85, no. 2, p. 310-326.

Wilson, M., E.R. Neuman, G.R. Davies, M.J. Timmermans, M. Heeremans, and B.T. Larsen, eds., 2005, Permo-Carboniferous magmatism and rifting in Europe: Mineralogical Magazine, Geology society of London, Special Publication, no. 223, 498 p.

Ziegler, M.A., 2001, Late Permian to Holocene paleofacies evolution of the Arabian plate and its hydrocarbon occurrences: GeoArabia, Gulf PetroLink, Bahrain, v. 6, no. 3 p. 445-504.

Zumberge, J., 2010, pers. comm.

APPENDEX

CONTENTS OF THE CD-ROM

Plate Ia: Tectonic map of Iraq (Al-Kadhimi, J.A.M., and V.K., Sissakian "compiled", F.A.   Ibrahim, and V.K., Sissakian "editing and cartographic completion", R.M. Al-Jumaily, and H.Kh. Mahmoud "approved", E.I. Ibrahim, and N.M. Al-Ali "cartographic execution", 1996).

Plate Ib: Structure map on the top Middle Jurassic at Middle Miocene (Pitman et al., 2004).

Plate II: Stratigraphic column of the Middle Jurassic Sargelu Formation at Sargelu village, northern Iraq.

Plate III: Stratigraphic column of the Middle Jurassic Sargelu Formation at Barsarin village, northern Iraq (modified from Balaky, 2004).

Plate IVa: Stratigraphic column of the Middle Jurassic Sargelu Formation at Hanjeera village, northern Iraq.

Plate IVb: Geologic cross-section of Shawoor valley, NW Rania town, shows Jurassic formations—not to scale (modified from Karim, 2009, pers. comm.).

Plate V: Stratigraphic column of the Middle Jurassic Sargelu Formation at Gara Mountain, northern Iraq (modified from Wetzel, 1948; Balaky, 2004).

Plate VI: Shows photograph images, thin section photomicrograph, and scanning electron microscope images of the Middle Jurassic Sargelu Formation at depth 2207-2208 m below the sea level at Guwear-2 Well, northern Iraq.

Plate VII: Correlation of lithofacies among the studied sections of the Sargelu Formation in northern Iraq (modified from Balaky, 2004).